2017

Insights into coral recovery based on symbiont state and environmental conditions in the temperate, facultatively symbiotic coral Astrangia poculata

BOSTON UNIVERSITY

Graduate School of Arts and Sciences

Dissertation

INSIGHTS INTO CORAL RECOVERY BASED ON SYMBIONT STATE AND ENVIRONMENTAL CONDITIONS IN THE TEMPERATE, FACULTATIVELY SYMBIOTIC CORAL *ASTRANGIA POCULATA*

by

ELIZABETH M. BURMESTER

B.A., Franklin & Marshall College, 2010

Submitted in partial fulfillment of the

requirements for the degree of

Doctor of Philosophy

2017

Approved by

First Reader _____

John R. Finnerty, Ph.D.
Associate Professor of Biology

Second Reader _____

Randi D. Rotjan, Ph.D.
Research Assistant Professor of Biology

Third Reader _____

Les Kaufman, Ph.D.
Professor of Biology

The people you love will change you,

The things you have learned will guide you,

And nothing on earth can silence

The quiet voice still inside you.

Moana

For my Dad.

ACKNOWLEDGMENTS

This dissertation would not have been possible without the support, guidance, and encouragement of many people. First, I would like to thank my advisors: John Finnerty, Randi Rotjan, and Les Kaufman. I am so grateful for your optimism, your advice, your assurance, and your patience. I also appreciate the guidance and support of my PhD committee members: Sean Mullen, Pete Buston, and Sarah Davies.

Many thanks to past and present members of the Finnerty, Kaufman, and Rotjan labs, who have made an indelible impact on me as a person and as a professional by being my colleagues and friends.

Thanks to my wonderful research assistants, interns, and volunteers that have assisted me over the years. This work is the collaborative effort of many hands and would not have been completed without the invaluable contributions of each and every single one. To all of my colleagues at the New England Aquarium, thank you for your enthusiasm and your support.

I want to thank my friends and my roommates, whose kind words, laughter, and advice have carried me throughout the highs and lows of this intellectual journey.

To my sister, Caroline, and to my parents: thank you for your continued and unwavering support in everything I do. It has been a source of unlimited inspiration. Lastly, I thank Perry Oddo, who has been a brilliant and indispensable partner throughout this entire adventure.

INSIGHTS INTO CORAL RECOVERY BASED ON SYMBIONT STATE AND ENVIRONMENTAL CONDITIONS IN THE TEMPERATE, FACULTATIVELY SYMBIOTIC CORAL *ASTRANGIA POCULATA*

ELIZABETH M. BURMESTER

Boston University, Graduate School of Arts and Sciences, 2017

Major Professors: John R. Finnerty, Associate Professor of Biology,
Randi D. Rotjan, Research Assistant Professor of Biology,
and Les Kaufman, Professor of Biology

ABSTRACT

Coral reefs are declining globally, calling for better ways to quantify coral health and predict resilience to future stress. The relationship between bleaching and fitness is key, as is reserve capacity to deal with physical trauma. This dissertation is an integrative study of the coral-algal symbiosis, holobiont performance under varied environmental conditions, and interactions between holobiont and environment on coral colony health and ability to recover from routine partial damage. I utilize the facultatively symbiotic, temperate coral *Astrangia poculata* as a natural model to explore the dynamics of colony health, performance, and the influence of environmental and nutritional stress under

stable aposymbiotic and symbiotic states. Unlike most tropical hermatypic corals that rely heavily upon photosynthetic symbionts for energy, *A. poculata* can (1) flexibly use both heterotrophic and autotrophic nutritional pathways and (2) exist in naturally occurring, stable, and measurable aposymbiotic and symbiotic states. I begin by describing the impacts of environmentally relevant (winter, summer, and above range) temperatures on small-scale wound healing and recovery. Next, I explore the effects of nutritional and symbiotic states by comparing wound recovery, total colony health, host behavior, and symbiont performance in fed and starved colonies. Finally, I generate a novel reference transcriptome for *A. poculata,* and use computational approaches to characterize variation in gene expression between the symbiotic and aposymbiotic states. This analysis reveals that regardless of temperature, and with or without the potential for heterotrophic nutritional sources, a relationship with *Symbiodinium* enhances wound recovery and resilience to stress. Compromised healing ability and tissue cover at low temperatures suggest that in temperate stony corals, recovery and survival are more impacted by winter conditions than by exposure to high summer temperatures. Differential expression analysis revealed predictable enhancements to photosynthesis-related gene expression in symbiotic colonies. Together these results illuminate the complex interactions among symbiotic state, stress, recovery, and performance. We propose that studies like ours that examine the effects of combined stressors, as opposed to a monotonic focus on coral bleaching *per se*, are essential to clinical diagnosis and stewardship for coral reefs subjected to intense, cumulative human impacts.

TABLE OF CONTENTS

LIST OF TABLES

LIST OF FIGURES

LIST OF ABBREVIATIONS

ΔAIC_c	change in Aikake information criterion
AIC	Aikake information criterion
AIC_c	Aikake information criterion adjusted for small sample size
ANOVA	analysis of variance
bp	base pair
BLAST	Basic Local Alignment Search Tool
BUSCO	Benchmarking Universal Single Orthologs
cDNA	copy deoxyribonucleic acid
CI	colony integration
CO1	cytochrome oxidase subunit 1
DE	differentially expressed
E	expect value
EDGE	extraction of differential gene expression
F_0	minimal fluorescence
F_m	maximal fluorescence
F_v/ F_m	maximum quantum yield
FDR	false discovery rate
GLMM	generalized linear mixed model
GO	gene ontology
h	hour
HO	high output
ID	identification
kmer	a motif of length k observed more than once in a sequence
LME	linear mixed effects model
LR	localized regeneration
MA	Massachusetts
MUSCLE	Multiple Sequence Comparison by Log-Expectation
MRD	Marine Resources Department
n	sample size
N50	the shortest sequence length at 50% of the genome
NCBI	National Center for Biotechnology Information

NIH	National Institutes of Health
NOAA	National Oceanic and Atmospheric Association
nt	nucleotide
nr	non-redundant
RPKM	reads per kilobase of transcript per million reads
P:SA	perimeter to surface area
PAM	pulse-amplitude modulated fluorescence
PAR	photosynthetically active radiation
PCA	principle components analysis
PE	phoenix effect
PSII	photosystem II
REML	restricted maximum likelihood
RGB	red-green-blue
RI	Rhode Island
SAM	sequence alignment map
SEM	standard error of mean
UV	ultraviolet

Chapter 1

INTRODUCTION

Coral reefs are among the most biodiverse ecosystems on the globe, but they are also among the most highly at risk from degradation (Mulhall 2008). For numerous ecological, sociological, and economic reasons, these ecosystems are highly valued (Knowlton 2001, Baker *et al.* 2008, Brainard *et al*. 2013). As such, there is an emergent global effort to steward coral reef species and communities through the time required to arrest anthropogenic climate change and local human impacts. In order to maintain sustainable populations through periods of extreme stress, conservationists must understand and be able to predict the ability of reef-building corals to recover from localized perturbations and exhibit resilience to environmental stress over time. However, how can we quantify such complex dynamics in coral health and survival?

With the importance of lesion repair to colony integrity, health, and resilience, there is a growing effort to use wound healing as a measurable proxy for determining recovery capacity and coral health in response to environmental stress (Meesters *et al.* 1994, Downs *et al.* 2005, Work & Aeby 2010). Coral colonies are regularly abraded by a host of biotic and abiotic factors, including predation

(corallivory), human activity, storm surge, and disease (Bak *et al.* 1980, Bythell *et al.* 1993, Bonaldo *et al.* 2011). The ability of colonies to recover and replace lost tissue is vital to restoring colony integrity and enhancing long term survival. As a result, a multitude of studies have explored several intrinsic (colony size, morphology, and genotype) and extrinsic factors (parameters of the wound itself as well as environmental factors such as temperature and sedimentation) that may influence which mode of recovery a colony might utilize, the pace of that recovery, or whether a colony may recover at all (for example: Fishelson 1973, Bak *et al.* 1980, Woodley *et al.* 1981, Bak 1983, Hughes & Jackson 1985, Riegl & Velimirov 1991, Bythell *et al.* 1993, Harmelin & Marinopoulos 1994, Bak & Meesters 1998, Van Woesik 1998, Mascarelli & Bunkley-Williams 1999, Lirman 2000, Edmunds & Lenihan 2010, Jayewardene 2010, Rotjan & Dimond 2010, Bonaldo & Krajewski 2011, Roff *et al* 2014; as suggested by Kramarsky-Winter & Loya (2000) and reviewed by Henry & Hart 2005).

Intrinsically, lesion recovery can vary by the size of the colony (Bak *et al.* 1977, Woodley *et al.* 1981, Hughes & Jackson 1984, Bythell *et al.* 1993, Bak & Meesters 1998, Kramarsky Winter 2000). Without regard to regenerative capacity, colony size plays an important role in the likelihood that a coral colony will need to engage in lesion repair. By probability of the interaction of lesion agents with a

greater surface area, larger corals tend to be more vulnerable to wounds than smaller corals (Jackson 1979). However, even though injuries may occur more frequently in larger colonies, they disrupt a smaller proportion of colony integrity. Therefore, wounds on smaller colonies have a greater ratio of circumference to surface area by virtue of having less undisturbed tissue surrounding the wound border, through which resources necessary for successful regeneration might be translocated (Meesters *et al.* 1997b). Additionally, increasing colonial morphological complexity encourages faster post-lesion regeneration. Likely because of their enhanced need for regular tissue maintenance and repair due to their growth forms, more complex morphologies should have greater colonial integration and higher investment in lesion repair (Jackson 1979, Kojis & Quinn 1985). Thus, for example, massive mounding forms have been shown to recover more quickly from surface lesions than do plating forms (Fishelson 1973, Bak & Engel 1979, Riegl & Velimirov 1991, Nagelkerken & Bak 1998). Branching corals with apical tips (such as *Acroporids*) are rapid regenerators, however, it should be noted that rapid growth in these colonies may impair the pace of regeneration in these fast-growing species (Denis *et al.* 2013). Polyp morphology can also play an important role in predicting tissue recovery rate. Taxa with smaller polyps have

been found to have more rapid healing rates than their larger polyp counterparts (Fishelson 1973, Riegl & Velimirov 1991).

Extrinsically, features of the wound itself play an important role in the success and pace of recovery. On the colony level, there are several hypotheses that attempt to predict the direction and capacity of a coral's regenerative power. Two of these hypotheses ("Localized Regeneration" and "Colony Integration") function primarily on lesions in which recovered tissue originates from the leading edge of the wound (Meesters *et al.* 1994, 1997a, Bak & Steward-Van Es 1980; Oren *et al.* 1997, 2001). Under the Localized Regeneration hypothesis, healing capacity is determined by the ratio of the wound's perimeter to surface area (P:SA), whereby healing rate increases as this ratio increases (Meesters *et al.* 1997a, VanWoesik 1998). In this mode of recovery, colony size seems to have little to no influence on regenerative capacity. On the other hand, the Colony Integration model posits that lesion recovery involves the translocation of resources from tissues proximal or distant from the wound site (Oren *et al.* 1997, 2001). Therefore, under this model, small wounds might behave according to the Localized Regeneration model, but the recovery of larger wounds depends on the size of a colony and its energetic resources (Oren *et al.* 1996, 2001). The third hypothesis, Phoenix Effect recovery, describes lesion healing that originates from remaining

tissue within the corallites that are able to regenerate and rejoin to restore polyp-wide and colonial integrity (Krupp *et al.* 1992, Meesters *et al.* 1992, Jokiel *et al.* 1993, Roff *et al.* 2014, DeFilippo *et al.* 2016).

Together, these studies suggest that wound recovery and colony resilience are the context dependent results of the interplay of a myriad of driving factors. However, despite the large body of observational and experimental work devoted to the study of coral recovery and resilience, little is known about what role a key, defining characteristic of a coral reef – the coral-algal symbiosis— plays in the recovery process.

The term "holobiont" is used to describe as assemblage of different symbiotic species – of sorts, an ecosystem within an organism (Rowan 2004). Among the key components of the coral holobiont are the photosynthetic algal endosymbionts of the genus *Symbiodinium* (Downs *et al.* 2002, LaJeunesse *et al.* 2012). For many tropical hermatypic corals, the vast majority of carbon resources are derived from photosynthate transfer from *Symbiodinium* cells kept within specialized gastrodermal cells called symbiosomes (Muscatine & Hand 1958, Roth *et al.* 1988). Because the nutritional needs of tropical coral hosts are obligately tied to their photosynthetic endosymbionts (Downs *et al.* 2002, Rowan 2004), it can be difficult to tease apart the relative contributions of host and symbiont to the

recovery process. Colony health suffers when the symbiotic relationship is disrupted during "bleaching" events, where zooxanthellae are expelled from their hosts. This mass expulsion of symbionts has been linked to changes in temperature (Lesser and Farrell 2004), solar radiation (Roth 2014), reduced salinity (Brown 1994), as well as bacterial infection (Kushmaro 1996). While bleaching can be adaptive in the short term because it prevents the overproduction of oxygen free-radicals during periods of photosynthetic inhibition, it poses a major threat to corals in the long term. Most corals cannot survive long as heterotrophs (Rowan 2004). Moreover, the physiological stress caused by bleaching can undermine the ability of corals to heal and regenerate after incurring routine physical wounds (Diaz-Pulido & McCook 2002). Therefore, studies characterizing the impact of a coral's reserve capacity for recovery are of crucial importance to conservation.

In this dissertation, I use the temperate northern star coral *Astrangia poculata* as a tractable study organism to investigate the impacts of symbiotic, environmental, and nutritional states on the recovery, health, and performance of hermatypic corals. Because of its facultative relationship with *Symbiodinium psygmophilum* (clade B2), *A. poculata* has the potential to be a uniquely informative model for studying the health impacts and reserve potential of the coral-algal symbiosis. Unlike their tropical counterparts, colonies of *A. poculata* can be found

sympatrically in nature in measurable and healthy symbiotic and aposymbiotic states. This creates a natural experiment for exploring holobiont function and health under stable conditions.

Thus, in the Appendix (an undergraduate-driven mentored work), we begin by exploring the mechanistic patterns of lesion recovery by experimentally manipulating physical characteristics of an induced multi-polyp lesion and their interactions with symbiont state. Informed by these patterns, in Chapter 2, I generate a staged developmental scheme as well as quantifiable recovery metrics for single polyp recovery. I utilize naturally occurring symbiont states and mimic environmentally relevant temperatures in a controlled laboratory setting to observe lesion recovery under temperate winter, summer, and above range scenarios. In Chapter 3, I expand this work to explore the impacts of reserve capacity on lesion recovery, colony health, and behavior in both host and symbiont by experimentally controlling colony exposure to heterotrophic sources of nutrition.

Having described several examples of differential phenotypic performance based on symbiont state in the previous chapters, in Chapter 3, I apply transcriptomic and computational approaches to characterize differential gene expression between aposymbiotic and symbiotic colonies. As part of this work, I

generate a novel transcriptome for *Astrangia poculata*, producing the first available transcriptomic data resources for a facultatively symbiotic coral, as well as the first naturally occurring (i.e. not induced) aposymbiotic cnidarian-algal holobiont model.

Taken together, these chapters represent comprehensive insights into dynamics of symbiont state and environmental condition as drivers of holobiont performance and recovery in a temperate and facultatively symbiotic coral model system.

Chapter 2

TEMPERATURE AND SYMBIOSIS AFFECT LESION RECOVERY IN EXPERIMENTALLY WOUNDED, FACULTATIVELY SYMBIOTIC TEMPERATE CORALS

2.1 ABSTRACT

The health of most reef-building corals depends upon an intracellular symbiosis with photosynthetic dinoflagellates of the genus *Symbiodinium* that is acutely sensitive to increasing ocean temperatures. However, distinguishing the individual effects of both temperature and symbiotic state on coral health is difficult to investigate experimentally in most tropical corals because the symbiosis is obligate. Here, we varied temperature (9, 18, 24°C) and symbiotic state (symbiotic, aposymbiotic) in the facultatively symbiotic, temperate scleractinian coral *Astrangia poculata* to distinguish the impacts of temperature and symbiosis on wound healing, an important component of coral resilience. We used wound size using calibrated photographs to characterize the developmental stages of the healing process over time. Symbiotic corals demonstrated a significant healing advantage over corals with lower densities of *S. psygmophilum* (aposymbiotic state), regardless of temperature. In addition, overall recovery success of both symbiotic states increased with temperature. These data suggest

that a functional symbiotic relationship with *S. psygmophilum* promotes lesion recovery despite heterotrophic energy sources. Reductions in healing rate and tissue cover near the wound site under cold temperatures suggest that wound healing is compromised during the winter in these temperate corals. This study demonstrates that supplemental energy sources from symbiosis, coupled with optimal growth conditions, promote wound healing and may offer insight into factors enhancing wound recovery in tropical corals.

2.2 INTRODUCTION

One key determinant of coral resilience is the ability to heal from wounds. In nature, corals sustain lesions regularly, and from multiple causes, including corallivory (Kaufman 1981, Jompa & McCook 2003, Jayewardene & Birkeland 2006, Rotjan & Lewis 2008, Cole *et al.* 2008), algal abrasion (Coyer *et al.* 1993, Grace 2004), sedimentation (Nugues & Roberts 2003a,b), and hurricane activity (Bythell *et al.* 1993). Tissue regeneration (by which tissue has re-grown and/or polyp body plan is reimposed) and full wound recovery (by which colony integrity is restored, including calcification) are energetically demanding (Oren *et al.* 2001, Henry & Hart 2005, Jayewardene 2009, Lenihan & Edmunds 2010). As a result, wounding can lead to reductions in colony fecundity (Oren *et al.* 2001, Rotjan & Dimond 2010) and growth (Meesters *et al.* 1994, Jayewardene *et al.* 2010, Lenihan & Edmunds

2010). Furthermore, until epithelial integrity is reestablished, wounded colonies are left with patches of bare calcium carbonate that are susceptible to overgrowth by benthic competitors such as algae and sponges (Meesters *et al.* 1996, 1997, Diaz-Pulido & McCook 2002, Jompa & McCook 2003, Rotjan & Lewis 2005). Such overgrowth may inhibit the recovery of coral tissue and overall colony growth (River & Edmunds 2001). Therefore, the pace of healing and regeneration is critical to coral survival.

Healing rate can be influenced by a number of factors, including coral species (Bak & Steward-Van Es 1980), the size of the lesion (Meesters *et al.* 1996), and the ratio of wound perimeter to surface area (Meesters *et al.* 1997). Infrequent high-energy traumas tend to cause larger injuries, whereas due to their greater frequency, the fine-scale wounds that result from smaller disturbances (such as fish bites) can account for a greater loss of live tissue than large-scale wounds (Hughes & Jackson 1985, Bythell *et al.* 1993, Rotjan & Lewis 2006). Therefore, it is particularly important to understand the factors that impact how rapidly corals heal from these small lesions.

Environmental stress also influences the rate of healing and regeneration (Fisher *et al.* 2007). For example, temperature-induced bleaching (Meesters & Bak 1993, Rotjan *et al.* 2006) and high sedimentation (Meesters *et al.* 1994, Cróquer *et al.*

2002) impair healing capability in corals. Because of their importance to coral resilience and sensitivity to environmental conditions, wound recovery and regeneration have been used as metrics to assess colony health in the field (Meesters *et al.* 1994) and in the laboratory (Work & Aeby 2010), and to forecast the ability of a coral to survive prevailing environmental conditions (Downs *et al.* 2005).

While lesion healing has been studied extensively in a variety of species (reviewed by Henry & Hart 2005, and for example: Nagelkerken & Bak 1998, Denis *et al.* 2001, Cameron & Edmunds 2014) as well as across a range of intrinsic and extrinsic factors (e.g. Van Veghel & Bak 1994, Nagelkerken *et al.* 1999, Kramarsky-Winter & Loya 2000, Edmunds 2009), few studies have directly studied the impact of symbiosis on the healing process. In tropical corals, photosynthetic endosymbiotic alga of the genus *Symbiodinium* can provide up to 95% of the coral host's energy (Muscatine 1990); however, environmental stress (such as rising temperatures or changes in salinity) can decouple this obligate symbiosis, resulting in 'bleaching' (Hoegh-Guldberg 1999, Rowan 2004). This bleached state is not stable because of the resulting nutritional deficiency, and those colonies that are unable to shift or re-gain symbiotic partners will die (Grottoli *et al.* 2006, Baker *et al.* 2008). Because it is difficult to maintain tropical corals in a bleached state, and

because high temperatures result in bleaching, it is difficult to experimentally distinguish the impacts of bleaching and temperature on wound healing (Henry & Hart 2005), although this is of particular interest to coral conservation (Edmunds & Lenihan 2010).

The northern star coral *Astrangia poculata* (= *A. danae*; Peters *et al.* 1988) is an ideal organism to decouple the effects of temperature and symbiosis because its distribution spans a wide range of temperatures and it exhibits a facultative symbiosis with *Symbiodinium*. *A. poculata* is a temperate species whose native range extends along the US east coast, from Florida and the Gulf of Mexico to Rhode Island (RI) (Dimond & Carrington 2007, Thornhill *et al.* 2008). In nature, *A. poculata* may be found in symbiosis with *S. psygmophilum* (LaJeunesse *et al.* 2012), but colonies may also be found in an aposymbiotic (relatively low density of *S. psygmophilum*) state in the same habitat with symbiotic colonies (Dimond *et al.* 2013). Even within a colony, symbiont densities can vary markedly among polyps, resulting in mixed or mottled phenotypes (Figure 1). Regardless of symbiont state, all colonies of *A. poculata* rely heavily on heterotrophy as a source of energy (Szmant-Froelich & Pilson 1980). The symbiotic state of the colony is a function of zooxanthellae expulsion rates, i.e. aposymbiotic colonies actively maintain a very low density of *S. psygmophilum* through high expulsion rates (Dimond &

Carrington 2007). Polyps of *A. poculata* remain functionally aposymbiotic until *S. psygmophilum* density reaches or exceeds 10^6 cells cm^{-2}, after which polyps appear consistently brown throughout the body column (Dimond & Carrington 2007). As a result, these functionally aposymbiotic colonies differ significantly from bleached corals, as the low density of *Symbiodinium* sp. within host cells is (1) not indicative of stress and (2) not the result of a breakdown in symbiotic pathways between alga and host. Thus, unlike corals in obligate symbioses, qualitative differences in symbiont density exist as stable states in nature. Additionally, the sympatric overlap of different symbiont states provides a natural experiment for exploring the relative roles of symbiont and host on different biological functions. Previous studies have exploited the facultative symbiosis of *A. poculata* to investigate the effects of the coral–algal symbiosis on coral health, including the effect of symbiont density on coral nutrition (Szmant-Froelich & Pilson 1980, 1984), resistance to ocean acidification (Holcomb *et al.* 2010, 2012), post-sedimentation recovery (Cohen *et al.* 2002), calcification and metabolism (Jacques & Pilson 1980, Cummings 1983, Jacques *et al.* 1983), and physical parameters of wound recovery (DeFeilippo *et al.* 2016).

The objective of this study was to determine the effects of temperature and symbiont state on wound recovery in *A. poculata* coral colonies. We conducted

controlled laboratory experiments to investigate tissue recovery in naturally occurring symbiotic (high density of *S. psygmophilum*) and aposymbiotic (low density or absence of *S. psygmophilum*) colonies of *A. poculata* at 3 environmentally relevant temperatures characteristic of winter (9°C), fall/spring (18°C), and summer (24°C) in New England. Several healing metrics indicate that symbiotic corals exhibit significantly greater healing ability at 18 and 24°C.

2.3 METHODS

2.3.1 Collection and husbandry

Colonies exhibiting a range of symbiont densities were collected from depths of 6 to 10 m at Fort Wetherill State Park in Jamestown, RI (41° 28' 40" N, 71° 21' 34" W) from late spring through early fall 2014. As described by DeFeilippo *et al.* (2016), specimens were housed in a flow-through aquarium system at the New England Aquarium. Seawater was filtered using a protein skimmer and UV treatment, and water quality was measured weekly. Tanks were illuminated for 10 h d^{-1} using T5 HO fluorescent lighting fixtures (Hamilton Technology, Aruba Sun T5-V Series). Photosynthetically active radiation (PAR) was kept constant at an average of 37.5 ± 10.1 μmol m^{-2} s^{-1}. Corals were fed daily with frozen copepods (JEHM) directed to all polyps within each colony using a turkey baster. All colonies were acclimated to 18°C for at least 2 wk prior to commencing healing

trials. Throughout the duration of the initial acclimation and the experimental trials, all colonies were cleaned weekly using a soft nylon brush to remove algae and forceps to remove epibionts (e.g. polychaetes). Only bare skeletal regions (i.e. no live tissue) were brushed in this manner to avoid inflicting additional wounds or tissue damage. Colonies were assigned symbiont state as described by Dimond & Carrington (2007) and demonstrated by Dimond *et al.* (2013) and DeFilippo *et al.* (2016), where symbiont state was determined visually using color as a proxy for chlorophyll density. Additionally, to ensure this method accurately represented our system, a random subset of photos of 20 symbiotic and 20 aposymbiotic colonies were analyzed for approximated chlorophyll density using the protocol of Dimond & Carrington (2007). On average, the approximated chlorophyll densities for symbiotic colonies (mean +/- SEM: 0.45 ± 0.04 $\mu g\ cm^{-2}$) were significantly higher than those of aposymbiotic colonies (mean +/- SEM: 0.13 ± 0.02 $\mu g\ cm^{-2}$; ANOVA, $F_{1,38} = 53.4058$, $p < 0.0001$).

2.3.2 Experimental setup and temperature manipulation

Symbiotic and aposymbiotic colonies were sorted into pairs for treatment. Colony pairs were randomly placed into treatment groups, controlling for size between treatments. Sizing was based on colony mass, a measurement of whole

colony mass after the removal of excess water from bare skeletal regions. This measurement exhibited a high degree of precision; 5 separate mass measurements were performed on each of 37 colonies, and the mean variation in measurements performed on the same individual was 0.69%. Overall, average colony mass was 6.32 ± 0.27 g (SE). Paired colonies were placed adjacent to one another on a submerged platform in a randomized fashion in order to control for tank microclimate (lighting, flow, etc.). However, each pair of colonies was kept at a distance of 6–10 cm to avoid direct interaction. Three temperature treatments were tested: 9°C (within the natural range for winter), 18°C (within the natural range for summer), and 24°C (outside the typical temperature range for this site). Experimental temperatures were chosen based on environmental data for the area (NOAA Tides & Currents, Newport, RI: site 8452660), where sea surface temperatures ranged from 0.5 to 23°C during the 2014 calendar year. To account for seasonality and to accommodate the limitations of our system (i.e. tank space, ability to manipulate multiple temperatures simultaneously), 9°C treatments were performed in the winter months and 24°C treatments were performed in the summer and early fall. For continuity between seasonal experiments and to control for captivity duration, 2 trials of the 18°C group were carried out: 1 in winter and 1 in summer. Winter and summer 18°C trials were then compared to determine

any potential changes due to season, captivity duration, or husbandry (there were none). Therefore, at 18°C, 40 colonies of each symbiont state were sampled; meanwhile, 20 colonies of each symbiont type were sampled at 9 and 24°C. At 18°C, 1 wounded aposymbiotic colony was lost during routine tank cleaning (non-mortality), reducing the sample size of that group to 39 colonies (and a total of 159 colonies overall). Corals in the 9 and 24°C tanks were subjected to a temperature increase or decrease from 18°C at a rate of 1°C every 12 h. Colonies in these tanks were acclimated at their final experimental temperatures for 1 wk prior to wounding.

2.3.3. Wounding

All experimental corals were wounded in a consistent fashion: a single polyp, centrally located in the colony, was removed using a scalpel, and the calyx was cleared of tissue using a Waterpik (Figure 1) before the immediate surrounding skeleton was filed to a uniform basal skeletal height using a diamond-coated file, followed by a final cleaning with a Waterpik. These lesions were designed to mimic destructive forces that remove both tissue and skeleton (i.e. predation, mechanical injury, storm damage, etc.), but were inflicted in such a way to create as uniform a wound as possible between replicates. Colony mass

for each colony was measured before and after wounding to determine wound size (via change in mass)

2.3.4 Lesion recovery

Lesions were photographed using a Leica M165FC stereomicroscope immediately after wounding (Day 0) and at 10 time points post-wounding (5, 10, 15, 20, 25, 30, 40, 50, 60, and 75 d). Photographs from Day 0 were used to calibrate post-wound photos to ensure consistent magnification as well as colony angle and position. Photographs were scored for whether or not colonies exhibited signs of healing (i.e. new tissue within the wound site) as well as the developmental state of new tissue (undifferentiated tissue, tentacle nubs, or full polyp; Figure 1A [panels c-e, respectively]). These 3 stages were chosen because they can be identified unambiguously, and they represent important developmental landmarks on the way towards full healing, which begins with the formation of undifferentiated tissue, followed by initiation of tentacle formation, and concludes with the formation of a full polyp that has the ability to feed (as evidenced by tentacular contraction; Figure 1A). Achievement of this final developmental landmark was recognized as the indicator of healing success. Wound surface area

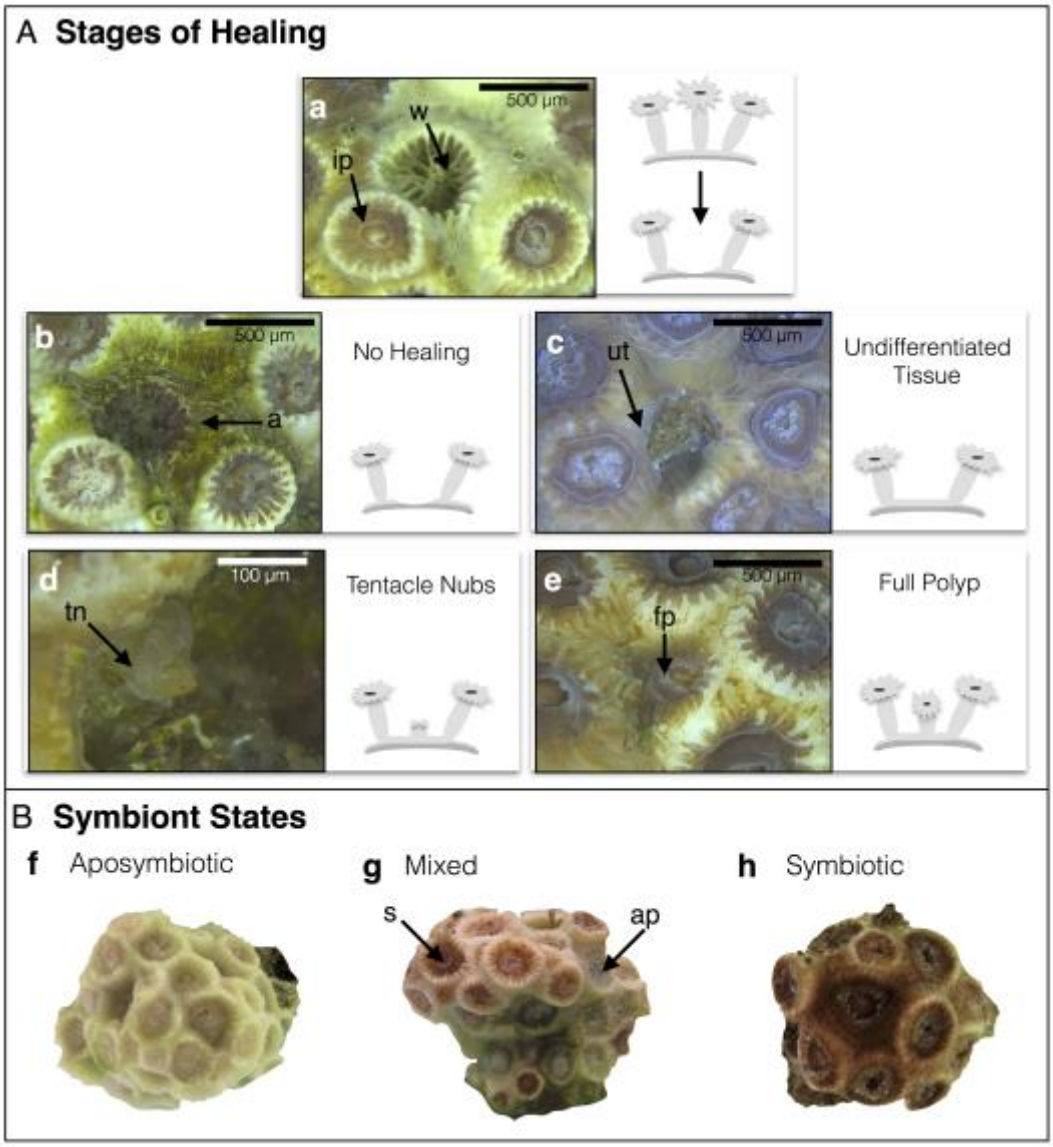

Figure 2.1. (A) Stages of wound healing as demonstrated in A. poculata*:* [a] experimentally-induced bare skeleton wound (*w*) from initial polyps (*i*); [b] no demonstration of recovery with wound size covered in algae (*a*); [c] formation of undifferentiated tissue (*ut*) from wound edges (as shown) or from within calice; [d] formation of tentacle nubs (*tn*); re-establishment of full polyp (*fp*) with fully functional tentacles. (B) Symbiont states in *A. poculata*: [f] aposymbiotic colonies appear white in color; [g] mixed symbiont colonies have a range of symbiotic (*s*) and aposymbiotic (*ap*) polyps; [h] fully symbiotic colonies appear brown in color.

was determined for Days 0 and 75 using hand-drawn area tools that are part of the Leica M165FC software. Three measurements were taken for each photo, and the wound surface area was estimated as their average. The percent change in wound surface area was calculated as final wound area minus the initial wound area divided by the initial wound area.

2.3.5 Colony Mass

Bare skeletal regions of each colony were thoroughly cleaned, avoiding live tissue, with a soft nylon brush and forceps prior to each measurement of mass to prevent confounding colony growth with algal growth. The difference between the initial post-wound mass (Day 0) and final mass (Day 75) was used to calculate a healing mass differential, i.e. the gain or loss of mass over the healing process. We also determined the mass of the wound itself by subtracting the colony's post-wound mass from its pre-wound mass. Two specimens were removed from the analysis (1 each from the 9°C symbiotic and aposymbiotic groups) because their colony mass at the time of wounding had not been accurately recorded.

2.3.6 Photosynthetic efficiency

In order to test for symbiont performance, photosynthetic efficiency (maximum quantum yield: F_v/F_m) was measured for each colony at 3 time points

over the course of the experiment (0, 30, and 60 d) using a Walz JUNIOR-PAM pulse-amplitude modulated fluorescence meter. All readings were taken between 11:00 and 13:00 h on each day to reduce diel fluctuations between readings across time points. As described by DeFilippo *et al.* (2016), colonies were acclimated to darkness for 30 min in a closed dark container and then transferred individually to a glass beaker with 5–7 cm of seawater stored within a dark box to reduce light exposure during measurement. For each measurement, polyps were first exposed to 6 s of far-red illumination to determine minimal fluorescence while dark-adapted (F_0). They were then exposed to 0.6 s of a saturating pulse (10000 μmol m^{-2} s^{-1}) to determine maximal fluorescence (F_m). The change in fluorescence between F_0 and F_m (ΔF) was divided by maximal fluorescence (F_m) to calculate maximum quantum yield (F_v/F_m; Suggett *et al.* 2010). Readings were taken with a light fiber held approximately 1 mm from the oral groove of 3 haphazardly selected polyps per colony, and the resulting average maximum quantum was used to represent the colony.

2.3.7 Documentation of altered symbiotic state

We visually inspected microscope photos from Day 75 to qualitatively assess whether any of the polyps within a 2-polyp radius of the wound had

undergone a change in symbiont density as evidenced by a shift in color. Shifts in symbiont density were quantified as the percentage of polyps changing symbiont state between Day 0 and Day 75; only polyp-level shifts from aposymbiotic to symbiotic were observed. Such shifts became apparent when individual polyps in a colony would develop clusters of brown spots (i.e. symbiosomes) detectable under the microscope.

2.3.8 Statistics

Healing initiation (proportion of colonies having developed any of the 3 landmark stages of healing) and healing success (proportion of colonies having regenerated new full polyps) were analyzed using generalized logistic mixed models (GLMMs) in the lme4 package in R. Logistic models were compared using Akaike's information criterion (AIC) scores, and a reduction in AIC of at least 2 was required to accept a given model over another or to validate the inclusion of a new variable in the model (Burnham & Anderson 2002). In the case of 2 models whose AIC scores differed by less than 2, the simpler model was chosen (Burnham & Anderson 2002). Odds ratios were generated using exponentiated estimates. The effects of symbiont state and temperature on colony mass and surface area were compared using Laplace-approximated generalized linear mixed models on the

nlme package in R (Pinheiro *et al.* 2017, R Core Team 2013). In order to test for the potential effect of colony size and wound size on recovery and colony mass, we included wound mass, initial mass, and initial wound surface area as fixed effects in addition to symbiont state and temperature in the analyses of healing initiation, healing success, wound closure, and colony mass. The impacts of added fixed, interaction, and random effects were determined using a forward and reverse stepwise approach (using AIC for logistic models and likelihood ratio tests for linear models). Additionally, tank assignment was designated as a random effect in all generalized logistic and linear models to control for potential consequences of multiple colony pairs in the same tank.

In order to test for changes in photosynthetic efficiency over time, maximum quantum yield was analyzed between symbiont states and temperatures over time using a restricted maximum likelihood (REML)-fitted GLMM in the lme4 package in R (Bates *et al.* 2015, R Core Team 2013). Individual coral identity was nested within tank in order to control for changes in an individual across time points and to account for potential confounds of tank housing. Model selection criteria were based on reductions in AIC in the same manner as logistic model selections.

Fisher's exact tests and ANOVAs were used to determine the effect of shifts in symbiont density on the relative ratios of healing ability and stage, and relative means of colony mass and surface area recovery, respectively, for aposymbiotic corals at 18 and 24°C. No colonies at 9°C showed signs of shifts in symbiont density, and this group was therefore excluded from this analysis.

2.4 RESULTS

2.4.1 Healing initiation and success

Overall, there was a significant impact of symbiosis on the healing process (Figure 2). Adjusted for tank grouping, symbiotic corals (40 of 80 total colonies) were 2.4 times as likely as aposymbiotic corals (25/79 colonies) to have initiated healing (developed new tissue of any kind) at the wound site (Table 1) and 5.8 times as likely to have successfully completed healing (reached the full polyp stage) by the end of the trial (15/80 symbiotic; 3/79 aposymbiotic; Table 2). Healing initiation also increased with temperature (Figure 2): with random effects, the odds ratio of exhibiting any healing at 24°C (23/40) was 4.7 times greater than at 9°C (9/40) and 1.6 times greater than at 18°C (33/79), while the odds ratio for corals at 18°C was 2.9 times that of corals kept at 9°C. None of the 9°C colonies developed full polyps by the end of the trial; however, among those colonies that did successfully

complete the healing process, the odds ratio of complete healing at 24°C (10/40) was 3.2 times greater than at 18°C (8/79). Consistent with these observations, both symbiont state and temperature were found to be significant predictors of healing initiation in a GLMM analysis (Table 3). However, neither the interaction between these 2 variables nor the added fixed effects of mass, wound mass, and wound surface area significantly improved the model (AIC 208.6, Table 3). Likewise, only symbiont state and temperature were found to be significant predictors of full polyp formation (i.e. healing success) in corals at 18 and 24°C (AIC 68.64, Table 4).

2.4.2 Wound closure

On average, the inflicted wounds were (mean ± SEM) 38.4 ± 1.2 mm^2 in area and accounted for a loss in mass of 0.14 ± 0.01 g. With the exception of symbiotic corals housed at 24°C, colonies, on average, experienced an increase in wound surface area, representing an expansion of the wound site (Figure 3). All (100%) symbiotic colonies experienced a decrease in wound size at 24°C, while none (0%) of the colonies (regardless of symbiont density) experienced such a decline at 9°C. More symbiotic colonies (32.5%) saw reductions in wound size at 18°C than did aposymbiotic colonies (18%). A similar proportion of aposymbiotic colonies were able to restore any lost surface area at 18°C (18%) and 24°C (15%). The proportion of tissue loss was lower in symbiotic corals (group mean= 0.098) than aposymbiotic

Table 2.1. Odds ratios (with 95% confidence) for fixed effect comparisons of healing ability.

Effect	**Odds Ratio (*95% Confidence*)**
Symbiont State	2.370 (*1.205, 4.663*)
9°C : 18°C	2.856 *(1.033, 7.898)*
9°C : 24°C	4.664 *(1.459, 14.910)*
18°C : 24°C	1.633 *(0.6325, 4.215)*

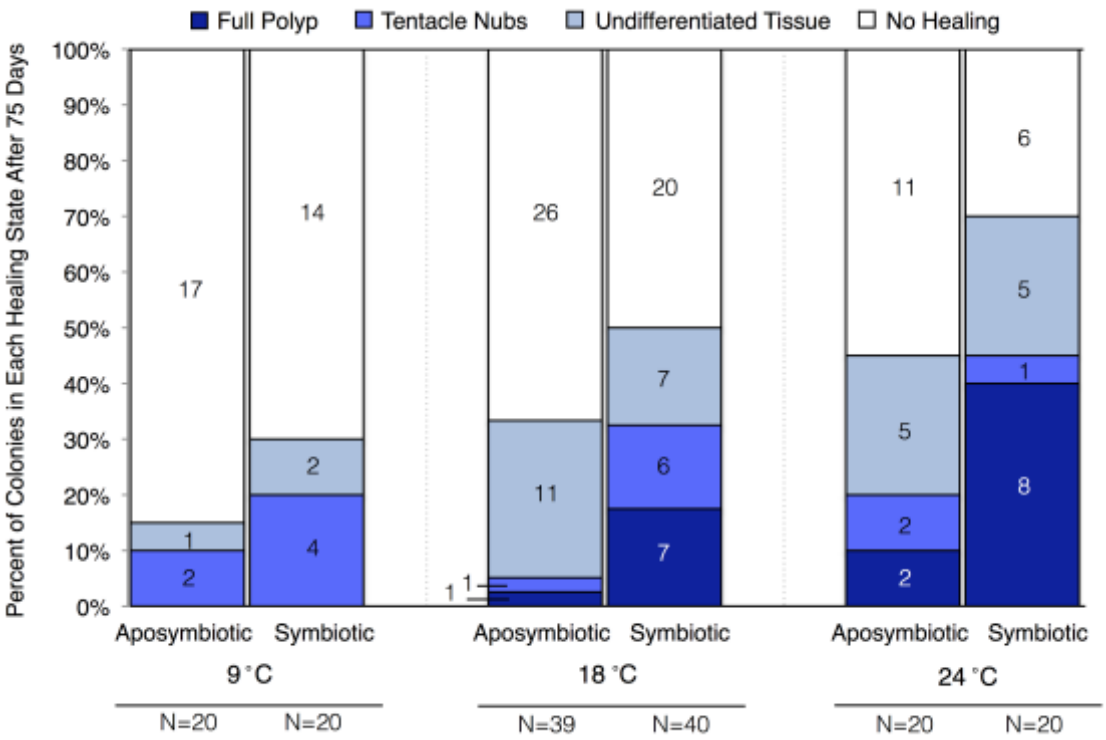

Figure 2.2. Proportion in each healing stage of symbiotic and aposymbiotic colonies maintained at three temperatures (9, 18, 24°C) 75 days post-wounding. Numbers in each column represent total number of colonies at that healing stage. Cumulative areas in blue delineate colonies that have demonstrated signs of healing, while bars in dark blue indicate only those colonies that have achieved successful healing through the formation of a complete polyp.

Table 2.2. Odds ratios (with 95% confidence) for fixed effect comparisons of healing success (polyp formation).

Effect	Odds Ratio (*95% Confidence*)
Symbiont State	5.769 *(1.346, 24.732)*
Temperature	3.253 *(0.927, 11.418)*

Table 2.3. Laplace approximated generalized mixed logistic regression for healing ability (AIC 208.6). For fixed effects, ** indicates significance at $\alpha < 0.001$, * indicates significance at $\alpha = 0.05$, $^{+}$ indicates significance at $\alpha = 0.1$.

Effect	Estimate	Standard Error	Z-Value	P-Value
Intercept[#]	-1.7812	0.4876	-3.653	0.0003**
Symbiont State (S)	0.8627	0.3452	2.499	0.0124*
18°C	1.0496	0.5189	2.023	0.0431*
24°C	1.5399	0.5929	2.597	0.0094*

[#]Rooted under Aposymbiotic and 9°C conditions

Effect	Estimate	Standard Error	Z-Value	P-Value
Intercept[#]	0.1311	0.3193	0.411	0.6813
Symbiont State (A)	-0.8627	0.3452	-2.499	0.0124*
9°C	-1.0496	0.5189	-2.023	0.0431*
24°C	0.4903	0.4839	1.013	0.3109

[#]Rooted under Symbiotic and 18°C conditions

Table 2.4. Laplace approximated generalized mixed logistic regression for healing success (AIC 68.64). For fixed effects, ** indicates significance at $\alpha < 0.001$, * indicates significance at $\alpha = 0.05$, $^{+}$ indicates significance at $\alpha = 0.1$.

Effect	Estimate	Standard Error	Z-Value	P-Value
Intercept[#]	-2.4522	0.7477	-3.280	0.0010**
Symbiont State (S)	1.7525	0.7427	2.360	0.0183*
Temperature (24)	1.1796	0.6406	1.842	0.0655^{+}

[#]Rooted under Aposymbiotic and 18°C conditions

corals (group mean = 0.195). Temperature also had a significant effect on wound surface area (Table 5), as corals in warmer water recovered a higher proportion of tissue than those in cooler water ($mean_9 = -0.349$, $mean_{18} = -0.137$, $mean_{24} = 0.046$). Again, symbiont state and temperature were significant contributors to the best mixed model (Table 5), although the effect of temperature was reduced ($p = 0.0918$).

2.4.3 Colony Mass

Except for the 24°C symbiotic group, colonies lost mass over time (Figure 4). Symbiotic colonies (group mean = –0.004 g) lost less mass than did aposymbiotic colonies (group mean = –0.409 g). Similarly, corals kept at higher temperatures experienced less tissue loss than colonies at lower temperatures,

with the colonies at 24°C experiencing a slight gain in mass on average ($mean_9$ = –0.345 g, $mean_{18}$ = –0.242 g, $mean_{24}$= 0.021 g; Figure 4). Both symbiont state and temperature had a significant impact on colony mass, but there was no significant interaction between these 2 variables (Table 6). Colony mass, wound mass, and initial wound surface area had no significant effects.

2.4.4 Photosynthetic efficiency

Regardless of symbiont state, measurable levels of photosynthesis were observed in all treatment groups (Figure 5). Symbiotic colonies had higher values for maximum quantum yield (F_v/F_m), with the exception of symbiotic colonies kept at 9°C (which demonstrated photosynthetic efficiency levels similar to those of aposymbiotic corals). Aposymbiotic colonies, on the other hand, demonstrated consistently similar F_v/F_m values regardless of temperature. The data show a slight significant decline in photochemical efficiency for symbiotic corals over time, but a slight significant increase for aposymbiotic corals. The preferred model included only symbiont state and the interactions between symbiont state and temperature as well as symbiont state and time (Table 7). Based on our model selection criteria (requiring a reduction in AIC of at least 2 to permit the inclusion of new fixed

effects), there was little support for the inclusion of other fixed effects (temperature and time) or interactions of fixed effects (temperature/time).

2.4.5 Symbiont state switching

At 18 and 24°C, some polyps of aposymbiotic corals were found to switch symbiont states, as indicated by pockets of high *Symbiodinium psygmophilum* density along the body column or oral groove. This phenomenon was significantly more likely in colonies at 24°C (15/20; 75%) than in colonies kept at 18°C (18/39; 46.15%; 1-tailed Fisher's exact test; n = 59, p = 0.0319). However, among these corals, there was no significant effect of symbiont switching on healing initiation (2-tailed Fisher's exact test; n = 59, p = 0.4232), colony mass ($mean_{switch}$ = –0.1244 g; $mean_{non\text{-}switch}$ = –0.1313 g; n = 59, $F_{1,57}$ = 0.0075, p = 0.9310), or wound closure ($mean_{switch}$ = –0.441; $mean_{non\text{-}switch}$ = –0.303; n = 59, $F_{1,57}$ = 1.1012, p = 0.2984). It should be noted that no aposymbiotic colonies ever completely switched states where every polyp in the colony transitioned from white to brown.

2.5 DISCUSSION

Overall, our data suggest that symbiotic colonies exhibit a clear advantage over aposymbiotic colonies with respect to single-polyp wound healing. At all

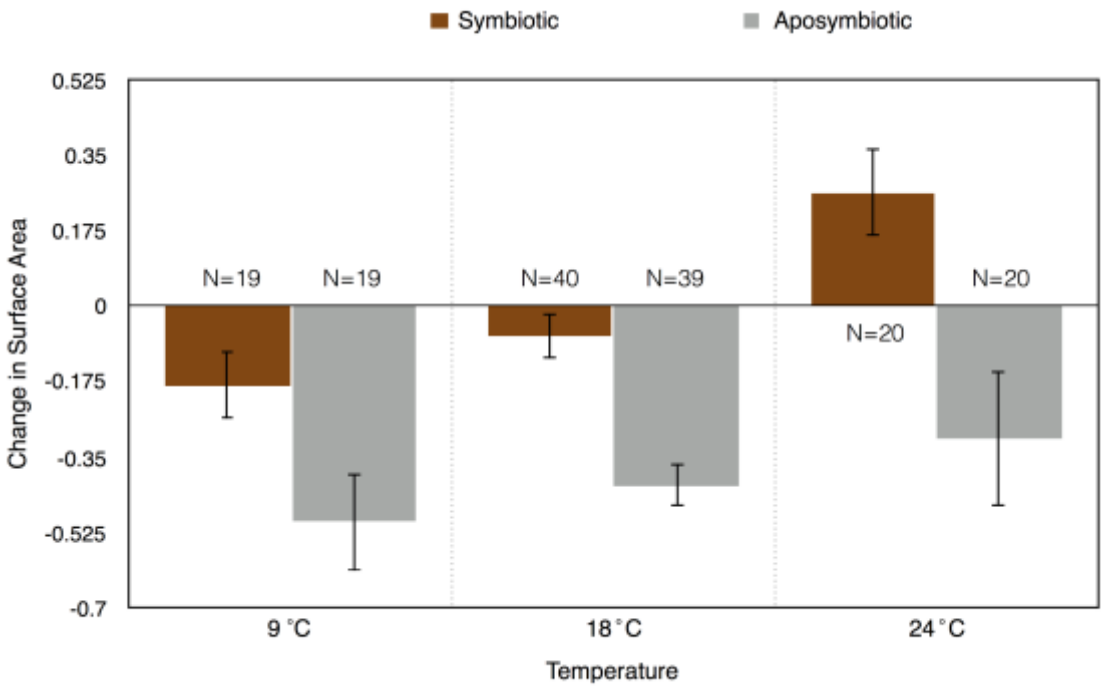

Figure 2.3. Change in wound surface area after 75 days normalized over the initial wound surface area. Values were measured from aligned photographs by dividing the final wound surface area at Day 75 by the initial wound surface area at Day 0. Negative values indicate an increase in wound size while positive values indicate a decline in wound size. Error bars represent standard error.

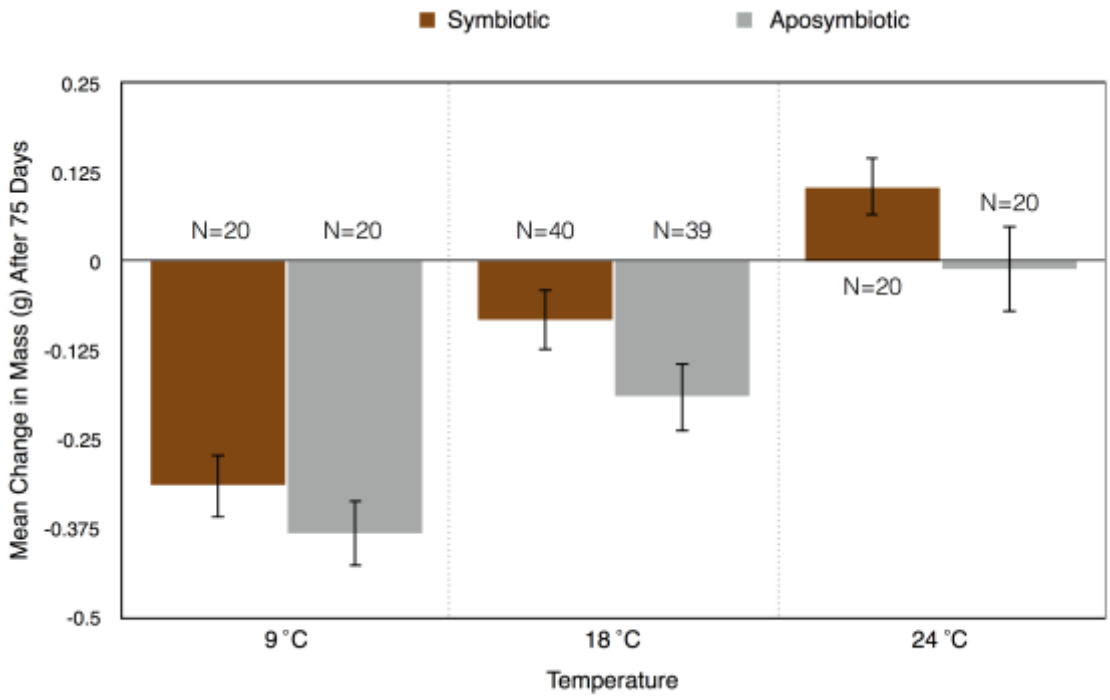

Figure 2.4. Mean change in colony mass 75 days after wounding. Values were calculated by subtracting the final mass of each colony from its post-wound mass. Error bars represent standard error.

Table 2.5. Laplace-approximated generalized linear mixed model for surface area (AIC 218.8). For fixed effects, ** indicates significance at $\alpha < 0.001$, * indicates significance at $\alpha = 0.05$, $^{+}$ indicates significance at $\alpha = 0.1$.

Effect	Estimate	Standard Error	DF	T-Value	P-Value
Intercept[#]	-0.5382	0.1138	136	-4.7289	<0.0001**
Symbiont State (S)	0.3977	0.0670	136	5.9463	<0.0001**
18°C	0.0908	0.1347	19	0.6737	0.5086
24°C	0.2822	0.1588	18	1.7761	0.0918[+]

[#]Rooted under Aposymbiotic and 9°C conditions

Effect	Estimate	Standard Error	DF	T-Value	P-Value
Intercept[#]	-0.0497	0.0860	136	-0.5774	0.5646
Symbiont State (A)	-0.3977	0.0670	136	-5.9463	<0.0001**
9°C	-0.0908	0.1347	19	-0.6737	0.5086
24°C	0.1914	0.1404	19	1.3631	0.1888

[#]Rooted under Symbiotic and 18°C conditions

Table 2.6. Laplace approximated generalized linear mixed model for growth (AIC -8.535). ** indicates significance at $\alpha < 0.001$, * indicates significance at $\alpha = 0.05$, $^{+}$ indicates significance at $\alpha = 0.1$.

Effect	Estimate	Standard Error	DF	T-Value	P-Value
Intercept[#]	-0.2686	0.0569	133	-4.7214	<0.0001**
Symbiont State (S)	0.1073	0.0322	133	3.3317	0.0011*
18°C	0.1700	0.0673	19	2.5258	0.0206*
24°C	0.2364	0.0794	19	2.9784	0.0077*

[#]Rooted under Aposymbiotic and 9°C conditions

Effect	Estimate	Standard Error	DF	T-Value	P-Value
Intercept[#]	0.0087	0.0426	133	0.2040	0.8387
Symbiont State (A)	-0.1073	0.0322	133	3.3317	0.0011*
9°C	-0.1700	0.0673	19	-2.5258	0.0206*
24°C	0.0664	0.0698	19	0.9516	0.3533

[#]Rooted under Symbiotic and 18°C conditions

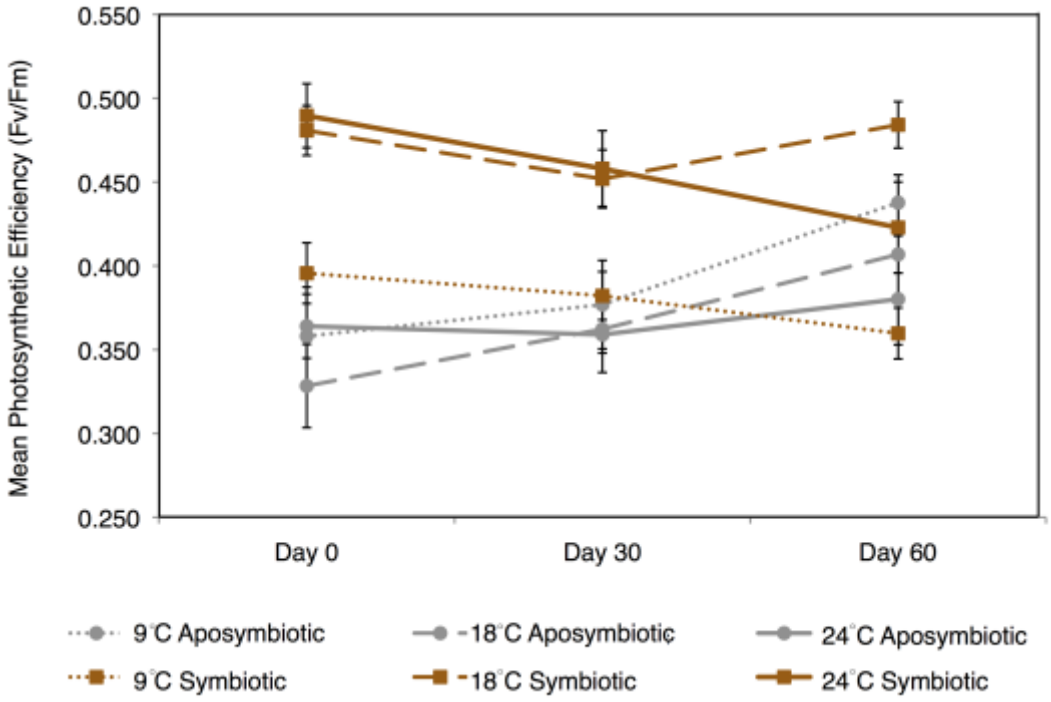

Figure 2.5. Mean photosynthetic efficiency (F_v/F_m) as measured via pulse-amplitude modulated fluorescence (Walz JUNIOR-PAM). Error bars represent standard error. For all 9°C and 24°C groups, N=20; N=40 for 18°C symbiotic corals and N=39 for 18°C aposymbiotic corals.

Table 2.7. REML-fitted generalized linear mixed model for photosynthetic efficiency (AIC -678.4). Significance (*) assumed from t-values (DF= 452) at α= 0.05.

Effect	Estimate	Standard Error	T-Value
Intercept[#]	0.3292	0.0220	14.950*
Symbiont State (S)	0.1569	0.0228	6.877*
Symbiont State (A): Temperature (9°C)	0.0342	0.0370	0.925
Symbiont State (S): Temperature (9°C)	-0.0926	0.0254	-3.652*
Symbiont State (A): Temperature (24°C)	-0.0048	0.0328	-0.145
Symbiont State (S): Temperature (24°C)	-0.0044	0.0260	-0.171
Symbiont State (A): Time	0.0012	0.0003	4.239*
Symbiont State (S): Time	-0.0005	0.0003	-1.940*

[#]Rooted under Aposymbiotic and 18°C conditions

Effect	Estimate	Standard Error	T-Value
Intercept[#]	0.3634	0.0318	11.414*
Symbiont State (S)	0.1569	0.0228	6.877*
Symbiont State (A): Temperature (18°C)	-0.0342	0.0370	-0.925
Symbiont State (S): Temperature (18°C)	0.0926	0.0254	3.652*
Symbiont State (A): Temperature (24°C)	-0.0390	0.0413	-0.942
Symbiont State (S): Temperature (24°C)	-0.0881	0.0298	2.958*
Symbiont State (A): Time	0.0012	0.0003	4.239*
Symbiont State (S): Time	-0.0005	0.0003	-1.940*

[#]Rooted under Aposymbiotic and 9°C conditions

temperatures, a greater proportion of symbiotic corals developed new tissue at the wound site and went on to develop full polyps. Likewise, regardless of temperature, symbiotic corals lost less mass and less tissue area at the lesion site after wounding (to the point of partially to fully closing lesions at 24°C). Therefore, symbiotic corals proved more successful at resisting wound expansion and achieving wound closure for single polyp lesions. These results are consistent with previous studies, which suggested that symbiotic colonies of *Astrangia poculata* may be able to recover a higher proportion of multipolyp wounds from small pockets of residual tissue (DeFeilippo *et al.* 2016). Additionally, wounding experiments on another temperate and facultatively symbiotic coral, *Oculina patagonica* (Fine et al 2001), demonstrated a similar advantage to symbiosis, whereby the percentage recovery of lesions was greater in unbleached colonies than partially bleached or fully bleached (which did not recover at all) colonies (Fine *et al.* 2002).

The positive effect of symbiosis on healing observed here could be attributed to a number of benefits conferred to the corals by their symbiotic partners, including (1) higher energy reserves and tissue content at the time of wounding, (2) added energy availability during healing due to active photosynthesis, or (3) potential direct symbiont contribution to the healing

pathway (Fine *et al.* 2002). Because we also found that aposymbiotic polyps can switch partially or fully to a symbiotic state—and that these switches did not significantly impact the colony's ability to heal or grow—it is possible that symbiotic advantage accrues from a long-term association. Alternatively, a related study on the facultatively symbiotic *O. patagonica* (Fine *et al.* 2002) determined that carbon can be preferentially translocated to recovering tissue from a distance of 4–5 cm away; however, translocation only occurs in fully unbleached (and not partially bleached, 30–80%) colonies. This suggests a bleaching threshold (or a minimum density of *Symbiodinium* spp.) below which colonial integration and resource translocation is disrupted. There could also be an energetic cost to symbiont acquisition that overcomes the potential immediate energy gain from photosynthesis (Hill & Hill 2012). In tropical corals, which rely more heavily on photosynthesis to supply their nutritional needs, this disparity in healing ability between the symbiotic and aposymbiotic states could have significant impacts on coral health, particularly after bleaching. Even after returning to a full symbiont load, the diminishment of energetic reserves that results from a prolonged period of bleaching could undermine wound recovery for an extended period of time (Meesters & Bak 1993). This could compound the impact of bleaching and elevate post-bleaching mortality rates.

While our study does not directly address the possible advantages of a facultatively symbiotic life history, it does raise some important questions about the costs, benefits, and dynamics of the coral–algal symbiosis. While symbiosis clearly enhanced healing initiation, wound closure, and the development of full polyps in the current study, naturally occurring, aposymbiotic colonies of *A. poculata* are abundant in the field (Dimond *et al.* 2013). Furthermore, while symbiont state can be manipulated, switching between symbiont states does not appear to be common in nature (Dimond and Carrington 2008). The prevalence of aposymbiotic colonies in nature therefore suggests a cost to maintaining a high density of *Symbiodinium* that outweighs the observed advantages of the symbiotic state on colony health and recovery. Dimond *et al.* (2013) suggested that this cost may be most pronounced at cold, winter temperatures when colonies are dormant. In winter, all colonies experience a net loss of tissue, but aposymbiotic colonies lose less tissue than symbiotic colonies (Dimond *et al.* 2013). Thus, while symbiotic colonies have enhanced healing potential in summer, they may also need to compensate for greater tissue loss during the winter.

Environmental temperature had a direct effect on tissue loss and replacement in this experiment, regardless of symbiotic state. At 9°C, a natural winter temperature, both aposymbiotic and symbiotic colonies experienced

greater tissue loss at the wound site and lost more total mass over time than at 18°C (a temperature more typical of summer) or 24°C (a temperature not typically encountered by *A. poculata* in Rhode Island). Similarly, the smallest statistical difference between symbiotic and aposymbiotic colonies occurred at 9°C, as colonies of both symbiont states had low rates of wound recovery; these cold-exposed colonies were less likely to develop new tissue at the wound site, and no colonies were able to successfully complete the regeneration process. These results are consistent with previous studies that found temperature to be a major driver of calcification and growth in both obligate and facultative zooxanthellate and azooxanthellate corals (Jacques *et al.* 1983, Miller 1995, Marshall & Clode 2004, Edmunds 2005, Dimond *et al.* 2013). However, it should be noted that growth and regeneration may be unrelated or even competing life traits, particularly in times of stress (Denis *et al.* 2013). The drop in healing initiation, healing completion, and colony mass likely derives from a significant decline in photosynthetic efficiency with decreasing temperature as well as a potential decrease in oxidative respiration below 11.5°C (Jacques *et al.* 1983). Previous studies (Jacques *et al.* 1983, Dimond *et al.* 2013) have noted a state of metabolic dormancy in *A. poculata* below 10°C, characterized by the retraction of polyps into their calices and the inability to feed. Interestingly, in our study, all colonies at 9°C were actively feeding over

the course of the experiment, potentially explaining the ability of some colonies to exhibit some healing despite their potentially reduced metabolism and lack of energetic input from photosynthesis. Additionally, while 9°C represents a typical winter temperature for this habitat, it is far from the lowest temperature encountered by wild colonies of *A. poculata* (0.3°C, NOAA Tides & Currents, Newport, RI: site 8452660). Therefore, as documented by Dimond *et al.* (2013), it is possible that quiescence could have a significant and inverse impact on healing with regards to symbiont state than observed in this study.

In contrast to 9°C, colonies at 24°C demonstrated the greatest wound recovery, despite experiencing a temperature outside the typical range of their natural habitat (which ranged from 0.3 to 23°C in 2014 [the year of this study]). Therefore, for this coral, these data support that survivability and, therefore, habitat range are more likely being limited by exposure to cold, winter temperatures than prolonged exposure to very warm summer temperatures (Dimond *et al.* 2013).

One hypothesis for the observed increase in healing and survivability by symbiotic corals is increased photosynthetic efficiency. Over time, there was an increase in photosynthetic efficiency in aposymbiotic colonies. Surprisingly, there was an inverse relationship with temperature (i.e. corals at 9°C experienced the

greatest rise in photosynthetic efficiency). However, this is very likely due to the fact that, in colder temperatures, colonies tended to lose more live tissue and, subsequently, bare skeletal scars were covered in adventitious algae. Additionally, the limited Gain settings on the JUNIOR-PAM may obscure fluorescence values when chlorophyll densities are low. Cold-treated symbiotic corals exhibited photosynthetic efficiency levels similar to aposymbiotic corals, but again, it is difficult to determine how much of this photochemical activity was generated by *S. psygmophilum* versus other potentially non-symbiotic photosynthetic organisms. *S. psygmophilum* is a cold-tolerant species whose photosynthetic efficiency peaks between 18 and 25°C and reaches a minimum (but does not cease altogether) at 10°C (Thornhill *et al.* 2008). Following this pattern, symbiotic corals at 18 and 24°C demonstrated higher levels of photosynthetic activity, although warm-treated corals (24°C) seemed to experience a reduction in photosynthetic efficiency over time.

A. poculata is a gonochoristic coral (Peters *et al.* 1988), and production of gametes occurs at warmer temperatures. Given the cost of producing gametes, and the generally greater cost of producing eggs relative to sperm (Holcomb *et al.* 2012), it is possible that corals at warmer temperatures might experience a trade-off between gamete production and healing, and this trade-off might differ

between males and females. However, because gametes can only be identified and quantified using destructive methods, we were unable to investigate the potential impact of gamete production on recovery without producing additional wounds, which would have confounded our experiments. We hypothesize that (1) wounds may confer a loss in fecundity, (2) gamete production may incur a cost to lesion recovery, or (3) reproductive dynamics promote a synergistic loss for both tissue recovery and fecundity (Rinkevich 1996).

Wound healing is a dynamic process impacted by a number of different environmental and biological factors. In addition to symbiotic state and temperature, lesion healing is affected by the perimeter to surface area ratio of the wound (Van Woesik 1988) as well as by the size of the lesion (Rotjan & Lewis 2008) and the size of the colony (Meesters *et al.* 1996). However, the influences of these physical parameters may vary by species and developmental timing (Bak 1983, Meesters *et al.* 1992, 1997, Oren *et al.* 1997, Van Woesik 1998). One previous study found that 'Phoenix Effect' recovery, whereby tissue is regenerated from within the calice rather than across wound edges, is the primary mode of recovery in *A. poculata* (DeFilippo *et al.* 2016). A similar pattern of recovery was observed in the experimentally wounded colonies in our trials. The wounds inflicted in this experiment most closely resembled those created through colony breakage or

corallivory, where regions of both skeleton and tissue are removed. In the field, colonies of *A. poculata* are most often abraded by foliose algae. Colony morphology is significantly impacted (flattened) by repeat interactions in regions with high macroalgal density (Grace 2004). While no predators have yet been characterized in the field for this coral, its ability to recover from such extremes (deep and well cleared of residual tissue) demonstrates its utility as a laboratory model for these studies.

Here, we have demonstrated that wound recovery is affected by symbiont state and temperature in a facultatively symbiotic coral. Comparable experiments cannot be conducted in tropical corals because elevated temperatures induce bleaching, and tropical corals cannot exist in a stable aposymbiotic state. By allowing us to decouple 2 key parameters that are conflated in tropical corals, *A. poculata* can provide unique insight into how particular biological and environmental states or stressors may impact coral health. While the study of temperate corals offers limited direct comparisons to tropical corals in their metabolism and physiology, it is likely that core mechanisms of the molecular stress response machinery are deeply conserved. Additionally, we can exploit the wide environmental tolerances of this temperate coral to investigate how a range of stressors and their intensities can affect coral health under non-lethal conditions.

Indeed, determining the threshold for lethal stress is a critical area of study; using temperate corals in controlled laboratory studies may yield valuable insights into the effects of synergistic stressors, and the relative role of symbiosis.

2.6 ACKNOWLEDGEMENTS

This work was funded by the PADI foundation, the Boston University Marine Program, and the New England Aquarium. We would like to thank Kiki Ballotti, Georgie Burruss, Nicholas Lawrence, Samantha Pelletier, Aaron Pilnick, and Ryan Schosberg for assistance with photography and data collection. We are also grateful to Tasia Blough, Julio Camperio-Ciani, Gregory Coote, Lukas DeFilippo, Corbin Kuntz, Georgia Luddecke, Katrina Malakhoff, Jessie Matthews, and Matthew Tohl for their roles in the husbandry and maintenance of coral specimens. The authors respectfully appreciate the input of the anonymous reviewers that contributed to the improvement of this manuscript.

2.7 PUBLICATION

Burmester, EM, JR Finnerty, L Kaufman, R Rotjan (2017) Temperature and symbiosis affect lesion recovery in experimentally wounded temperate corals. *Mar. Ecol. Prog. Ser.* 570: 87-99

Chapter 3

INTERPLAY BETWEEN FOOD AVAILABILITY AND SYMBIONT STATE AFFECT TOTAL COLONY HEALTH AND WOUND RECOVERY IN TEMPERATE CORALS

3.1 ABSTRACT

For animals that harbor photosynthetic symbionts within their tissues, such as corals, the different relative contributions of autotrophy versus heterotrophy to organismal energetic requirements have direct impacts on fitness. This is especially true for facultatively symbiotic corals, where the balance between host-caught and symbiont-produced energy can be altered substantially to meet the variable demands of a shifting environment. In this study, we utilized a temperate coral-algal system (the northern star coral, *Astrangia poculata,* and its photosynthetic endosymiont, *Symbiodinium psygmophilum*) to explore the impacts of nutritional sourcing on the host's health and ability to heal wounds, as well as host and symbiont performance by controlling each colony's access to food. For fed and starved colonies, wound healing and total colony tissue cover were differentially impacted by heterotrophy and autotrophy. There was an additive impact of nutritional and symbiotic states on a coral's ability to initiate healing, but a greater influence of symbiont state on the success (full development) of

recovery and the surface area recovery of lost tissue at the lesion site. On the other hand, regardless of symbiont state, fed corals maintained a higher overall colony tissue cover. This analysis also suggests an impact of food ability on host behavior (polyp extension) and on the photosynthetic ability of *Symbiondinium* endosymbionts. Overall, we determined that the impact of nutritional state and symbiotic state varied between biological functions, suggesting a diversity in energetic sourcing for each of these processes.

3.2 INTRODUCTION

The differential utilization of alternative energy sources can directly influence an organism's growth, reproduction, behavior, and survival. In organisms that can obtain carbon from multiple qualitatively different sources, energetic dynamics can be particularly complex. For example, corals harboring photosynthetic algal symbionts (*Symbiodinium*), can obtain energy through transfer of photosynthate from the endosymbiont or by predation on plankton (Grottoli *et al.* 2006; Palardy *et al.* 2008). When obtaining energy via photosynthesis, the coral holobiont (host animal plus symbionts) is functioning as an autotroph, and when obtaining its energy via predation, it is functioning as a heterotroph.

However, corals often obtain energy through multiple sources simultaneously, and there may be interactions between autotrophy and heterotrophy.

For tropical corals in well-lit, shallow environments, host colonies can meet or exceed their metabolic needs through transfer of photosynthate from *Symbiodinium spp.* (Muscatine 1990). It has been hypothesized that these corals prey on zooplankton mainly to supplement the energy they receive from the endosymbiont and to supply essential nutrients (such as phosphorus and nitrogen; Johannes *et al.* 1970; Tanaka *et al.* 2006) and that prolonged heterotrophic compensation may be a stress response that increases resilience under conditions unfavorable to autotrophy (Hughes and Grottoli 2013, Levas *et al.* 2015). Additionally, heterotrophic feeding can enhance growth rate, protein and chlorophyll concentrations, as well as calcification rates in daylight and in darkness (Ferrier-Pagès *et al.* 2003, Houlbrèque *et al.* 2003). However, the degree to which a colony can supplement lost photosynthetic resources appears to vary by species (Anthony and Fabricius 2000, Grottoli *et al.* 2006), and recent studies have suggested that the balance between energy sources might not be fixed (Piniak 2002).

In the temperate realm, a highly variable environment can lead to a wide variety of flexible feeding strategies, such as those employed by facultatively

symbiotic corals like *Astrangia poculata* (= *A. danae*; Peters *et al.* 1988), *Oculina patagonica* (Fine *et al.* 2001), and *Oculina arbuscula* (Leal *et al.* 2014). Heterotrophy has many effects on the metabolism and physiology of these facultatively symbiotic temperate corals: (1) it can mitigate thermally-induced "bleaching" (a sharp reduction in symbiont density caused by exposure to elevated temperatures; Aichelman *et al.* 2016); (2) it increases nitrogen uptake and excretion (Szmant-Froelich & Pilson 1984); (3) it increases calcification and growth (Jacques & Pilson 1980; Jacques *et al.* 1983; Miller 1995); (4) it reduces damage from sedimentation (Peters and Pilson 1985). Symbiotic state can impact the effects of heterotrophy, although the presence of photosynthetic symbionts does not preclude heterotrophy. For example, symbiotic colonies of *A. poculata* actually retained more carbon (^{14}C) from heterotrophic sources than aposymbiotic colonies (Szmant-Froelich 1981), and there is evidence for transfer of photosynthetic carbon to coral host tissue (Schiller 1993). Additionally, *S. psygmophilum* in fed colonies fix carbon more efficiently (but translocate less ^{14}C) than their starved counterparts (Szmant-Froelich 1981). This suggests a potentially higher degree of interconnectivity between energy strategies than previously assumed (Piniak 2002), as well as a complex dynamic between simultaneous autotrophy and heterotrophy.

The northern star coral *Astrangia poculata* has an expansive range along the east coast of North America, from Florida and the Gulf of Mexico to southern Massachusetts (Dimond & Carrington 2007; Dimond *et al.* 2014). In nature, these corals can exist in one of three basic symbiotic states with *Symbiodinium psygmophilum* (Lajeunesse *et al.* 2012): fully symbiotic corals appear brown; aposymbiotic corals harbor far fewer symbionts, and they appear white; symbiont density can also vary from polyp to polyp, producing a mottled, mixed colony comprising both white and brown polyps (Cummings 1983). Unlike in tropical corals, in *A. poculata*, the aposymbiotic state is not the result of stress (i.e. bleaching); white colonies of *A. poculata* are as "healthy" as brown colonies and can persist indefinitely in nature (Grace 2004). Their relatively low density of *S. psygmophilum* is actively maintained by the regular expulsion of the symbiont (Dimond & Carrington 2008). Regardless of symbiont state, temperate colonies rely heavily on heterotrophy (Szmant-Froelich & Pilson 1984; Farrant *et al.* 1987), with symbiont density only explaining an estimated 23% of growth in the field (Dimond & Carrington 2007).

This study investigates the interaction of feeding and symbiotic state on wound healing in *Astrangia poculata*. As corals regularly incur abrasions and wounds, wound healing is critical to resilience, and for this reason, there is a

growing history of wound-healing studies on corals in the laboratory and field (for example: Meesters *et al.* 1994, Downs *et al.* 2005, Edmunds 2009, Work & Aeby 2010). There is ample evidence to suggest that both lesion recovery and colony maintenance are energetically costly activities that are often in conflict with each other and other critical physiological functions such as reproduction, calcification, and growth (Richmond 1987; Ward 1995; Rinkevich 1996; Anthony *et al.* 2002; Rotjan and Lewis 2009). In addition, the process of lesion repair can require a high degree of colonial energy integration, which can vary by wound and colony characteristics (Oren *et al.* 2001). Given the premium that wound-healing places on the acquisition of energy and the redistribution of energy throughout the colony, delineating the roles of host and symbiont nutrition to regeneration and tissue maintenance is critical to our understanding of coral recovery and resilience.

Because of its flexibility and tractability, *A. poculata* makes an ideal study organism for investigating the dynamics between energy sourcing and colony health. This study uses (1) small-scale wound lesion and total colony tissue recovery, (2) foraging behavior, and (3) symbiont density and photosynthetic efficiency metrics to assess colony health and stress response in the presence and absence of both autotrophic and heterotrophic nutritional strategies in naturally-occurring symbiotic and aposymbiotic *A. poculata* colonies.

3.3 MATERIALS AND METHODS

3.3.1 Collection and husbandry

Colonies of *Astrangia poculata* in both symbiotic or aposymbiotic states were collected between 6-10m at Fort Wetherhill State Park in Jamestown RI (41 28°40°° N, 71 21°34°° W) in Summer 2014. Collected specimens were housed at the New England Aquarium and provided lighting in 10-hour cycles via T5 HO fluorescent lighting fixtures (Hamilton Technology, Gardena, CA, Aruba Sun T5-V Series) as well as filtered, UV-treated seawater from the Boston Harbor. Light levels (PAR) and water quality (pH, nitrate, ammonia, alkalinity) were measured weekly to ensure consistent water quality parameters. All experimental colonies were acclimated at 18°C for at least two weeks before the start of experimentation. During this acclimation period, colonies were given individualized, daily *ad libitum* feedings of a mixture of 50g/L of frozen copepods (JEHM Co., Inc.) using a pipette.

3.3.2 Experimental setup and nutrition manipulation

Symbiotic and aposymbiotic colonies were randomly assigned in approximately size-matched pairs, and these pairs were subsequently sorted into one of four treatment groups: fed (non-wounded control or wounded) or starved

(non-wounded control or wounded). In order to control for differences in colony size, colony mass was recorded, and no significant differences were found between groups (ANOVA, $F_{(3,220)} = 1.3864$, $P = 0.2478$; average mass – 6.34 (± 0.25 SEM)). Overall, twenty-eight paired symbiotic and aposymbiotic colonies were included in each treatment group (resulting in a total of 224 corals). Specimens were housed on a raised, gridded plastic rack such that paired colonies were adjacent, but kept at a distance of at least 10 cm, to ensure consistent lighting and surrounding flow for both symbiont types without risk of intercolonial aggression. All colonies were acclimated to their nutritional treatment condition for three days prior to the start of the experiment so that starved colonies began the trial period with minimum potential benefit of stored nutrition from a previous feeding. During the course of the entire eight-week (60 day) experiment, the starved group received no food while the fed treatment continued to receive *ad libitum* offerings of frozen copepods (at a concentration of 50g/L/feeding). Colonies were carefully observed during these feedings to ensure that each polyp mouth on each colony (1) was given a direct feeding opportunity and (2) demonstrated contraction due to food capture.

3.3.3 Experimental wounding

Colonies were experimentally wounded after the 3-day treatment acclimation period. A single polyp and the surrounding connective tissue (coenchyme) was removed from the center of the colony (to control for wound position) using a scalpel before the wound site was cleaned with seawater via Waterpik®. Mean wound size was 34.28 mm^2 (+/- SE 2.27) with no statistical difference in wound size between groups (ANOVA, $F_{(3,108)} = 0.9400$, $P = 0.4240$).

3.3.4 Assessing wound recovery

As demonstrated by Burmester *et al.* (2017), wound recovery was assessed using three different metrics after 60 days: (1) determination of unambiguous developmental landmark stages of recovery ("healing initiation:" no recovery, undifferentiated tissue, the formation of non-functional tentacle nubs, and full polyps), (2) "healing completion:" the proportion of colonies in full recovery as determined by the formation of fully functional tentacles, and (3) the change in wound surface area. Colonies were observed under a Leica M165FC stereomicroscope after wounding and at the close of the experiment (60 days) as well as over 8 observational time-points (5, 10, 15, 20, 25, 30, 40, 50 days) over the course of the experiment. Photographs for each of these time-points were

calibrated so that magnification as well as colony angle and position were consistent for each colony across all photographs. These photographs were used to determine the developmental landmark recovery stage of colonies after 60 days as well as the wound surface area at Days 0 and 60. Wound surface area was measured three times using Leica M165FC software, using the resulting mean as the representative surface area of that colony for each time-point. Proportional recovery (or tissue loss) was calculated as the difference between Day 0 and Day 60 divided by the initial (Day 0) surface area.

3.3.5 Colony-wide tissue surface area

Colonies were photographed in a shallow dish of seawater with a size standard from 6 different angles (top, base, and over 4 sides) at Day 0 and Day 60. Each colony was labeled at the skeletal base with a distinct honey-bee tag (betterbee.com) using super glue, and the location of this tag was used to enforce directionality to each of the colony's 4 sides. All 6 photographs for each colony at both time points were used to manually generate a composite image of the entire colony. To do this, photographs were carefully reviewed for regions of the colony that were included in multiple angles, and only the single photographic angle that best represented that region were used for analysis. For the base of the colony,

only obvious areas of live tissue growth (and not the entire surface area) were included. The composite area of best represented regions across all photographs was termed the "standard area" for a colony. Both the standard area and surface area of living tissue within the designated standard area ("live area") using Image J (NIH). We calculated the proportional live tissue cover (live: standard area) for each colony at Day 0 and Day 60, and the proportional difference in total colony surface area was determined as the difference between the initial and final proportional live tissue cover.

3.3.6 Polyp activity

Each week, as a measure of behavioral change and foraging effort, polyp activity was determined using a seven-scale extension matrix (Figure 1): A score of 0 indicated that all polyps were retracted (Figure 1: A, D), while a score of 6 indicated the full extension of all polyps within a colony (Figure 1: B, E). Scores between 0 and 6 specified intermediate states of increasing polyp extension (Figure 1: B, E).

For fed corals, overall polyp state for each colony was measured prior to the introduction of a stimulus (i.e. before feeding) and a half hour after feeding. Polyp extension was determined for starved corals at the same time points;

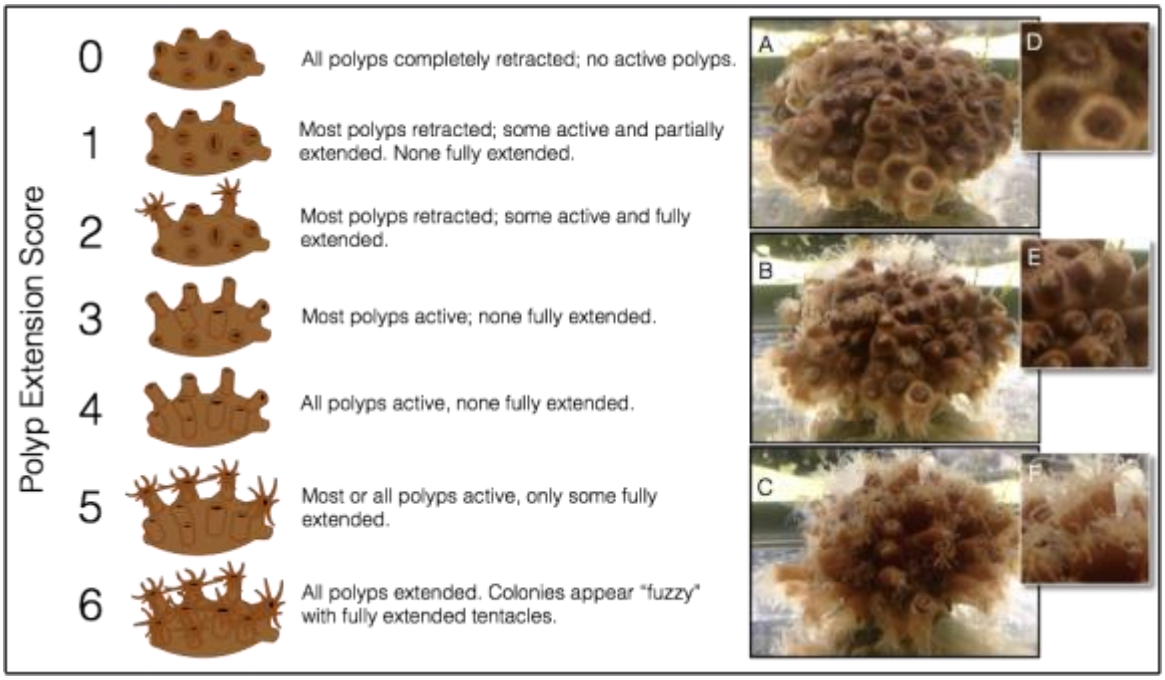

Figure 3.1. Polyp extension matrix for *Astrangia poculata*. Scores ranged from 0-6, with 0 indicating all polyps were fully contracted (A, D) and 6 indicating all polyps are fully extended (C, F). Scores between 1 and 5 represent an intermediate state of polyp extension (B) where different proportions of polyps within a colony are fully contracted (D), active but not fully extended (E), and fully extended (F).

however, no food-related stimulus was applied to this treatment group. Therefore, polyp extension values were recorded twice for both treatment groups, but only the activity of fed colonies was observed in response to a feeding stimulus. All measurements were taken within the same two-hour range (1100h and 1300h) for each time point to avoid confounds inflicted by diel behavioral cycles.

3.3.7 Quantification of chlorophyll density

Symbiont state was determined visually using color as a proxy. For this

species, host coral tissue is translucent, bearing no pigment and causing polyps to appear white when in the aposymbiotic state. Because colonies in a functional symbiosis (with a density of greater than 10^6 cells/cm^3) with *Symbiodinium psygmophilum* appear brown in color, Dimond and Carrington (2007) showed that it is possible to use polyp color as a proxy for chlorophyll density for *A. poculata*. Following this method, colonies were photographed prior to experimentation (Day 0) and at the close of the trial (Day 60) against red-green-blue (RGB) color standards. Photos were analyzed using custom scripts on Matlab R2007b (The Mathworks, Natick, MA), whereby the average of five randomly chosen polyps in a colony was used as the final measurement for each color (red, green, and blue). RGB quantities were condensed to a single principle component (representing overall polyp color) via PCA using a correlation matrix with oblimin rotation. Component loadings were 0.917 for red, 0.721 for green, and 0.870 for blue at Day 0 and 0.898 for red, 0.774 for green, and 0.858 for blue at Day 60. Color PCA values were multiplied by -1 to more accurately depict data directionality, and the absolute value of the lowest value was added to all color measurements to normalize the data for comparison. As prescribed by Dimond and Carrington (2007) and demonstrated in DeFilippo *et al.* (2016), transformed PCA values were

calculated into chlorophyll density proxies with the equation $y = 0.044x^2 + 0.0335x$ ($R^2 = 0.89$). Photograph quality was not suitable for analysis for 60 corals at Day 0 and 35 colonies at Day 60 (due to lighting inconsistencies between colonies and their RGB standards), reducing the overall sample size to 164 specimens at Day 0 and 189 specimens at Day 60.

3.3.8 Photosynthetic efficiency

Photosynthetic efficiency (F_v/F_m) was measured every other week (Weeks 0, 2, 4, 6, 8) for each colony with a Walz Junior-PAM pulse-amplitude modulated fluorescence meter. After a thirty-minute acclimation to darkness, three polyps per colony were selected haphazardly, where photosynthetic efficiency was calculated as described in DeFilippo *et al.* (2016) and Burmester *et al.* (2017). Briefly, minimal fluorescence (F_0) was measured by exposing polyps to 6s of far-red illumination while dark adapted; subsequently, maximal fluorescence (F_m) was determined after exposing polyps to a 0.6s saturating pulse of 10,000 μmol m^{-2} s^{-1}. Maximum quantum yield (F_v/F_m) represents the change between maximal and minimal fluorescence over the maximal fluorescence (Suggett *et al.* 2010). The resulting F_v/F_m values were averaged for each individual at each time point to obtain a single representative value.

3.3.9 Statistics

All statistics were performed using stepwise generalized linear and logistic mixed models (GLMMs) on the lme4 (Bates *et al.* 2015) and nlme (Pinheiro *et al.* 2017) packages in R (R Core Team 2013). Model selection was based on Akaike's information criterion (AIC) scores, where the decision to include a new fixed effect variable or accept one iteration of a model over another required a reduction in AIC of at least 2 (Burnham & Anderson 2002). The simpler model was always chosen in the case of equal models (Burnham & Anderson 2002). Additionally, linear models were compared using maximum likelihood tests. For logistic models, odds ratios were calculated using exponentiated estimates. In order to control for the potential impacts of pseudo-replication that could result from housing multiple colony pairs in the same tank, we used tank as a random effect in all statistical analyses.

Healing initiation (measured as the proportion of colonies in any of the 3 landmark stages) and healing success (measured as the proportion of colonies that regenerated fully functional polyps) were tested using Laplace-approximated logistic GLMMs. The proportional change in wound surface area and total colony surface area were analyzed using Restricted Maximum Likelihood (REML)-fitted linear GLMMs. In order to test for the impacts of the treatment dependent

variables as well as independent variables such as lighting and morphological features of the colony and the wound itself, we used a stepwise analysis using nutritional state, symbiont state, mean photosynthetically active radiation (PAR), initial mass, and initial wound size as fixed effect variables for wound recovery models. For total colony surface area: nutritional state, symbiont state, initial mass, PAR, and wounding treatment were used as variables.

Chlorophyll density and polyp extension were analyzed using REML-fitted linear GLMMs over time with PAR, wounding treatment, nutritional state, initial mass, and symbiotic state as additional variables. In order to control for repeated measurements made on the same individuals over time, colony identity was nested within tank as a random effect. Photosynthetic efficiency was initially tested similarly; however, since time bore no statistically significant effect, a mean maximum quantum yield was calculated over time for each individual colony. Mean photosynthetic efficiency was analyzed using a REML-fitted linear GLMM using PAR, symbiont state, and nutritional state as fixed effect variables.

3.4 RESULTS

3.4.1 Assessing wound recovery

Both nutritional state and symbiont state played a significant role on healing initiation. After accounting for tank grouping using random effects, symbiotic colonies (31 of 56 colonies) were 3.021 times more likely than aposymbiotic colonies (18 of 56 colonies) to reach any of the three landmark developmental stages (undifferentiated tissue, tentacle nubs, or full polyps; Figure 2, Table 1). Likewise, nutritional state had a strong impact on healing success: fed colonies (34/56) were 4.692 times more successful than starved colonies (15/56; Figure 2). Both symbiont state and nutritional state (but not their interaction, PAR, initial mass, and initial wound size) were significant predictors of healing initiation (Table 1). Only symbiont state significantly impacted healing success (the formation of fully functional tentacles) according to GLMM analysis (Table 2). In order to adjust for the small sampling of aposymbiotic colonies with full polyp development (1/56 colonies, Figure 2), a second GLMM was performed on only the subset of symbiotic colonies. However, this model did not find nutritional state to be significant ($P = 0.07474$, Table 2), which could potentially derive from a lack of statistical power. Accounting for the tank random effect, symbiotic (7/56)

colonies were 8.013 times more likely than aposymbiotic colonies (1/56) to successfully complete the developmental recovery process (Figure 2).

Symbiont state, but not any other fixed effects (nutritional state, PAR, initial mass, and initial wound size or their interactions), was a significant predictor of proportional wound surface area recovery (Table 4). On average, only the symbiotic fed treatment group (mean +/- SEM: 0.0791 +/- 0.0968) exhibited wound recovery via a reduction in wound size (shown here as a proportional increase in live tissue surface area; Figure 3). Wound size increased over time for aposymbiotic colonies (mean +/- SEM: starved, -0.3416 +/- 0.0748; fed, -0.2183 +/- 0.0928) and starved, symbiotic colonies (-0.1836 +/- 0.0874; Figure 3). While no group demonstrated full recovery across all colonies, the greatest proportion (16/28 or 57.14%) of colonies with wound closure was for the symbiotic, fed treatment group. In the remaining groups, less than half of the wounded colonies exhibited live tissue recovery at the wound site: 9/28 (32.14%) for aposymbiotic fed, 8/28 (28.57%) for symbiotic starved, and 4/28 (14.29%) for aposymbiotic starved corals.

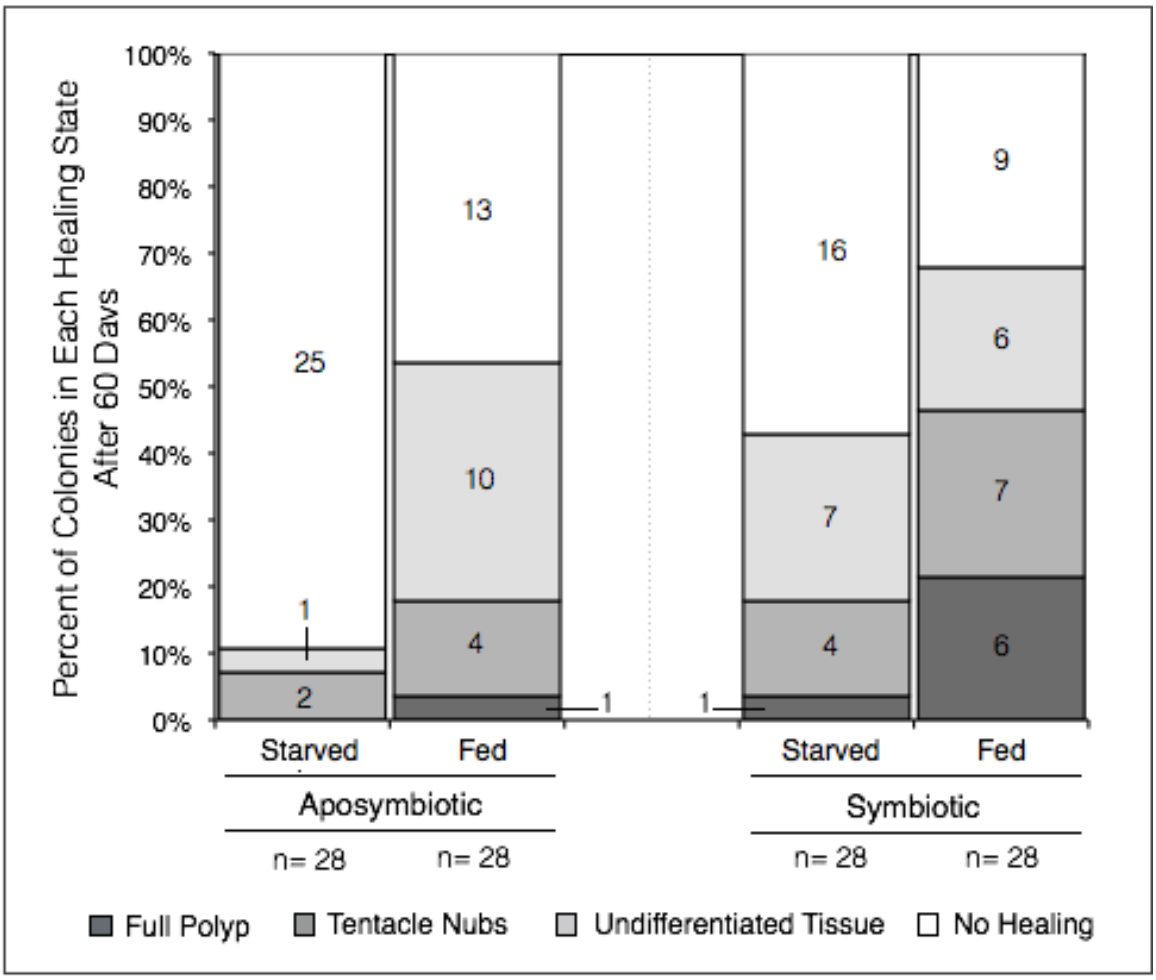

Figure 3.2. Proportion of colonies in landmark recovery stages (full polyp, tentacle nubs, undifferentiated tissue, or no healing) after 60 days. Bars in all shades of grey collectively represent healing initiation, while bars in dark grey represent developmental healing success. Numbers in bars signify total number of colonies in each stage.

Table 3.1. Laplace approximated generalized mixed logistic regression for healing initiation (AIC = 141.1). For fixed effects, ** indicates significance at $\alpha < 0.001$, * indicates significance at $\alpha = 0.05$.

Effect	Estimate	Standard Error	Z-Value	P-Value
Intercept	-0.08403	0.33976	-0.247	0.8047
Symbiont State (S)	1.10561	0.42719	2.588	0.0096*
Nutritional State (F)	1.54582	0.42838	-3.609	0.0003**

[#]Rooted under Aposymbiotic (A) and Starved (St) conditions

Table 3.2. Laplace approximated generalized mixed logistic regression for healing success (polyp formation) (AIC = 58.1). For fixed effects, ** indicates significance at $\alpha < 0.001$, * indicates significance at $\alpha = 0.05$.

Effect	Estimate	Standard Error	Z-Value	P-Value
Intercept	-4.099128	0.009418	-435.2	<0.0001**
Symbiont State (S)	2.081012	0.009417	221.0	<0.0001**

Table 3.3. Laplace approximated generalized mixed logistic regression for healing success (polyp formation) for symbiotic corals only (AIC = 43.7). For fixed effects, ** indicates significance at $\alpha < 0.001$, * indicates significance at $\alpha = 0.05$, $^{+}$ indicates significance at $\alpha = 0.1$.

Effect	Estimate	Standard Error	Z-Value	P-Value
Intercept	-1.2993	0.4606	-2.821	0.00479*
Nutritional State (F)	1.9966	1.1177	-1.786	0.07474^{+}

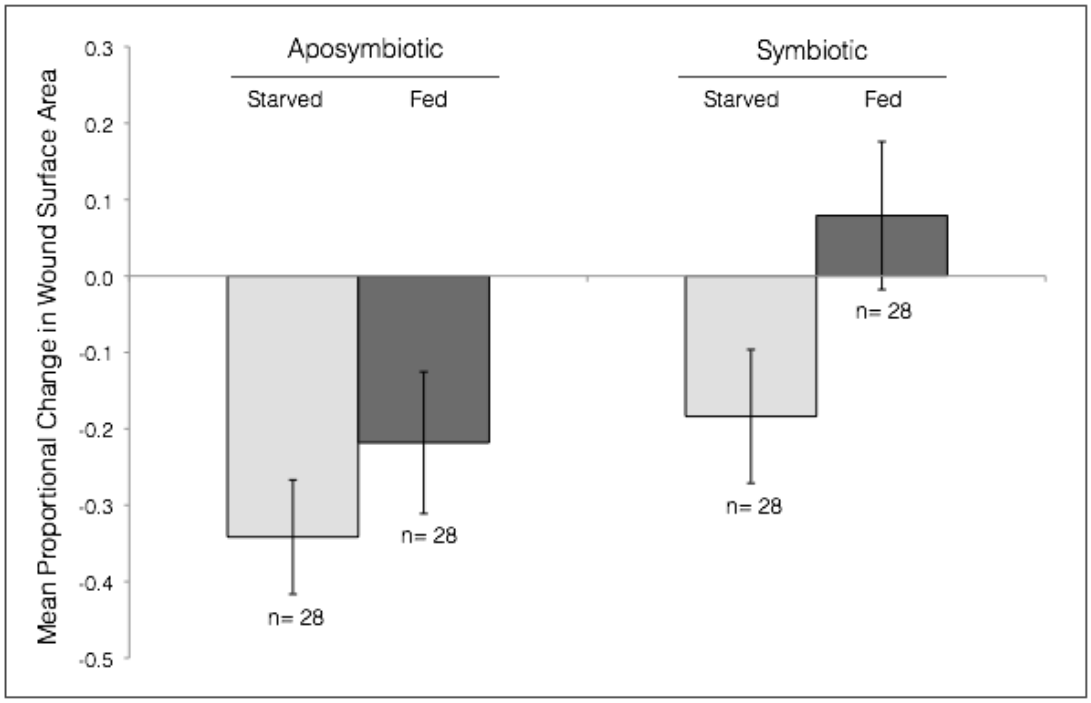

Figure 3.3. Mean proportional change in wound surface area 60 days after lesions were induced. Error bars signify standard error.

Table 3.4. REML-fitted linear mixed model for wound surface area (AIC 152.4). For fixed effects, ** indicates significance at $\alpha < 0.001$, * indicates significance at $\alpha = 0.05$.

Effect	Estimate	Standard Error	DF	T-Value	P-Value
Intercept	-0.2787	0.0956	103	-2.9142	0.0044*
Symbiont State (S)	0.2277	0.0810	103	2.8122	0.0059*

Table 3.5. REML-fitted linear mixed model for total colony surface area (AIC -354.9). For fixed effects, ** indicates significance at $\alpha < 0.001$, * indicates significance at $\alpha = 0.05$.

Effect	Estimate	Standard Error	DF	T-Value	P-Value
Intercept	-0.0755	0.0126	182	-6.0034	<0.0001**
Nutritional State (F)	0.0497	0.0173	6	-2.8729	0.0283*

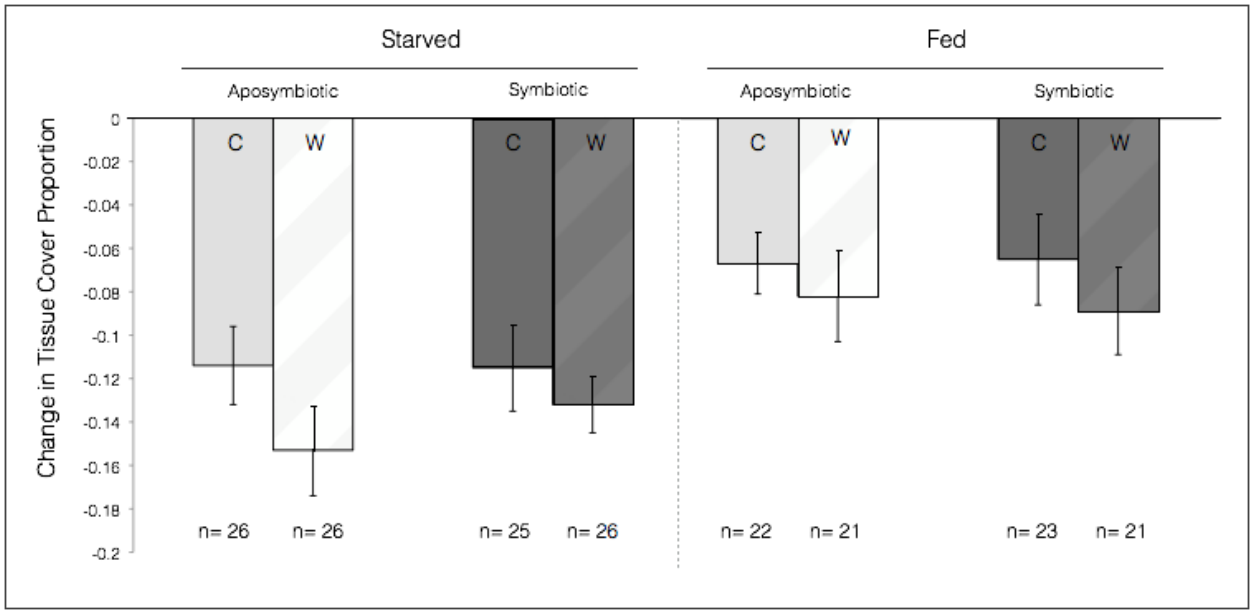

Figure 3.4. Mean proportional change in total colony tissue cover proportion after 60 days for control (C) and wounded (W) fed and starved colonies of different symbiont states (aposymbiotic, symbiotic). Error bars signify standard error.

3.4.2 Colony-wide tissue surface area

Overall, starved colonies (mean +/- SEM, -0.1253 +/ 0.0126) experienced a greater (nearly double) decline in proportional colony surface area than did fed colonies (mean +/- SEM, -0.0728 +/- 0.0138; Figure 4). According to the most parsimonious model, there was no significant impact of wounding treatment, symbiotic state, initial mass, or PAR; however, nutritional state did play a slight but significant role in predicting changes in total colony surface area (Table 5). Additionally, fed treatment groups experienced a higher proportion of colonies with increased total colony live tissue surface area (8/44 or 18.18% for symbiotic colonies; 7/43 or 16.28% for aposymbiotic colonies) than did starved colonies (3/51 or 5.88% for symbiotic colonies; 5/52 or 9.61% for aposymbiotic colonies).

3.4.3 Polyp activity

Fed colonies consistently exhibited higher polyp extension scores than did starved corals both before and after a stimulus was provided to fed colonies (Figure 5). For both pre- and post- stimulus models, wounding treatment, symbiotic state, PAR, and initial mass had no significant impact on polyp extension (Tables 6 & 7). The best models for both stimulus regimes selected nutritional state, time, and the interaction of time and nutritional state as

significant predictive fixed effects. In order to test for the impact of applying a food-related stimulus, an additional REML-fitted GLMM was performed on the subset of fed corals (pre- and post- stimulus). This model found both time and applied stimulus to be significant predictors of polyp extension (Table 8), whereby polyp extension varied over time but was consistently higher in colonies after food was supplied.

3.4.4 Quantification of chlorophyll density

Regardless of symbiotic state, there was no significant difference between fed and starved colonies in chlorophyll density. Symbiotic colonies had greater approximated chlorophyll density (ACD) (mean +/- SEM, 0.837 μg cm^{-2} +/- 0.016) than aposymbiotic colonies (mean +/- SEM, 0.347 μg cm^{-2} +/- 0.013) at all time points and under all experimental conditions. The most parsimonious model selected three significant fixed effects (symbiotic state, time, and the interaction of nutritional state and time) as well as one non-significant predictor (nutritional state, Table 9). This analysis is congruous with a variation in ACD between the initial (Day 0) and final (Day 60) measurements and a consistent decline in ACD over time amongst fed corals. The strongest predictor (by estimate), however, was symbiotic state (Table 9).

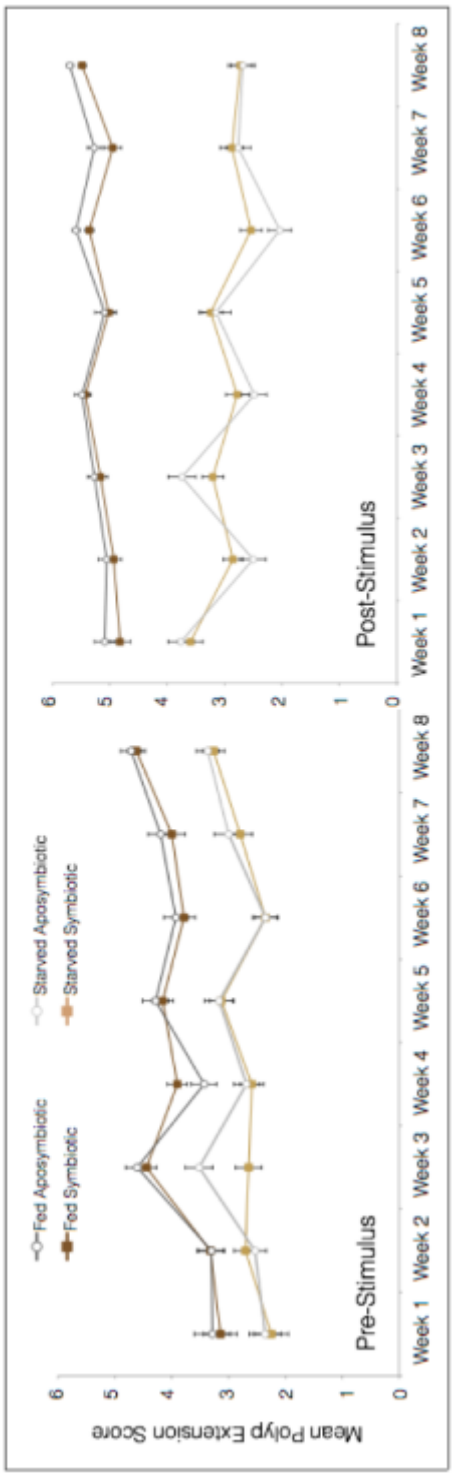

Figure 3.5. Mean polyp extension scores across a 60 day (8 week) period both before (pre-) and after (post-) a food stimulus had been supplied to the fed treatment group. Starved (symbiotic and aposymbiotic) colonies were provided no food stimulus.

Table 3.6. REML-fitted generalized linear mixed model for pre-stimulus mean polyp extension scores (AIC 5874.1). Significance (*) assumed from t-values (DF= 7) at α= 0.05.

Effect	Estimate	Standard Error	T-Value
Intercept	4.9416	0.1061	46.59*
Nutritional State (St)	-1.5248	-0.1517	-10.05*
Time	0.0643	0.0160	4.02*
Nutritional State (St): Time	-0.1718	0.0231	-7.45*

Table 3.7. REML-fitted generalized linear mixed model for post-stimulus mean polyp extension scores (AIC 5611.4). Significance (*) assumed from t-values (DF= 7) at α= 0.05.

Effect	Estimate	Standard Error	T-Value
Intercept	3.4621	0.1404	24.658*
Nutritional State (St)	-0.8249	0.2001	-4.123*
Week	0.1200	0.0210	5.727*
Nutritional State (St): Week	-0.0744	0.0300	-2.476*

Table 3.8. REML-fitted generalized linear mixed model for mean polyp extension scores (pre- and post-stimulus) for fed corals (AIC 5642.9). Significance (*) assumed from t-values (DF= 5) at α= 0.05.

Effect	Estimate	Standard Error	T-Value
Intercept	4.8161	0.0879	54.82*
Stimulus (Pre)	-1.2406	0.0572	-21.68*
Time	0.0934	0.0127	7.36*

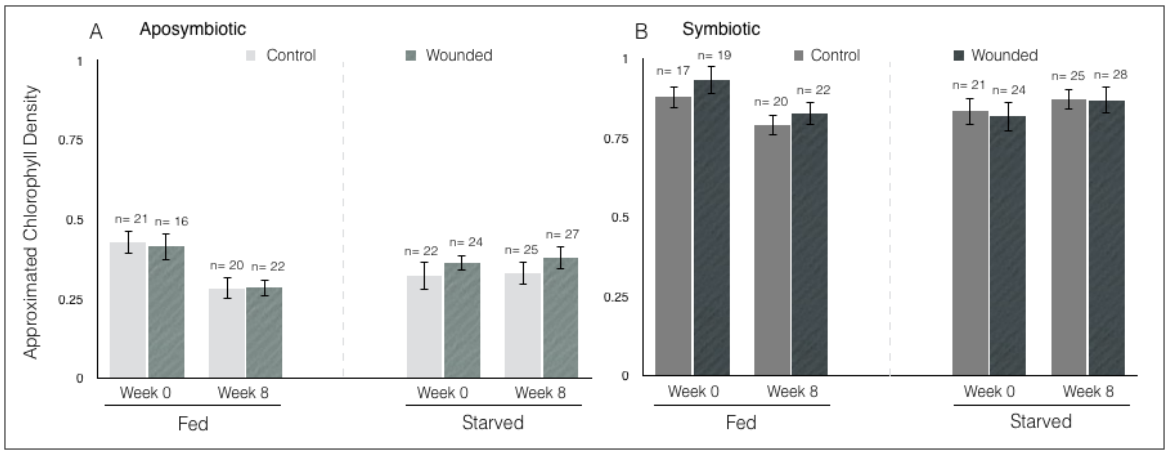

Figure 3.6. Mean chlorophyll density as determined by RGB color values. Error bars represent standard error.

Table 3.9. REML-fitted generalized linear mixed model for approximated chlorophyll density (AIC -239.93). Significance (*) assumed from t-values (DF= 8) at α= 0.05.

Effect	Estimate	Standard Error	T-Value
Intercept	0.4129	0.0223	18.494*
Symbiotic State (S)	0.4966	0.0202	24.601*
Nutritional State (St)	-0.0487	0.0268	-1.816
Week	-0.0149	0.0031	-4.856*
Nutritional State (St): Week	0.0108	0.0041	2.644*

3.4.5 Photosynthetic efficiency

Because time was not found to be a significant predictor of photosynthetic efficiency, we analyzed mean maximum quantum yield (F_v/F_m) across all five time points. Symbiotic, fed colonies exhibited significantly greater photosynthetic

efficiency (mean +/- SEM, 0.394 +/- 0.011) than all other groups at all time points (Figure 7). Starved, symbiotic colonies shared similar mean maximum quantum yields with aposymbiotic colonies s (symbiotic mean +/- SEM, 0.394 +/- 0.011; (aposymbiotic fed 0.382 +/- 0.009, starved: 0.364 +/- 0.007; Figure 7). Consistent with these results, the model with best support found symbiont state and the interaction between symbiotic state and nutritional state (particularly amongst symbiotic and not aposymbiotic colonies) to be the most significant predictors of photosynthetic efficiency (Table 10).

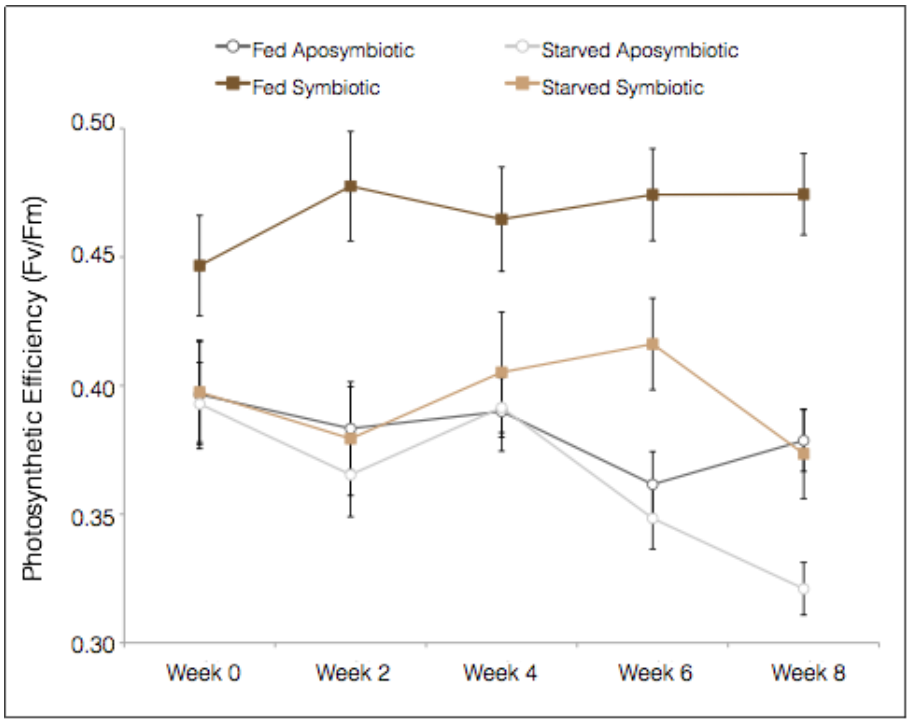

Figure 3.7. Mean maximum quantum yield (F_v/F_m) across a 60 day (8 week) period. Error bars signify standard error.

Table 3.10. REML-fitted linear mixed model for total colony surface area (AIC -486.8). For fixed effects, ** indicates significance at $\alpha < 0.001$, * indicates significance at $\alpha = 0.05$, $^{+}$ indicates significance at $\alpha = 0.1$.

Effect	Estimate	Standard Error	DF	T-Value	P-Value
Intercept	0.3795	0.0128	211	29.7495	<0.0001**
Symbiont State (S)	0.0846	0.0138	211	6.1153	<0.0001**
Symbiont State (A): Nutritional State (St)	-0.0119	0.0170	211	-0.7027	0.4830
Symbiont State (S): Nutritional State (St)	-0.0660	0.0170	211	-3.8850	0.0001**

3.5 DISCUSSION

Our findings highlight some of the dynamic pathways through which coral colonies might obtain, distribute, and utilize energetic resources during the process of recovering from physical abrasion. This study suggests that autotrophy plays an important role in wound recovery, and that there may be an important interplay and feedback (both positive and negative) between autotrophy and heterotrophy. As previously found in *A. poculata*, symbiotic state had a significant role on healing initiation and success as well as proportional surface area recovery to wounds (Burmester *et al.* 2017, DeFilippo *et al.* 2016). However, symbiont state

alone was not enough to maximize healing potential. Starved symbiotic and fed aposymbiotic healed comparably, while there was an additive negative feedback between starved aposymbiotic corals (no nutrition from either source; little/ no healing), and an additive positive feedback between fed symbiotic corals (nutrition from both sources; highest healing ability) (Figures 2, 3). This suggests that aposymbiotic, starved corals may experience a nutritional 'double jeopardy', and that energy allocation across wound healing, growth, and reproduction may be more complex than has previously been appreciated.

While nutritional state impacted healing initiation, it had no statistical effect on healing success or surface area recovery. On the other hand, only nutritional treatment (and not symbiont state) appeared to play a role in total colony tissue maintenance. These findings suggest that energy might not be regulated or distributed uniformly across levels of body organization. This is consistent with other studies, where branching growth tips of *Stylophora pistillata* had significantly less ^{14}C products than fragments from below branch tips (Rinkevich and Loya 1983). Additionally, both symbiotic state and lesion induction can alter the quantity and directionality of carbon translocation across a coral colony (Oren *et al.* 1997; Fine *et al.* 2002). In *O. patagonica*, preferential translocation to recovering tissue proceeded from a distance of 4-5 cm, but this phenomenon does not occur

in colonies that were fully or partially (30-80%) bleached (Fine *et al.* 2002). The pace and completion of wound recovery is subject to the impacts of several intrinsic and extrinsic factors (such as colony size, wound size, wound location, temperature, disease state, sedimentation, etc. [as reviewed by Henry & Hart 2005 and for example: Van Veghel & Bak 1994, Nagelkerken & Bak 1998, Nagelkerken *et al.* 1999, Kramarsky-Winter & Loya 2000, Edmunds 2009, Denis *et al.* 2011, Cameron & Edmunds 2014]), which also have the potential to interact with energy sourcing and nutritional state. The type of damage inflicted may also play a role in how energy is regulated or directed to recovery and other biological processes. Dislodged colonies of *Pocillopora damicornis* with edge damage experience a decrease in overall energy allocation, resulting in higher mortality rates and decreased growth and reproduction (Ward 1995). Meanwhile, fragmentation bears no significant impact on growth and mortality, but results in higher overall energy allocation and increased reproduction (Ward 1995). Therefore, it is likely that tissue maintenance and damage is regulated differently for small-scale local wounds (e.g. the single polyp removal demonstrated in this study) and across a coral's total-colony tissue cover. Interestingly, these results indicate that symbiont state is more important to the regulation of tissue surface area at the wound level while overall nutritional state is more greatly impacted by the presence or absence

of prey items. Therefore, there could be an added cost to lesion recovery during and after bleaching events that may not be fully supplemented via heterotrophy.

Both the availability (stimulus) of prey items as well as the history of heterotrophic opportunity significantly influenced polyp foraging behavior. Fed colonies maintained a higher degree of polyp expansion than unfed colonies at all time points, and the introduction of food particles induced even greater expansion. In tropical, obligate symbiotic scleractinians, symbiotic photosynthetic energy resources have been shown to influence heterotrophic activity. Colonies of *Pocillopora damicornis* maintained under dark conditions for 2 weeks ingested less *Artemia* nauplii than those in lighted conditions, suggesting a dependence on energy from photosynthesis to meet the metabolic needs required for sustainable foraging behavior (Clayton and Lasker 1982). In the present study, there was no observed statistical difference in foraging activity between symbiotic and aposymbiotic colonies. These results are similar to those found for other facultatively symbiotic corals. Piniak (2002) found that prey capture efficiency varied by prey type and flow rate, but observed no difference between (fed) symbiotic and aposymbiotic colonies of *Oculina arbuscula.* Coral colonies may also forage advantageously regardless of photosynthetic activity, as even obligate, tropical corals have been shown to seek heterotrophic nutrition even if metabolic

carbon requirements are met via autotrophy (Ferrier-Pagès *et al.* 1998). Additionally, the availability of heterotrophic food sources increased foraging activity in fed colonies both with and without a food stimulus. Therefore, colonies with a recent history of feeding are better able to maintain a fuller, long-term foraging effort, allowing them to not only respond to a food stimulus, but to also survey their environment. This suggests a heterotrophic, rather than autotrophic, mechanism for inducing appropriate behavior to meet metabolic demands in temperate, facultatively-symbiotic corals.

In this study, while the photosynthetic efficiency (maximum quantum yield) of fed symbiotic colonies was significantly higher than that of all aposymbiotic (fed and starved) colonies, there was no difference between aposymbiotic colonies and starved, symbiotic colonies. This phenomenon does not appear to derive from a loss of chlorophyll, which suggests an energetic cost to symbiont photosynthesis that must be fulfilled via host heterotrophic means. In fact, zooxanthellae have been documented to exhibit heterotrophic behavior inducing a parasitic metabolic burden on the facultatively symbiotic anemone *Aiptasia pulchella* (Steen 1986). Previous studies have documented an enhancement to photosynthesis in temperate corals after feeding (Jacques & Pilson 1980). Similarly, rates of photosynthesis increased (2-10x) after the introduction of

heterotrophic food sources to *Stylopora pistilla* (Houlbrèque *et al.* 2003). The decline in photosynthetic efficiency for starved, symbiotic colonies could also potentially be attributed to their higher rates of polyp contraction. Fabricius and Klumpp (1995) found reduced photosynthetic productivity and increased required levels of irradiance to achieve photosynthetic compensation and saturation in contracted large-polyped soft corals.

The dynamic relationship between *Astrangia poculata* and *Symbiodinium psygmophilum* is well-documented, with both symbiotic states characterized across its range (Dimond *et al.* 2013), and the potential for state-switching under experimental conditions (Dimond and Carrington 2007). The aposymbiotic state is common in nature (Grace 2004) despite relevant losses in recovery ability (DeFilippo *et al.* 2016, Burmester *et al.* 2017) as well as resilience to stress (Holcomb *et al.* 2010; 2012). It has been hypothesized that the persistence of the aposymbiotic life history reduces polyp loss under cold temperatures (Dimond *et al* 2013) during winter quiescence, when polyps enter a state of metabolic dormancy (Jacques *et al.* 1983) and tentacles no longer elicit a tactile feeding response (Grace 2017). Despite its thermal tolerance and resilience to chronic cold exposure (Thornhill *et al.* 2008), *S. psygmophilum* experiences a rapid decline and cessation in maximum quantum yield at winter temperatures. Combined with metabolic dormancy and a lack of

feeding response, the demonstrated decline in photosynthetic efficiency in the absence of heterotrophy in implied energetic cost of these symbionts to the host coral could explain the reduced polyp loss of aposymbiotic colonies under over-winter conditions.

While feeding behavior was ensured among all polyps for each colony, this study did not specifically determine the quantity of food consumed nor the amount of carbon incorporated. Likewise, while we recorded light availability (PAR) and photosynthetic efficiency (F_v/F_m), neither of these measurements provide accurate insight into photosynthetic carbon production for this coral. As such, it would be difficult to infer how specific pathways might be impacted by differences in symbiont state and experimental feeding treatments on the cellular level. However, the results of this study demonstrate significant and predictable morphological and stress-tolerant responses that influence key life history strategies in temperate corals, and importantly, are likely to be mirrored in their tropical counterparts.

3.5 ACKNOWLEDGEMENTS

This work was funded by a grant from the PADI foundation and a Boston University Marine Program Warren McLeod Fellowship awarded to EMB, and a

Cell Signaling Technologies grant to RDR, with additional support from the New England Aquarium. We would like to thank Abigail DeJohn, Carriel Cataldi, Lily Coughlin, Kiki Ballotti, Georgie Burruss, Samantha Pelletier, Aaron Pilnick, and Ryan Schosberg for assistance with data collection as well as Katey Lesneski, Karina Scavo Lord, Sam Herman, and Lukas DeFilippo for their help collecting research specimens. We are also grateful to Gregory Coote, Corbin Kuntze, Georgia Luddecke, Katrina Malakhoff, Jessie Matthews, and Matthew Tohl for their roles in the husbandry and maintenance of coral specimens. We also thank Jeff Chabot for programming RGB color analysis in MATLAB.

Chapter 4

A "HOLOBIONT" REFERENCE TRANSCRIPTOME FOR *ASTRANGIA POCULATA*, A FACULTATIVELY SYMBIOTIC SCLERACTINIAN, IN NATURALLY OCCURRING SYMBIOTIC STATES

4.1 ABSTRACT

The northern star coral *Astrangia poculata* (Ellis and Solander, 1786; =*A. danae*; =*A. astreiformis* {Peters, 1988}) is a temperate scleractinian coral with a wide latitudinal range that extends from Cape Cod to Florida. Like tropical reef-building corals, *A. poculata* calcifies, and can form symbioses with photosynthetic dinoflagellates of the genus *Symbiodinium*, However, unlike tropical corals, this symbiosis is facultative, and *Astrangia* can survive indefinitely in a functionally aposymbiotic condition where very few *Symbiodinium* are present. We generated a reference transcriptome for *A. poculata* from RNA sequencing data totaling 52.3 gigabases derived from four symbiotic colonies and two aposymbiotic colonies collected in Woods Hole, Massachusetts as well as single symbiotic and aposymbiotic polyps within one colony (presumably with identical genotypes) collected in Fort Wetherill, Rhode Island. The transcriptome comprises 368,277 contigs ranging in size from 200 to 22,801 nt (N50 = 789). All contigs and their associated annotations have been deposited at NCBI. The transcriptomic sequence

data and database described here provide a platform for studying the facultative symbiosis between *A. poculata* and *Symbiodinium*.

4.2 INTRODUCTION

The health of coral reefs is declining globally at a precipitous rate due to local human activities such as overfishing, destructive fishing practices, coastal development, pollution, and physical damage as well as pan-oceanic environmental disruptions such as thermal shock and ocean acidification (Reefs at Risk, 2011). In light of these crises, there has been a relatively recent and rapid accumulation of genomic and transcriptomic resources for scleractinian corals. Responding to the need for a better understanding of the coral stress response and reef resilience, hermatypic coral studies have focused on (1) adaptations for resilience (Barshis *et al.* 2012, Palumbi *et al.* 2014, Bay & Palumbi 2015) (2) stress response to environmental factors including heat stress (DeSalvo *et al.* 2010, Maor-Landaw *et al.* 2014, Mayfield *et al.* 2014., Rosic *et al.* 2014), ocean acidification (Davies *et al.* 2016), heavy metal exposure (Yuan *et al.* 2017), and eutrophication (Lin *et al.* 2017), as well as (3) disease (Daniels *et al.* 2015, Wright *et al.* 2015), and (4) processes related to development (Mansour *et al.* 2016) and homeostasis such as biomineralization (Mass *et al.* 2017) and circadian rhythm (Ruiz-Jones and

Palumbi 2015, Oldach *et al.* 2017). With the advent of publicly available genomic resources for hermatypic corals [such as the *Acropora digitifera* (Shinzato *et al.* 2011) and *Orbicella faveolata* (NCBI) genomes] as well as genomic data for their dinoflagellate endosymbionts [including *Symbiodinium microadriaticum* (Aranda *et al.* 2016), *S. minitum* (Shoguchi *et al.* 2013), and *S. kawagutii* (Lin *et al.* 2015)], the ability to work with molecular data for these non-model systems has become increasingly feasible.

However, despite the rise in availability of molecular data for corals, there are still some key challenges in establishing tropical scleractinian corals as model systems. First, the obligate nature of the tropical coral-*Symbiodinium* relationship and the inherent biological stress induced by bleaching make it difficult to create experimentally tractable systems for monitoring the establishment, maintenance, and breakdown of symbiosis. Likewise, the sensitivity of most coral species to minor changes in environmental conditions, as well as their slow growth rates and often endangered status make them difficult and expensive to maintain in a controlled laboratory setting. Additionally, wild caught samples have increased potential for genetic heterogeneity, which can result in individual variability that can make interpretation of gene-expression studies difficult (Lehnert *et al.* 2012).

Databases for non-calcifying cnidarian models like *Nematostella vectensis* (an Anthozoan cnidarian: Sullivan *et al.* 2006) and *Hydra magnipapillata* (a Hydrozoan cnidarian: Champan *et al.* 2010) exist, but these species are more distantly related and unique (i.e. *Hydra*) and/or lack the dinoflagellate symbiosis. For this reason, over the years, the sea anemone *Aiptasia* spp. (including *Exaiptasia pallida*; Grajales & Rodriguez 2014) has been established as a tractable model system for the cnidarian-dinoflagellate symbiosis. Like tropical corals, *Aiptasia* maintains an intracellular symbiotic relationship with *Symbiodinium* spp.; however, this symbiosis is highly flexible, and *Aiptasia* anemones can be manipulated to exist in fully aposymbiotic (without dinoflagellates) or symbiotic (in association with a variety of *Symbiodinium* types) states (Weis *et al.* 2008). Unlike most corals, *Aiptasia* is extremely hardy and easy to keep in a laboratory setting, with established husbandry protocols for the full life cycle including asexual reproduction and regular spawning and settlement (Lehnert *et al.* 2012). As such, *Aiptasia* has provided an optimal platform for studies investigating the molecular basis of the coral symbiosis, and related works have been conducted on multiple levels, including organismal (Perez *et al.* 2001, Dunn *et al.* 2002), genomic (Baumgarten *et al.* 2015), transcriptomic (Sunagawa *et al.* 2009, Lehnert *et al.* 2014, Wolfowicz *et al.* 2016), proteomic (Black *et al.* 1995; Oakley *et al.* 2016), and lipidomic (Garrett *et al.*

2011). However, this model, too, has its limitations. First, while *Aiptasia's* lack of calcareous skeleton and colonial lifestyle may facilitate easier manipulation of several biochemical and cell biological techniques (Lehnert *et al.* 2012), it also makes this model incompatible with understanding calcification. As biomineralization is an important biological process in colony growth as well as a significant energetic cost (Cohen & Holcomb 2009), the transcriptional profiles for *Aiptasia* do not provide a good model for the energetic and cellular repertoire of a stony coral. Additionally, energy and carbon resources can be translocated across multiple polyps within a colony (Fine *et al.* 2002). Therefore, focus on a solitary polyp can miss key components of colonial pathways.

The Northern Star coral, *Astrangia poculata* (Ellis and Solander, 1786; =*A. danae*; =*A. astreiformis* {Peters, 1988}), serves as a bridge between these two established research systems. Like *Aiptasia*, *A. poculata* shares a facultatively symbiotic relationship with *Symbiodinium* (*psygmophilum*, of the B2 clade; LaJeunesse et al. 2012) and can be kept in a laboratory setting (DeFilippo *et al.* 2016, Burmester *et al.* 2017). Additionally, the facultative symbiosis of *A. poculata* and *S. psygmophilum* is naturally occurring and stable, such that fully symbiotic, fully aposymbiotic, and mottled symbiotic colonies that vary by polyp (Figure 1) exist sympatrically in the same microhabitats (Dimond & Carrington 2007). In fact, the

aposymbiotic state is regularly maintained through the active expulsion of symbionts, and not the result of an intracellular stress response or experimental manipulation (Dimond & Carrington 2008). As such, this relationship offers a natural experimental system for deciphering the dynamics between a coral host and its dinoflagellate endosymbiont as well as the opportunity to maintain experimental lines of identical genets by separating symbiotic and aposymbiotic polyps of mottled colonies. Furthermore, as a temperate coral, *A. poculata* demonstrates a remarkable temperature tolerance across its wide geographic range (from as far south as Florida and the Gulf of Mexico north through southern Massachusetts; Thornhill *et al.* 2008). Thus, despite its temperate distribution, *A. poculata* serves as a prime candidate for understanding scleractinian stress resilience in light of the relative roles of both coral host and symbiont under healthy and stable conditions.

Towards the establishment of *Astrangia poculata* as a model system in its own right, this work generates a novel *de novo* transcriptome for *A. poculata* and tests its utility as a resource for pairwise comparisons between symbiotic states.

4.3 MATERIALS & METHODS

4.3.1 Animal collection

Colonies of *Astrangia poculata* in three symbiotic states were collected at two sites in New England: Woods Hole, MA and Fort Wetherill State Park in Jamestown, RI. Naturally occurring symbiotic and aposymbiotic colonies of *A. poculata* were supplied by the Marine Resources Department (MRD) at the Marine Biological Laboratory in Woods Hole, MA in the fall of 2012 while mottled colonies were collected from Fort Wetherill State Park in Jamestown, RI in the summer of 2012 (by Randi Rotjan). All colonies were gathered using SCUBA by chiseling the colonies away from rocky substrates at depths between 2 and 4 meters, fully within the range enabling photosynthesis.

4.3.2 RNA isolation, sequencing and assembly

Total RNA was isolated from four symbiotic and two aposymbiotic colonies from Woods Hole as well as a single apoysmbiotic and single symbiotic polyp from the same mottled colony from Fort Wetherill using the TRIzol RNA Isolation Method (Life Technologies, Chomczynski and Mackey 1995). A full polyp (including skeleton) was removed from the colony using bone-cutting scissors. Excised polyps were frozen with liquid nitrogen before being pulverized with a mortar and pestle. The pulverized tissue was soaked in TRIzol and homogenized

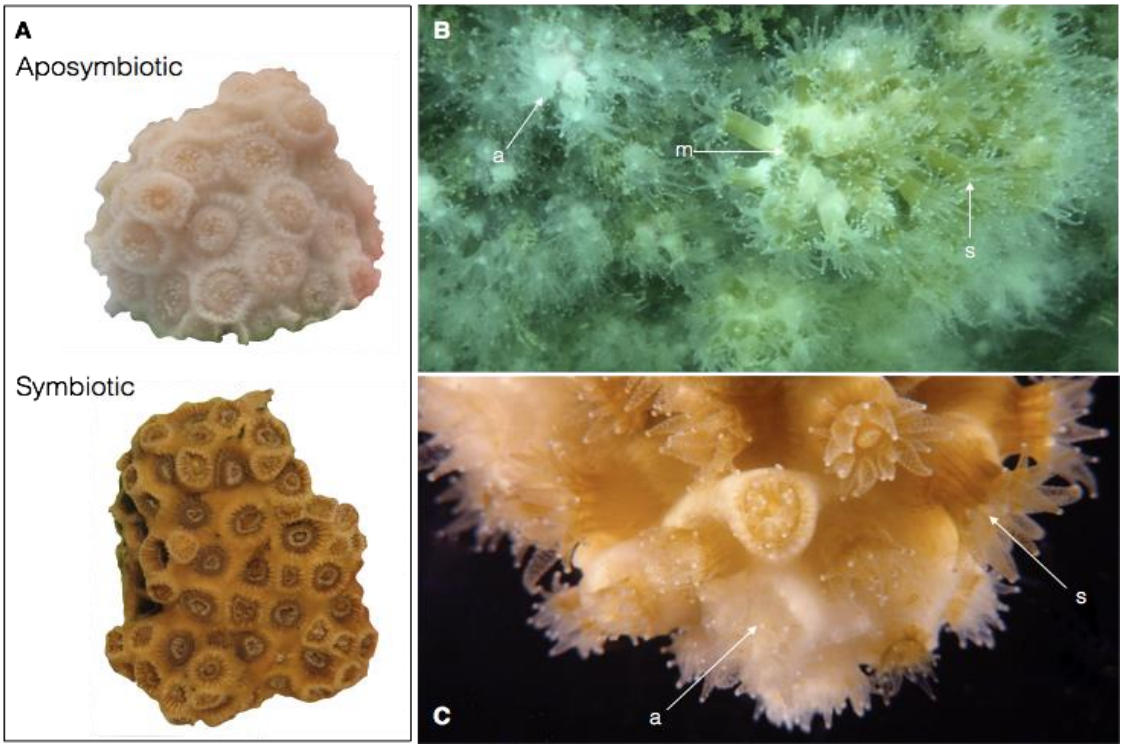

Figure 4.1. (A) Symbiont states in A. poculata: [f] fully aposymbiotic colonies appear white in color; [g] mixed symbiont state colonies have a range of symbiotic (s) and aposymbiotic (ap) polyps; [h] fully symbiotic colonies appear brown in color.

with ground glass homogenizers. Following isolation of RNA and resuspension in nuclease free water, the nucleotide concentration and purity were assessed by ultraviolet spectrophotometry using a NanoDrop 2000 (Thermo Scientific). Separate cDNA libraries were prepared for each RNA sample isolated, each with unique adaptor-primers using the TruSeq RNA Sample Prep Kit v2 (Illumina). The size range of the library inserts was determined with a 2100 Bioanalyzer Instrument (Agilent). RNA isolation and library preparation for Fort Wetherill

samples were performed in the laboratory of Iliana Baums at Penn State University by Nick Polato. Libraries were subsequently sequenced on the Illumina HiSeq 2000 platform to generate 100bp paired-end sequencing reads (for Woods Hole samples: at the Bauer Core Facility at Harvard University; for Fort Wetherill samples: through the Baums lab at the University of Maryland Institute for Genome Science). Multiple libraries from the same collection site were combined and sequenced on a single lane of a flow cell. After the removal of primers and adapter-dimers, low quality bases (Phred quality value, QV≥20) as well as overrepresented sequences from possible PCR duplicate contamination were identified and removed using the trim toolkit in CLC Genomics Workbench (Qiagen). Subsequent high-quality paired-end reads were assembled using CLC Genomic Workbench's assembly algorithm and a word size of 25. Contigs over 200bp in length were retained.

4.3.3 Assessing completeness and fragmentation

To assess the recovery of conserved metazoan genes, we used BUSCO (Benchmarking Universal Single Copy Orthologs; Université de Genève) to compare all contigs in the assembly to the Metazoa dataset (odb9, n=978 orthologs; Figure 3). This analysis generates quantifiable assembly assessments for ortholog

sequences that are (1) complete (single or duplicate copy), (2) fragmented, and (3) missing by identification and comparison to suspected near-universal and single copy orthologs selected from OrthoDB *v9*. For comparison, we performed the same analysis on 18 publicly available cnidarian and scleractinian transcriptomes (data obtained from reefgenomics.org).

4.3.4 Assessing sequencing coverage

We utilized a previously published python script (Stefanik *et al.* 2014) that uses a random re-sampling approach to assess the impact of sequencing depth on the recovery of individual transcripts. All reads were aligned to the reference assembly, and the resulting sequence alignment map (SAM) file was parsed through this custom script. Briefly, a subset of random sequencing reads were selected without replacement. Nominal coverage is estimated using the contig length, read length, and number of reads aligned to each contig. These alignments were then parsed to assess the percentage of contigs exhibiting a certain level of coverage (1x, 3x, 5x, 7x, 10x, 25x), where coverage represents the average number of reads mapping to each position in the contig. We calculated the percentage of contigs achieving each coverage threshold for randomly chosen subsets of sequencing reads in increments of 50 million reads from 0-500 million. For each

increment, three random samples of sequencing reads were evaluated, and the mean coverage and standard deviation were quantified. However, all standard deviation values were found to be negligible (less than 0.1% of total contigs at a given threshold) and were therefore not represented on the plot provided in the results.

4.3.5 Phylogenetic relationship to published scleractinians

From our transcriptome assembly, we recovered a complete mitochondrial cytochrome oxidase subunit (CO1). We aligned the putative CO1 gene generated by this study to previously published sequences from *A. poculata* [NCBI Accession Number: AY039209.1] and 41 other hermatypic corals. Nucleotide sequences from all taxa were converted into amino acid format using the translate tool on ExPASy. We evaluated the completeness of the CO1 protein sequences from all species by testing whether all conserved motifs were present using MEME (Bailey *et al.*, 2006). A phylogenetic tree was produced using the Phylogeny Analysis tool on the Phylogeny.fr interface via Information Genomique et Structurale via a four-step process: (1) sequences were aligned using MUSCLE (Multiple Sequence Comparison by Log-Expectation; settings: maximum 16 iterations with diagonals), (2) poorly aligned regions were removed from the alignment using Gblocks

(default setting), (3) a maximum-likelihood phylogeny was generated using PhyML, and (4) and the resulting phylogeny was rendered using TreeDyn.

4.3.6 Annotation of transcriptome assembly

Putative transcripts in the assembly were annotated using Blast2GO Pro by Linda Nguyen (Finnerty Lab, Boston University). All 368,277 contigs were first compared to sequences in the non-redundant database (NR) at NCBI (The National Center for Biotechnology) using BLASTx searches with a threshold Expect (E) value of 1E-03. For BLAST searches that produced a match to an annotated sequence in the database, Gene Ontology (GO) terms were extracted from the corresponding protein sequence in the Uniprot database at Swiss-Prot (The Uniprot Consortium 2016) and assigned to the matching *Astrangia* sequence.

4.3.7 Identifying host or symbiont-originated sequences

In order to identify and separate host and symbiont contributions to the overall holobiont transcriptome, assembled contigs were filtered through the protein databases for the *Acropora digitifera* genome and the *Symbiodinium microadriaticum* genome to identify putative coral- and symbiont-originated sequences, respectively. Analyses were performed using BLASTx with a filter E value of 1E-03.

4.3.8 Differential Expression Analyses

Sequence alignment and read counts were performed using the RNA-Seq Analysis tools on the CLC Genomics Workbench platform for all 8 samples. In order to determine overall similarity in gene expression across all contigs for all eight samples (five symbiotic and three aposymbiotic), a principle component analysis was performed on gene expression levels for each contig. Pairwise analyses were performed to identify transcripts that were differentially expressed between symbiotic (n=5) and aposymbiotic (n=3) samples. For each comparison between symbiotic and aposymbiotic samples, a volcano plot was generated using an Extraction of Differential Gene Expression (EDGE) test. We determined the identity of the most significantly differentially expressed contigs (those with a false discovery rate (FDR) of $P < 0.003$) using BLASTx searches against the NR database (NCBI). The taxonomic origin of the top hit in each search was extracted using BLAST2GO. Differentially expressed contigs of coral origin were analyzed using a motif analysis (MEME) and compared against the *Orbicella faveolata* sequence of closest similarity to validate sequence completion.

4.4 RESULTS AND DISCUSSION

4.4.1 Sequencing and assembly

Sequencing yielded a total of 52.29 gigabases of nucleotide data that passed Illumina's GAIIx quality filter (31.81 from Woods Hole; 20.48 from Fort Wetherill) from 8 samples, with the yield of individual specimens ranging from 1.62 to 11.06 gigabases. The overall sequencing yield for *A. poculata* greatly exceeds several previously published sequencing efforts (Table 1). After quality control and rimming, 445,607,644 of the 522,900,102 sequencing reads (with an average length of 90.5) were included in the assembly. Assembly on the CLC Genomics Workbench platform generated 368,277 total contigs (ranging from 200 – 22,801 bp in length; N50 = 789). This high number of contigs is comparable to other coral transcriptomes that encompass the entire holobiont (Figure 2); however, the N50 is at the low end of the range for recent scleractinian transcriptomes (749-2088 bp, Table 1), suggesting a higher number of incomplete gene assemblies.

4.4.2 Completeness and fragmentation

BUSCO analysis revealed that the *Astrangia poculata* transcriptome encompasses a large fraction of complete transcripts for conserved metazoan orthologs (86.9%), while only 10.7% of these conserved orthologs appear fragmented and 2.3% are missing (Figure 3). Comparison of 18 published scleractinian transcriptomes reveals wide variation in the recovery of complete

Table 4.1. Summary of sequencing statistics for a selection of recent coral sequencing efforts.

Species	Sequencing Reads(?)	N50	# Contigs	Putative Coral Contigs	Putative *Symbiodinium* Contigs	Reference
Astrangia poculata (APOC)	522 million (100bp paired end)	789	368,277	99,471 (27%)	85,057 (23%)	this study
Porites australiensis (PAUS)	71 million (100bp paired end)	2037	74,997	26,658 (35%)	26,627 (35%)	Shinzato *et al.* 2014
Orbicella faveolata (OFAV)	387 million (75bp paired end)	1551	442,294	178,943 (40%)	130,217 (29%)	Pinzón *et al.* 2015
Acropora millepora (AMIL)	2 million (454) > 400 million (single end) > 125 million (paired end)	2023	56,260	—	—	Moya *et al.* 2012
Stylophoroa pistillata (SPIL)	—	2088	470,497	—	—	Maor-Landaw *et al.* 2017
Balanophyllia europea (BEUR)	—	1246	961,667	—	—	Maor-Landaw *et al.* 2017
Platygyra carnosus (SPIL)	59.6 million 90bp paired end)	811	162,468	47,732 (29%)	—	Sun *et al.* 2013
Millepora alcicornis (MALC)	76.5 million (150bp paired end)	749	479,982	25.8%	—	Ortiz-González *et al.* 2017
Pocillopora damicornis (PDAM)	115 million (150bp single end)	1104	135,265	—	—	Mass *et al.* 2017
Porites astreoides (PAST)	594 million (150bp paired end)	763	867,255	129,718 (15%)	186,177 (21%)	Mansour *et al.* 2016

metazoan orthologs, from 24.6 - 91.7% complete, 2.4 – 29.1% fragmented, and 2.2-63.6% missing. Because the conserved orthologs evaluated by BUSCO are single-copy genes, complete and duplicated genes would not be expected unless there are variant alleles expressed within the sequenced RNA. The relatively high levels of duplication seen in this dataset (as well as that of *Nematostella vectensis*) could be the result of allelic variation between geographically distinct populations, resulting in the formation of "isotigs" corresponding to the same conserved ortholog.

4.4.3 Sequencing coverage

Although sequencing yield was high relative to other cnidarian transcriptome sequencing projects, the coverage of the transcriptome appears relatively low for the sequencing effort. The sequence saturation curves suggest that we achieved saturation for 1x coverage of the assembly at around 250 million reads (Figure 4.3). However, even at 500 million reads, we have not achieved saturation for 3x or 5x coverage of the assembly. By contrast, in the lined sea anemone, *Edwardsiella lineata*, another anthozoan cnidarian (Stefanik *et al.* 2014) 200 million reads provides 10x coverage for 100% of the transcriptome. However, *E. lineata* does not participate in a symbiosis with *Symbiodinium*, and therefore, the complexity of its transcriptome might be much lower. This suggests that because

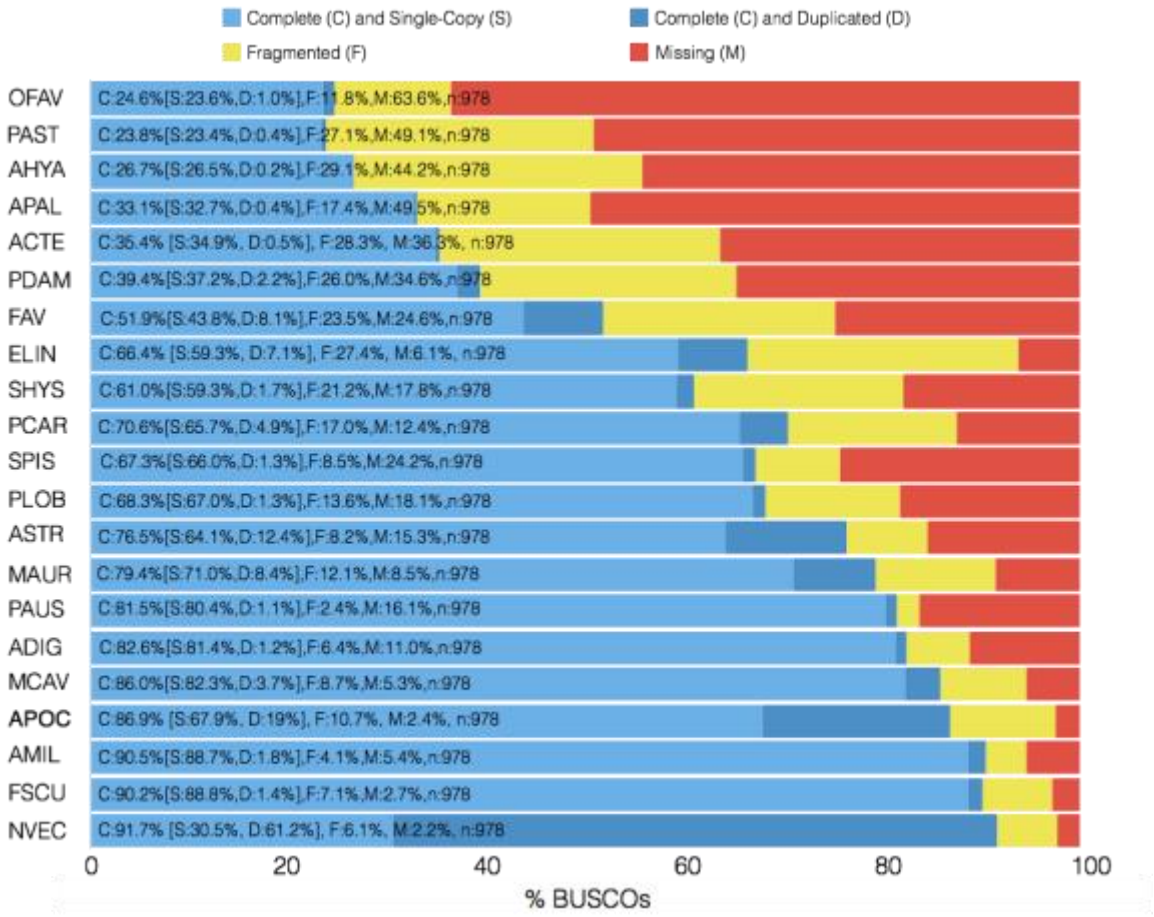

Figure 4.2. BUSCO analysis for published cnidarians and scleractinians. Data obtained from publicly available sources on reefgenomics.org. Transcriptomic completeness and fragmentation data for *Astrangia poculata* (APOC) against 18 scleractinians: PCAR (*Platygyra carnosus*), OFAV (*Orbicella faveolata*), MCAV (*Montastrea faveolata*), FSCU (*Fungia scutaria*), ASTR (*Astreopora* sp.), APAL (*Acropora palmata*), SPIS (*Stylophora pistillata*), SHYS (*Seriatopor hystrix*), PLOB (*Porites lobata*), PDAM (*Pocillopora damicornis*), PAUS (*Porites australiensis*), MAUR (*Madracis auretenra*), FAV (*Favia spp.*), PAST (*Porites astreoides*), MAUR (*Madracis auretenra*), AMIL (*Acropora millepora*), AHYA (*Acropora hyacinthus*), ADIG (*Acropora digitifera*), and ACTE (*Acropora tenuis*) as well as two sea anemones (Actinaria): ELIN (*Edwardsiella lineata*) and NVEC (*Nematostella vectensis*)

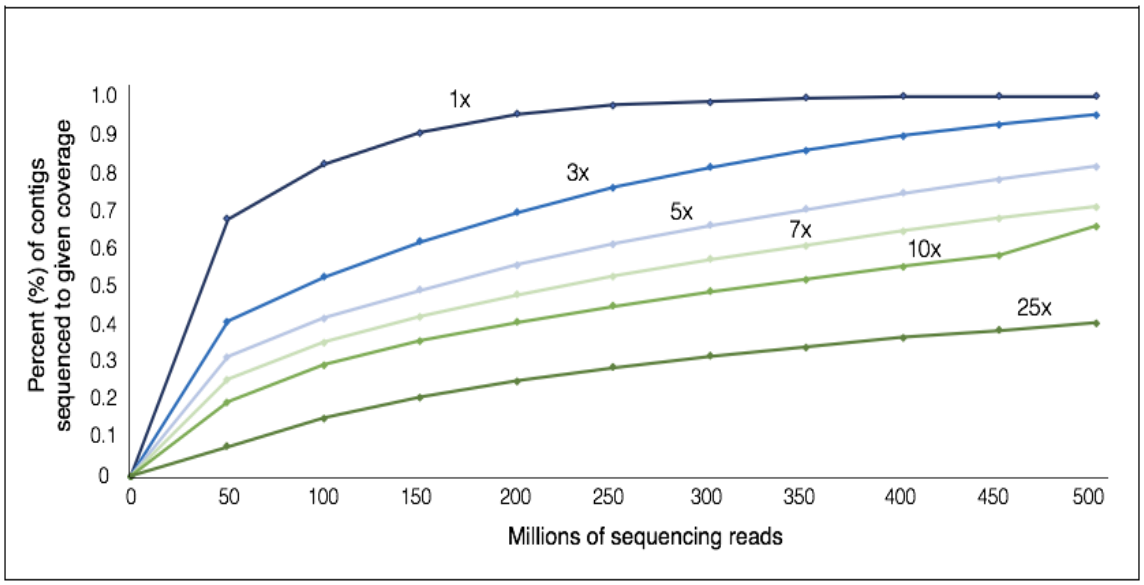

Figure 4.3. Sequencing saturation curve for percentage of contigs with nominal cover of n-fold plotted by the total number of sequencing reads. Sub-samples of sequencing reads of a given size were randomly selected from the complete pool of sequencing reads. Each data point represents the mean value of three replicates. Error bars are too small to be visually represented.

of (1) a diversity of contigs, likely due to the genetic biodiversity present within the holobiont samples and (2) high variety and quantity of symbiotic, endolithic, and epibiont community associates, we may require deeper sequencing than originally anticipated and historically sampled for corals (Table 1).

4.4.4 Annotation of transcriptome assembly

Of the 368,277 contigs in our transcriptome assembly, 40% (147,849) produced BLAST hits to sequences in NCBI's non-redundant (NR) protein

database, while 60% (220,428) had no BLAST hits (Fig. 4A). The greatest proportion of BLAST hits matched to one scleractinian species, *Acropora digitifera* (42,305 contigs; 27.3%) as well as two anthozoan cnidarian species: *Exaiptasia pallida* (9,504 contigs; 6.1%) and *Nematostella vectensis* (5,685 contigs; 3.7%).

Additionally, a fairly large fraction of the contigs producing hits matched a poriferan (*Amphimedon queenslandica*: 8,995 contigs, 5.8%) and a foraminiferan (5,727 contigs; 3.7%), suggesting that sponge and foraminifera may be relatively abundant components of the *Astrangia* holobiont (Figure 4B; e.g., the sponge *Cliona celata* is a frequent close associate of *Astrangia poculata* in Woods Hole).

Of the contigs that produced a BLAST hit, roughly 32% (46,742) could be associated with one or more GO annotation terms (Figure 4A). Because most contigs match many GO terms, there are a total of 450,695 pairings between contigs and GO terms: 197,219 of these GO terms belong to the category "biological process," 173,292 to "cellular component," and 80,184 to "molecular function" (Figure 5). Cellular process, metabolic process, single-organism process, biological regulation, and regulation of biological processes ranked as the top five GO categories for biological process (Figure 5). The most highly represented GO terms identified in this study overlapped substantially with another recent coral study. *Orbicella faveolata* (Pinzón *et al.* 2015) shared three of the top five most highly

represented GO terms with *A. poculata* in all three major categories: biological process (metabolic process, cellular process, and biological regulation), cellular component (cell part, organelle, and macromolecular complex), and molecular function (catalytic activity, binding, and structural molecule activity).

4.4.6 Identification of host and symbiont-originated sequences

Approximately 23% of all contigs (85,057) were matched to the *Symbiodinium microadriaticum* proteome via BLASTx. Meanwhile, approximately 23% of contigs (85,057) aligned via BLASTx to the *Acropora digitifera.* proteome (Figure 5). Although there does not appear to be a great deal of consistency between coral holobiont transcriptomes that have made this distinction, these identity values fall within the published range (Table 1). It is likely, however, that the proportion of coral, *Symbiodinium*, and other eukaryotes could vary greatly between different species and different populations.

4.4.8 Phylogenetic relationship to published scleractinians

A maximum-likelihood phylogeny of 41 scleractinian CO1 sequences and 2 actinarian outgroups is shown in figure 6. The tree typology is broadly consistent with a division between the widely recognized “robust” and “complex” coral

clades (Kitahara *et al.* (2010). The *Astrangia* CO1 sequence identified in this study grouped with a published CO1 sequence for *A. poculata* with bootstrap support of 100%, confirming its species identity. As expected, the *A. poculata* sequences are nested among other robust coral sequences, as *Astrangia* is a member of the family Rhizangiidae in the robust clade (Kitahara *et al.* 2010).

4.4.9 Differential expression analysis

Overall, 3,070 contigs were differentially expressed (DE) between symbiotic and aposymbiotic polyps (EDGE test with FDR $P < 0.003$). Most of these DE contigs exhibited enhanced expression values for symbiotic specimens (Figure 7A). Expression values varied greatly between individuals, particularly among symbiotic specimens, as evidenced by the wide dispersion of samples across the second principle component (Figure 7B). Symbiotic colonies and aposymbiotic colonies separate slightly from each other across the first component (which explains 80% of the overall variability in gene expression levels).

Of the 3,070, we were able to identify 2,088 (68%) using BLASTx against the NR database (NCBI) (Figure 8 inset). This represents a 70% increase in successful BLAST identification over the holobiont transcriptome as a whole. Of these, the top BLAST hit matched a member of the *Symbiodinium* genus for 1,513 (72%) of the

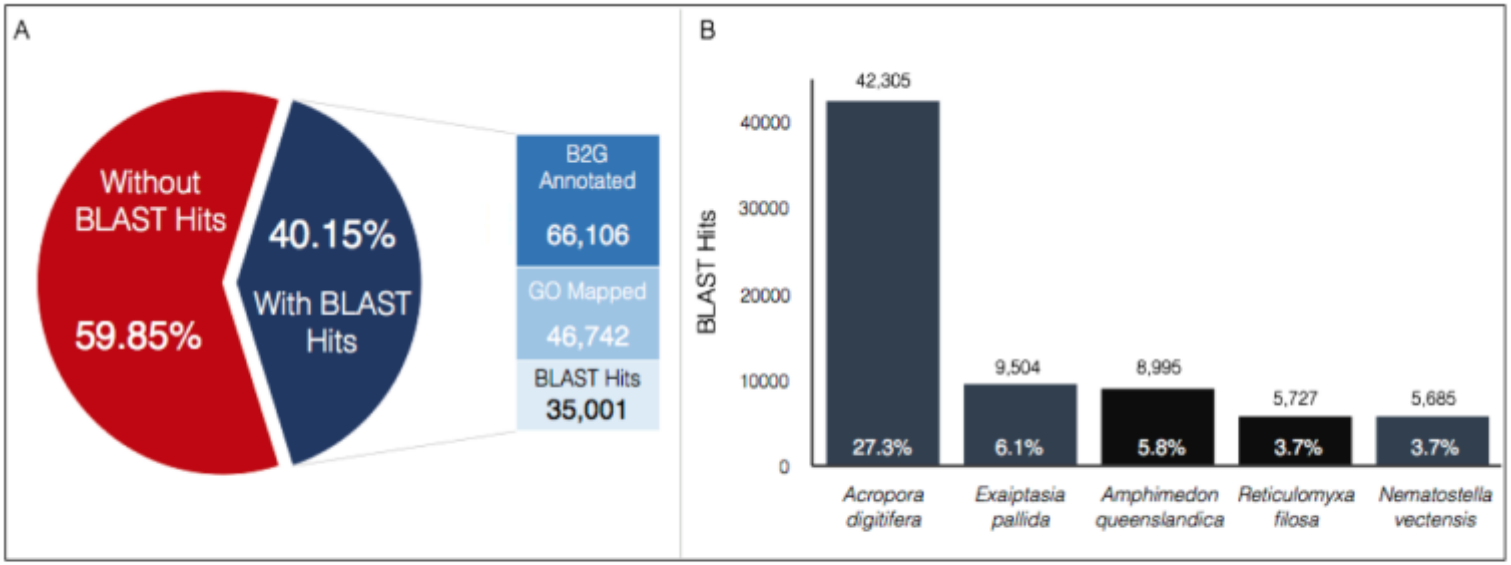

Figure 4.4. Summary of BLAST hits: (A) Comparison of all 368,277 assembled contigs against sequences in NCBI's non-redundant database using BLASTx and (B) Breakdown of top BLAST hits by species

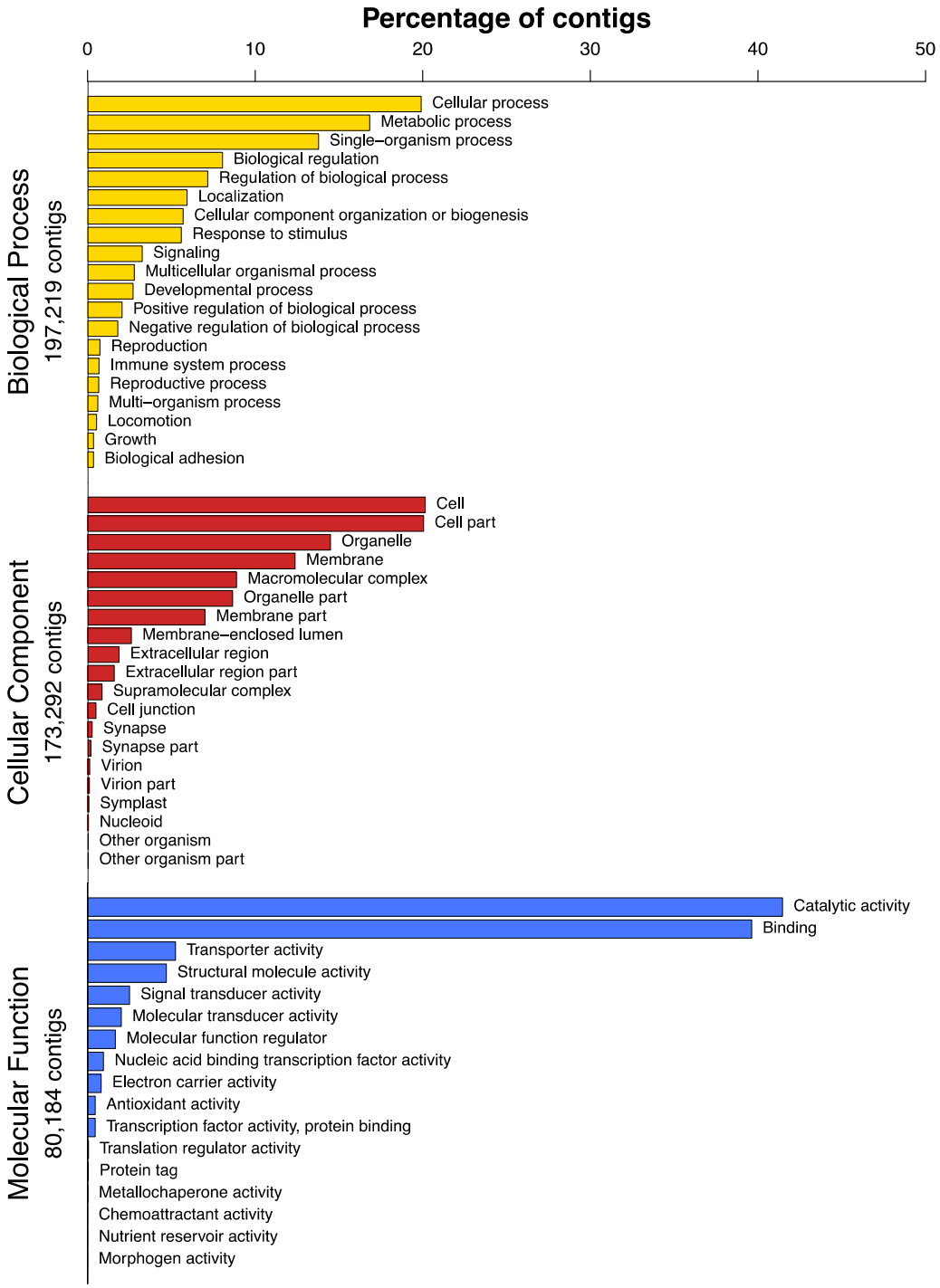

Figure 4.5. Recovery of GO terms for Molecular Function, Cellular Component, and Biological Process (Level 2).

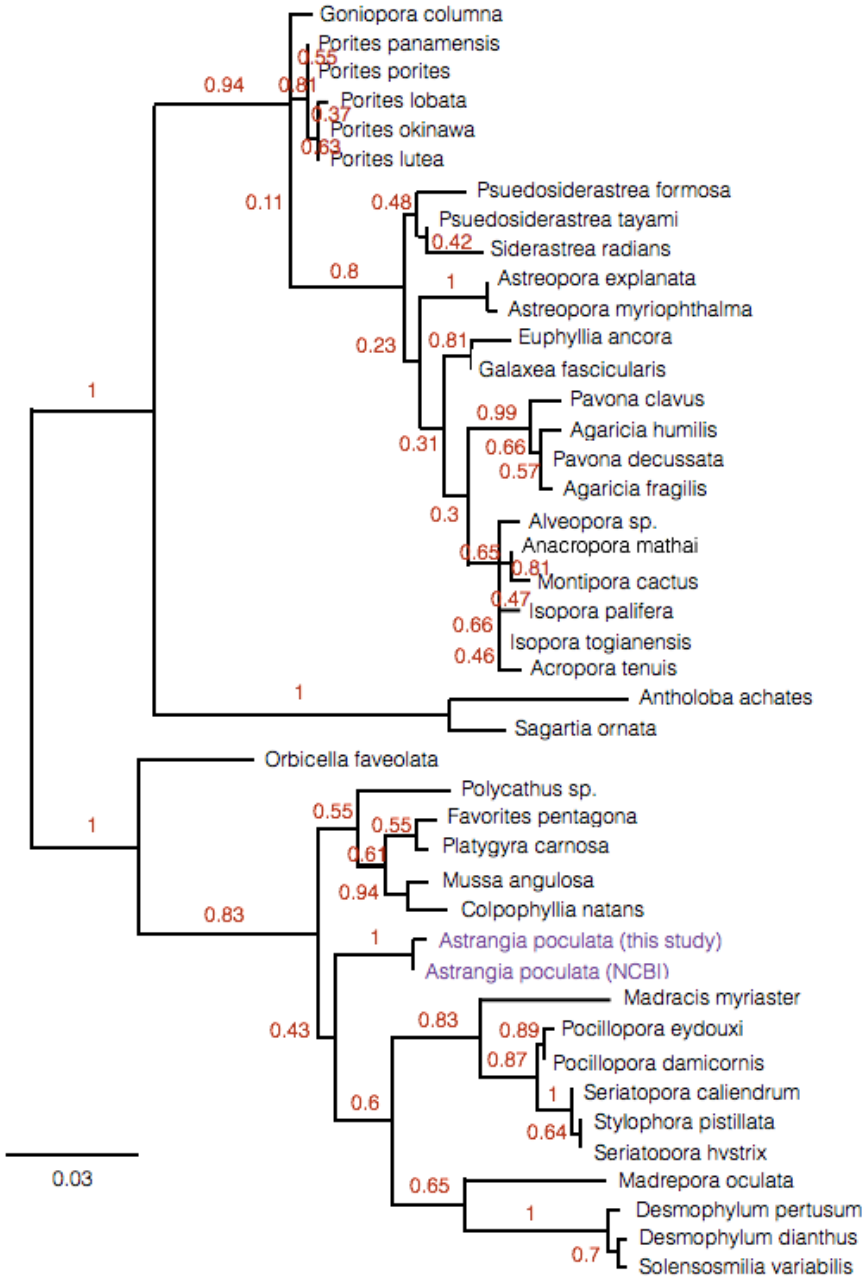

Figure 4.6. Phylogeny of mitochondrial cytochrome c oxidase (CO1) sequences for *A. poculata* (both generated by this study and obtained from NCBI) as well as 41 scleractinian corals. Numbers represent bootstrap evaluations after 100 iterations.

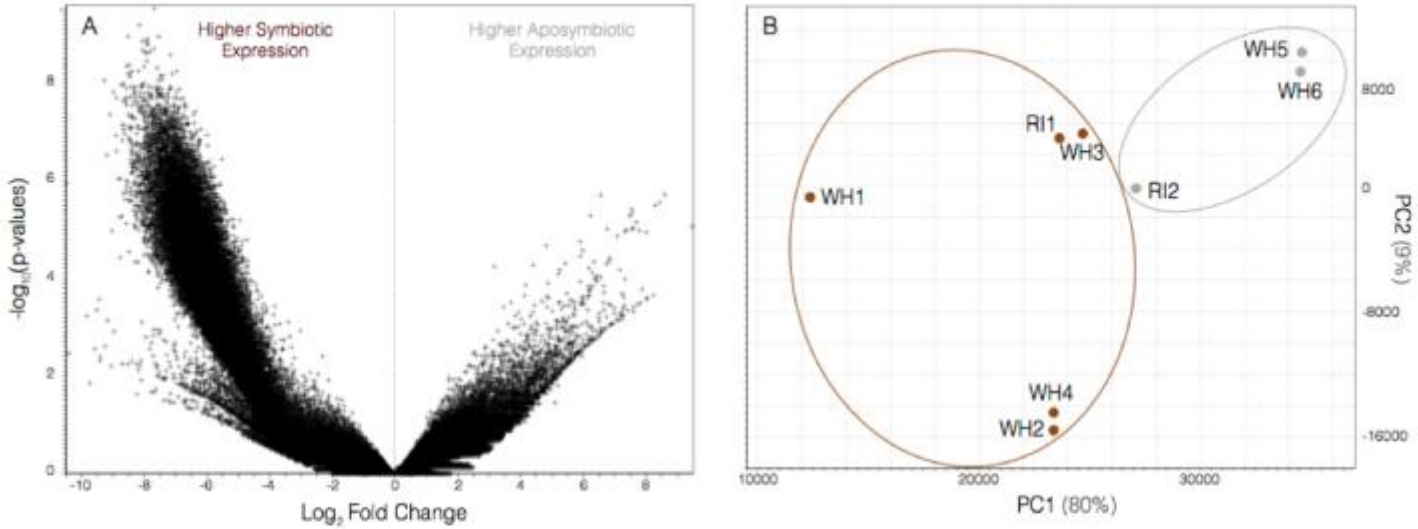

Figure 4.7. Differential expression between symbiotic and aposymbiotic states. (A) A volcano plot for the pairwise analysis between symbiotic (enhanced expression on the left) and aposymbiotic (enhance expression on the right) colonies. Expression are represented on a $\log_2$ fold-change scale. (B) A principle component analysis of expression for each sample. Component loadings (in %) are listed on the axis. Brown dots represent symbiotic colonies and grey dots depict aposymbiotic colonies of two populations (Woods Hole, WH and Rhode Island, RI). Samples are circled together by qualitative biological importance and not quantitative statistical importance.

contigs (Figure 8). The remaining top four species hits are likely *Symbiodinium* in origin as well as they belong to (1) dinoflagellates and (2) members of the phylum Alveolata, taxonomic categories that encompass the genus *Symbiodinium* (Shoguchi *et al.* 2015). Two species of the phylum Alveolata comprise 4.59% of top BLAST hits; 50 contigs matched *Vitrella brassicaformis* and 46 corresponded to *Perkinsus marinus*. An additional 2.15% (35 contigs) matched dinoflagellate species (*Pfiesteria piscicida*: 26 contigs, and *Karlodinium veneficum*: 19 contigs). Altogether, this analysis suggests over 79% DE contigs are from *Symbiodinium psygmophilum* (Figure 8).

Of interest, only two of the top 3,070 differentially expressed contigs (0.10%) matched scleractinian corals as a top hit (Figure 8). Both of these contigs (neurogenic locus notch-like and olfactomedin 2A) have putative immune function (Anderson *et al* 2016; Anholt 2014; Figure 9A,B). Immune-related genes have broadly generated interest for their potential roles in the onset and maintenance of cnidarian-dinoflagellate symbioses (Pinzón *et al.* 2015, Poole *et al.* 2016). Recent studies suggest neurogenic locus notch-like (Notch) genes play an important role in cnidarian innate immunity, whereby inhibition of the Notch pathway disrupts the wound healing ability of *Nematostella vectensis* (Dubuc *et al.* 2014). Despite the fact that Notch receptors have been relatively well described in

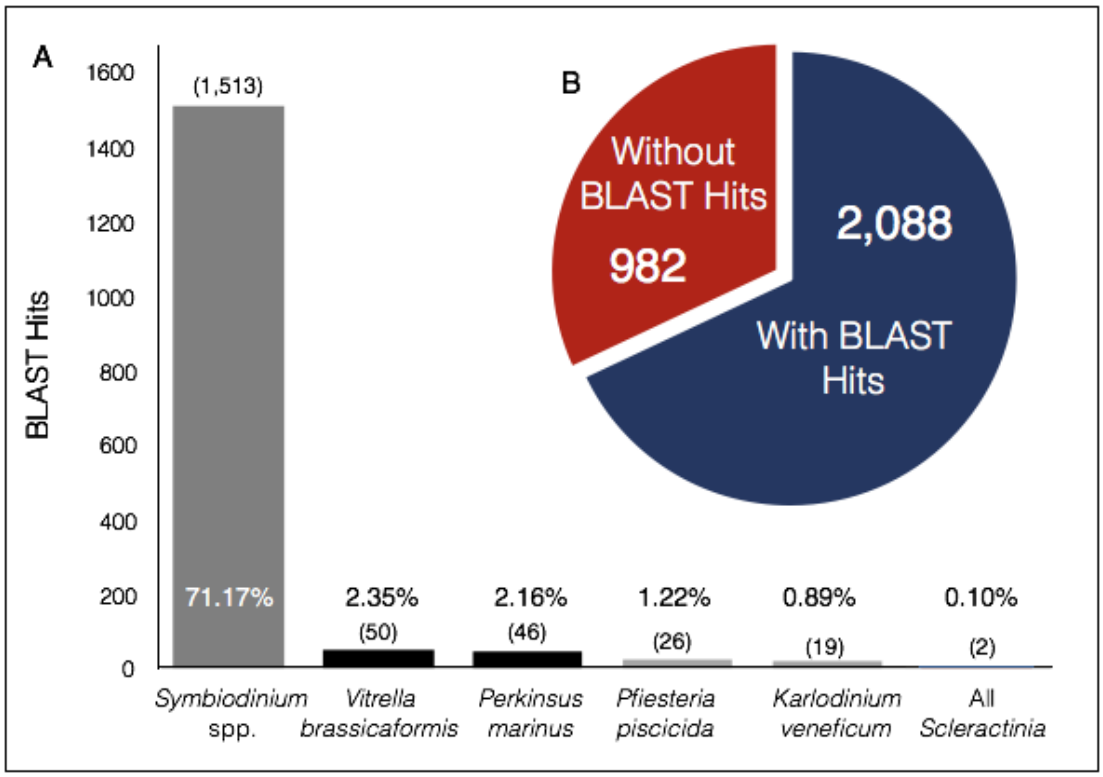

Figure 4.8. (A) Top BLAST hit species distribution for differentially expressed contigs. (B) Proportion of 3,070 DE contigs with (blue) and without (red) BLAST hits.

Table 4.2. Identified top-50 differentially expressed *Symbiodinium* contigs

	Contig Identification	Log2 Fold Change	GO Term Number
Photosynthesis	Ribulose 1,5- Bisphosphate Carboxylase Oxygenase	7.07	GO:0016021 GO:0031969 GO:0000287 GO:0004497 GO:0016984 GO:0019253 GO:0055114 GO:0009573 GO:0046487
	Ribulose 1,5- Bisphosphate Carboxylase Oxygenase	7.51	GO:0000287 GO:0004497 GO:0016984 GO:0019253 GO:0055114 GO:0009573 GO:0046487
	Fucoxanthin Chlorophyll a-c Binding Protein	7.48	GO:0009536 GO:0009579
	Light Harvesting Complex	7.04	GO:0009507 GO:0009579 GO:0016020 GO:0015979
	Ferredoxin	7.61	GO:0004324 GO:0055114 GO:0006118
	Photosystem I Reaction Center Subunit XI	7.50	GO:0009507 GO:0009522
	RBL2	7.13	GO:0009507 GO:0016020 GO:0016491 GO:0016829 GO:0046872 GO:0015977 GO:0015979
	Oxygen Evolving Complex	8.06	GO:0009654 GO:0016021 GO:0019898 GO:0005509 GO:0015979 GO:0042549
Metabolism	Glyceraldehyde-3-Phosphate Dehydrogenase	7.67	GO:0004365 GO:0050661 GO:0051287 GO:0006096 GO:0055114 GO:0006094
	S-Adenosyl-L-Homocysteine Hydrolase	8.42	GO:0005829 GO:0004013 GO:0006730 GO:0033353
	Alcohol Dehydrogenase	6.68	
	Methionine S-Adenosyl Transferase	7.87	GO:0005829 GO:0004478 GO:0005524 GO:0006556 GO:0006555
	Nitrate Reductase Small Subunit	6.48	GO:0097159 GO:1901363
	Ubiquinone Biosnthesis Methyltransferase	5.23	GO:0016740 GO:0008152
	3-Phosphoglycerate Deyhdrogenase	6.60	GO:0016616 GO:0008152
Stress	Heat Shock Protein Partial	7.67	GO:0005524
	Heat Shock Protein	8.42	GO:0005524 GO:0051082 GO:0006457 GO:0006950
	Calreticulin	6.68	GO:0005783 GO:0005509 GO:0016798 GO:0051082 GO:0006457

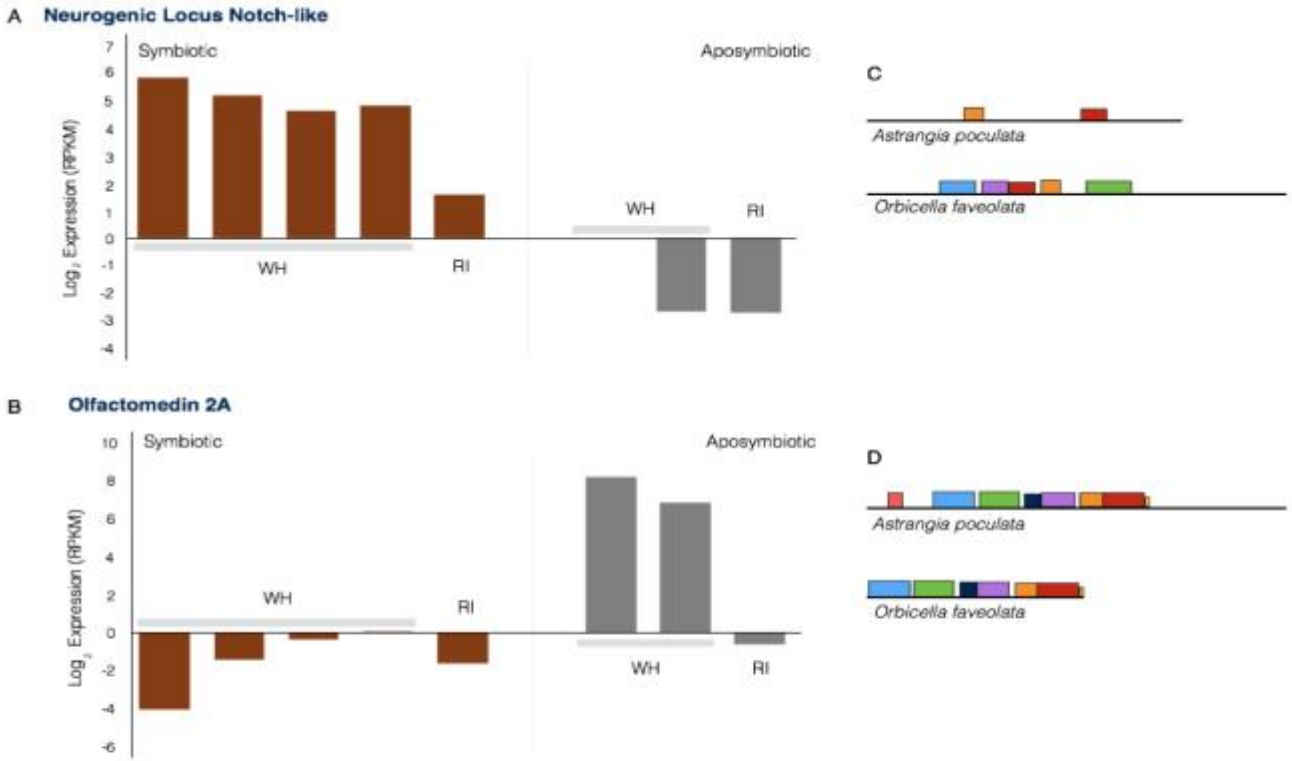

Figure 4.9. (A,B) Expression values for two differentially expressed contigs across two symbiotic types (symbiotic: brown, aposymbiotic, grey) and two populations (Woods Hole: WH, Rhode Island: RI). Values are given in RPKM on a $\log_2$ scale. (C,D) Motif analyses for neurogenic locus notch-like and olfactomedin 2A contigs, respectively, in *A. poculata* and *O. faveolata*. The height of colored boxes represents the statistical value of the motif while the width represents the length in nucleotides respective to other motifs.

cnidarians (Dunlap *et al* 2013, Käsbauer *et al* 2007, Marlow *et al* 2012, Münder *et al* 2010, Technau *et al* 2005), there is little motif homology between the transcript generated by this study and that of *Orbicella faveolata* (Figure 9C). It is unclear, however, whether this sequence is either (1) a result of spurious contig construction, or potentially (2) a different version of this gene unique for this species. The Notch-like contig is consistently more highly expressed in symbiotic relative to aposymbiotic samples. Olfactomedin, which plays a role in regulating apoptosis, has been shown to increase in expression in salamander cells with algal endosymbionts, suggesting a potential role in regulating symbiosis with a photosynthetic symbiont (Burns *et al* 2017). Interestingly, the olfactomedin transcripts in this study are relatively under-expressed in symbiotic corals compared to aposymbiotic corals. A motif analysis (MEME) with the most homologously similar gene model (in *O. faveolata*) indicates that this study's version of this gene is complete with a conserved suite of motifs (and in fact that the *O. faveolata* version might be truncated).

4.5 CONCLUSIONS

The present study describes a transcriptome assembly for *A. poculata* based on roughly 52 billion nucleotides of RNA sequencing and therefore represents one

of the largest transcriptomic datasets currently available for any scleractinian (Table 1). In order to ensure that we captured transcripts expressed throughout *A. poculata*'s complex relationship with *Symbiodinium*, we generated cDNA libraries from two naturally occurring and stable symbiont states as well as symbiotic and aposymbiotic polyps within a mixed symbiotic colony. Phylogenetic comparison of CO1 genes from this study and the previously sequenced type specimen for *Astrangia poculata* indicated extremely close homology and evidence for identification of the sequenced specimen (Figure 6). Further evidence that the transcriptome assembly is representative of the expressed gene repertoire of a scleractinian coral is the comparable recovery of GO terms from *A. poculata* and *O. faveolata*. Taken together, these data suggest that our sequencing effort was sufficient to generate a representative transcriptome that encompasses a large fraction of the transcript variety encoded by the *A. poculata* genome and its holobiont.

4.6 ACKNOWLEDGEMENTS

This research was supported by NSF grants MCB-0924749 and IOS-0818831 to JRF. Data generation and analysis were also supported by the budget of "Marine Genomics," a course in the Boston University Marine Semester. The authors are

grateful to Perry C. Oddo and William Caffrey for their expertise and advice in Python and R. We also thank Randi D. Rotjan for collection of coral specimens at Fort Wetherill State Park, RI.

4.7 AUTHOR CONTRIBUTIONS

The author and Nick Polato (Baums Lab, Pennsylvania State University) performed field collection of specimens, RNA isolation, and cDNA library synthesis. The author performed photography, assembled the reference transcriptome, carried out phylogenetic and MEME analyses, as well as BLAST, GO, and differential expression analyses. Linda Nguyen (Finnerty Lab, Boston University) performed initial BLAST2GO annotation for the reference transcriptome.

Chapter 5

Conclusion and future research directions

Contributions of the dissertation

This study is a multifaceted approach to understanding the impacts of combined stressors on hermatypic corals. I have combined health metrics at both the colony and polyp level, conducted an in-depth exploration of the coral-algal symbiosis by symbiont state, and employed a controlled, laboratory approach to understand coral recovery and resilience in the face of environmental stress. The work also elevates *Astrangia poculata* as a model organism for the lesion recovery process, including assays for performance (1) on the colony level and (2) at developmental landmarks on the polyp level (Appendix). Using a controlled single-polyp wounding schema, I explore the boundaries of this temperate coral's wide thermal tolerance and the influence of its facultative symbiosis with *Symbiodinium psygmophilum* on recovery from small-scale lesions (Chapter 2). I next utilize the natural and stable symbiotic states of *A. poculata* to examine the impact of a colony's energetic reserve capacity, with deference to the bleaching phenomenon, on the health, recovery, and performance of both host and symbiont (Chapter 3). Inspired by a discovered performance differential between

aposymbiotic and symbiotic colonies of *A. poculata*, I generate a transcriptome for this species and use computational approaches to determine differential gene expression between the holobionts of both symbiotic states (Chapter 4). Taken together, these research milestones shed light on the dynamic interactions between symbiosis, environmental stress, and the recovery and resiliency of corals.

This research project has made novel contributions to the fields of marine conservation and coral symbiosis, as discussed within each chapter. Here, I briefly note a few pertinent contributions. First, this work highlights the importance of a colony's symbiotic relationship with *Symbiodinium* to coral health and recovery. My work finds functional losses in performance for aposymbiotic corals, even in a system where aposymbiotic conditions are stable and actively maintained, and where heterotrophic food sources are abundantly available. These findings are broadly discussed across Chapters 2 and 3 as well as the Appendix, and suggest that an undisrupted long-term association with *S. psygmophilum* promotes not only quicker and more complete recovery from lesions, but also a greater ability to utilize smaller quantities of reserve tissue for to achieve recovery. Next, I examine the effect of symbiotic state, nutritional state, and reserve capacity, suggesting potential differential energetic allocation between biological processes as well as similar recovery processes on different organizational levels (Chapter 3). Taken

together, these findings hint at profound consequences to coral health after bleaching events, where there could be (1) an added cost to loss of symbiosis on small-scale recovery even after the uptake of new symbionts and (2) a possible decline in health and recovery ability even if a colony is able to supplement energy lost after symbiotic disruption by heterotrophic means. These results underscore the value of holistic studies characterizing coral energy dynamics, stress response, and recovery on multiple levels of function.

One pivotal step along the path to a robust comprehension of colony performance is to characterize the pathways and mechanisms that drive the recovery and stress responses. Toward that end, this dissertation presents a reference transcriptome for the full holobiont of *A. poculata* as well as a preliminary investigation into differential gene expression between the two main symbiont states.

Future directions

Astrangia poculata as a model system

The model organism of this dissertation, *Astrangia poculata*, has the potential to be a uniquely informative research system for coral conservation. This system provides a natural experiment through which we can explore the coral-

algal symbiosis in a controlled and measurable manner. Additionally, it can be kept in an aquarium and laboratory setting and, unlike many tropical corals, is abundant in nature with no imminent threat of endangerment. Given its phylogenetic relationship to other hermatypic corals, health diagnostics derived from *A. poculata* are very likely to be transportable to its tropical counterparts as well as other cnidarians. To that end, there is an established working group with the goal of expanding this system to answer multi-scale questions and to disseminate knowledge with collaborative engagement.

My work provides valuable input to this effort, including: (1) protocols for long term husbandry and maintenance, (2) quantifiable schemes for measuring lesion recovery, polyp extension behavior, and full colony tissue cover, (3) essential baseline knowledge of holobiont performance based on symbiont state, and (4) a reference transcriptome to serve as a platform for future studies.

Based on the conclusions of this work, there are several lines of future research that would be pertinent to explore in the future.

Genomic and transcriptomic resources

While the transcriptomic database for *A. poculata* presented here is an important first step, there is still a need for further deep sequencing of this coral.

Despite the large sequencing yield generated by this study, predicted sequence coverage is still low (3x coverage). A potential cause for the observed low sequence saturation is allelic diversity between multiple individuals in two geographically distinct populations (interpreted across a diverse holobiont species composition). A truly representative transcriptome would feature multiple individuals across several populations spanning this coral's extremely broad latitudinal range- in itself, another major advantage of using this coral as a model species. Additionally, characterizing gene expression after exposure to different controlled environments will be essential in moving from transcriptomic database to a full understanding of this corals' functional genomics. Future studies should focus on gene expression comparisons between symbiotic and aposymbiotic polyps of the same colony as well as between fully symbiotic and aposymbiotic colonies. Only taken together can we achieve an accurate picture of how (1) symbiosis influences gene expression within an individual genet and (2) how symbiosis is regulated on the colony level. Some of this work is underway collaboratively, investigating the relative impacts of controlled peroxide exposure and temperature stress (in the Finnerty lab at Boston University and Baums lab at Penn State University, respectively). Lastly, sampling the full holobiont (including the skeleton and its endolithic assemblage, as in this study) provides an opportunity to explore

epibiont and endolithic community structure not afforded by efforts that target only host cnidarian genetic material (i.e. sequencing gametes before horizontal acquisition of *Symbiodinium*, etc.). As these communities may be responding to stress and interacting with the coral colony as a whole in ways we cannot predict, I suggest that, moving forward, sequencing efforts for corals need to take a more holistic approach. Additionally, with increased interest in this model, sequencing and generating a genome database for this species would be also be a boon to our understanding and analysis of molecular and transcriptomic data for scleractinian corals.

Combinatorial approach to understanding coral stress and resilience

One of the more exciting avenues for future research is the use of *Astrangia poculata* as the basis for a controlled, combinatorial approach to understand coral stress and resilience. Pairing of organismal studies (phenotypic response) with molecular studies (genotypic variation and transcriptomic response) and/or directed energetics and carbon use measurements can be used to build a comprehensive picture of the processes involved in recovery from physical trauma, and stress responses.

Characterizing recovery pathways in corals

Finally, while the data generated in this dissertation have identified functional morphological pathways towards recovery and the impact of key environmental factors, this work is not able to identify mechanisms that drive or hinder recovery. As such, there is an urgent need to characterize the complete histological and molecular pathways through which lesion recovery is achieved. In doing so, we would generate not only descriptive indicators of success or failure of lesion healing, but permit predictive metrics for recovery and resilience. While we understand much of the general ecology of lesion recovery in corals, there is still much we do not understand about how these processes function mechanistically (including, as this dissertation has highlighted, resource allocation and energy dynamics as well as intra-species variation and acclimation). These functional questions are critical areas of study and could provide important information for conservation efforts, which often focus solely on thermotolerance as a standard for resilience.

Appendix

PATTERNS OF SURFACE LESION RECOVERY IN THE NORTHERN STAR CORAL, *ASTRANGIA POCULATA*

A.1 ABSTRACT

Corals regularly experience partial mortality due to grazing, sedimentation, disease, and abrasion. Because a colony's ability to heal such surface lesions can reflect its overall health, recovery from artificial wounds has been posed as a potential in situ measure of coral status and resilience. In this study, the response of a temperate, facultatively symbiotic coral, *Astrangia poculata*, to wounds of varying size and shape was measured, along with the influence of *Symbiodinium psygmophilum*. Because most tropical corals host an obligate symbiosis, the impact of the symbionts on lesion recovery cannot be quantified separately from the hosts. Here, symbiotic and aposymbiotic *A. poculata* colonies were subjected to lesions representing 25%, 50%, and 75% total colony loss, with varying wound shape. Colonies were monitored for recovery, mortality of living tissue, photosynthetic efficiency and approximated chlorophyll density. Recovery was observed to occur primarily from within the lesion site, demonstrating a 'Phoenix effect' healing pattern whereby recovery stems from tissue remnants in the wound area. Recovery was best explained by an interaction effect between symbiotic state

(symbiotic versus aposymbiotic) and the amount of residual tissue visible after wounding. Per unit area of residual tissue, healing was greater in symbiotic colonies. Symbiotic colonies also exhibited higher estimates of photochemical efficiency and approximated chlorophyll density, likely contributing to their enhanced healing capacity. These results support previously documented reductions in wound recovery among bleached corals, and suggest that symbiont loss itself, rather than associated stress or physiological disruption contributes to the diminished healing capacity of bleached colonies. Tissue mortality in un-wounded colony portions was greatest among symbiotic corals exposed to 50% colony loss amassed over two wounds, suggesting that corals with multiple injuries may experience greater tissue loss compared to single-wounded colonies, which can help inform methods for wound proxy metrics in the field. Dissected decalcified *A. poculata* colonies revealed deep (~4–6mm) corallite and polyp penetration, suggesting that surface lesions in this species are likely to leave tissue remnants buried within the skeleton. As such, it appears that *A. poculata* and corals with similar morphologies are predisposed to 'Phoenix effect' recovery, since most natural lesions would not fully penetrate the full depth of their corallites.

A.2 INTRODUCTION

Partial mortality is a constant source of sublethal stress for most colonial, sessile, and modular organisms (Mistri and Ceccherelli, 1995; Harmelin and Marinopoulos, 1994; Meszaros and Bigger, 1999; Jackson and Winston, 1981; Crawley, 1983). The ability of these organisms to repair wounds quickly and successfully can have major consequences for their survival, growth, and reproduction (Meesters *et al.*, 1996; Rinkevich, 1996; Rinkevich and Loya, 1989; Meesters *et al.*, 1994; Rotjan and Lewis, 2005). Because of the ecological and adaptive importance of wound healing, conservation and monitoring efforts are beginning to explore recovery from artificial wounds as a proxy for organismal status and resilience to a variety of stressors (as in Fisher *et al.*, 2007; Meesters and Bak, 1994; Meesters *et al.*, 1992). However, wounds are highly variable (Meesters *et al.*, 1997b; Lirman, 2000) and relationships between wound characteristics and recovery must be established before lesion healing can serve as a reliable proxy for organismal status.

Partly due to its utility as a proxy for colony health and performance, wound healing has been relatively well studied in corals. One of the earliest hypotheses generated by this research was 'localized regeneration' (LR), which posits that the energy for recovery is provided entirely by a narrow region of living

tissue directly bordering the lesion (Meesters *et al.*, 1994, 1997a; Bak and Steward-Van Es, 1980). Consequently, this hypothesis purports that the ratio of a wound's perimeter to its surface area (P:SA) is the primary determinant of healing capacity (Meesters *et al.*, 1997a; Van Woesik, 1998). Studies spanning multiple species support this hypothesis by demonstrating a positive functional relationship between healing rate and lesion P:SA (Meesters *et al.*, 1997a; Van Woesik, 1998). Under LR, colony size has no influence on healing capacity, although small colonies may be unable to withstand extensive lesioning and suffer whole colony mortality (Meesters *et al.*, 1996).

While the LR hypothesis is well supported in the literature, there are alternative healing patterns documented in corals. Oren *et al.* (1997, 2001) described a recovery model involving more widespread 'colony integration' (CI). These authors observed only relatively small lesions (<1 cm^2) behaving as expected under the LR hypothesis, with larger wounds drawing resources from portions of the colony as distant as 10–15 cm from the lesion site. Thus, for larger lesions, recovery did not depend solely on a thin band of adjacent tissue, but on the colony's total size and available energy reserves. Importantly, both CI and LR describe recovery that originates from the lateral margins of the wound, driven by contributions from the living colony (Meesters *et al.*, 1997a; Oren *et al.*, 1997, 2001).

In addition to the LR and CI models, there is a third, functionally distinct recovery pattern documented in corals. Krupp *et al.* (1992) observed recovery from osmotically induced mortality in *Fungia scutaria* to be driven by cryptic residual tissue within the skeleton. Despite complete withdrawal of surface tissues, the authors found intact messentarial filaments and undifferentiated tissue 2–7 mm beneath the skeletal surface. This recovery pattern, creatively dubbed the 'Phoenix effect' (PE), was also implicated in the rapid recovery of *Porites* colonies after a mass bleaching event (Roff *et al.*, 2014). Jokiel *et al.* (1993) also described recovery of *Porites* colonies after a freshwater kill to be driven by undifferentiated tissue within the coral skeleton, and Meesters *et al.* (1992) noted accelerated recovery of shallow lesions in *Porites asteroides* driven by tissue remnants in the skeleton. To date, most published descriptions of PE recovery have focused on ecosystem-wide patterns, and in depth descriptions at the organism level have yet to be reported.

Like most corals, the taxa in which wound healing has been previously researched, (*Acropora*, *Montipora*, *Diploria*, *Porites*, *Agaricia*, *Orbicella*, *Favia*, *Siderastrea*, and *Fungia*) (Hall, 2001; Meesters *et al.*, 1996; Titlyanov *et al.*, 2008; Denis *et al.*, 2011; Jayewardene, 2010; Van Woesik, 1998; Bak and Steward-Van Es, 1980; Meesters *et al.*, 1997a,b; Fisher *et al.*, 2007; Mascarelli and Bunkley-Williams, 1999; Oren *et al.*, 1997, 2001; Kramarsky-Winter and Loya, 2000; Kramarsky-Winter

and Loya, 1996) all maintain obligate symbioses with photosynthetic dinoflagellates (*Symbiodinium* spp.). Interruption of this symbiosis, commonly known as 'bleaching', is usually accompanied by stress and physiological disruption (Glynn *et al.*, 1985), confounding comparisons between bleached and healthy corals for assessing the role of *Symbiodinium* in wound recovery. While previous studies have been crucial to elucidating the general patterns and mechanisms of coral lesion healing, these efforts did not determine the role of algal symbiosis in recovery. As has been previously noted, determining the benefits of symbiosis to the host and symbionts under normal conditions has lagged behind understanding symbiosis during stress and bleaching (Edmunds and Gates, 2003).

The Northern Star Coral, *Astrangia poculata* (=Astrangia danae; Peters *et al.*, 1988), is a temperate coral that facultatively associates with *Symbiodinium psygmophilum* (LaJeunesse *et al.*, 2012; Dimond and Carrington, 2007, 2008), sympatrically displaying multiple visually distinct 'symbiotic states' (sensu Dimond and Carrington, 2007; Mitchelmore *et al.*, 2003) in shallow waters: brown, symbiotic, and white, aposymbiotic, with some intermediate colonies. The aposymbiotic state retains chronically reduced symbiont densities, maintained by proportionally greater expulsion rates than their fully symbiotic counterparts (Dimond and Carrington, 2008). As such, while aposymbiotic colonies are not

completely azooxanthellate, they do not functionally receive any photosynthetic benefits from *S. psygmophilum*. This unique intraspecific dichotomy allows examination of the impact of *Symbiodinium* on various aspects of coral biology, without the confounding effects of stress and physiological disruption associated with bleaching in obligate symbiotic taxa (Glynn *et al.*, 1985). The Northern Star Coral has already been used to investigate the impacts of algal symbiosis on host nutrition (Szmant-Froelich and Pilson, 1980, 1984), resistance to acidification (Holcomb *et al.*, 2010, 2012), vulnerability to sedimentation (Peters and Pilson, 1985), calcification, and metabolism (Jacques and Pilson, 1980; Jacques *et al.*, 1983; Cummings, 1983), and has proved to be a tractable experimental system with exciting potential for addressing fundamental questions of coral biology.

This study aimed to 1) directly evaluate the influence of *Symbiodinium* symbiosis on recovery and maintenance in *A. poculata*, and 2) describe the physical and temporal patterns of wound recovery in *A. poculata*, and the extent to which it adheres to any of the previously described healing models (localized regeneration (LR), colony integration (CI), or Phoenix effect (PE)). By evaluating the relationship between lesion P:SA, and colony size with healing capacity, as well as measuring any recovery from residual tissue fragments in the lesion site, it is possible to identify the dominant healing pattern(s) exhibited by *A. poculata*.

Additionally, comparing recovery between symbiotic and aposymbiotic *A. poculata* provides novel insights into the contributions of *Symbiodinium* to coral wound healing and resilience.

A.3 METHODS

A.3.1 Collection and Husbandry

Coral specimens were collected in October 2013 from depths of 6– 10 m at Fort Wetherill National Park in Jamestown, Rhode Island (41 28° 40°° N, 71 21° 34°° W) using SCUBA. Once collected, corals were acclimated for two months in an integrated, flow-through aquarium system supplied with ultraviolet-sterilized, particulate-filtered seawater from Boston Harbor. During acclimation, research specimens were removed of all visible epibionts, which included sponges, polychaete worms, and algae. After acclimation, colonies were randomly and evenly allocated among two integrated 30 gallon tanks such that approximately equal numbers from each symbiotic state and wound treatment group were present in each. Lighting was provided by high output (HO) T5 fluorescent fixtures (Hamilton Technology, Gardena, CA, Aruba Sun T5-V series) each housing one 54-watt daylight and actinic bulb. A stable temperature of 18 °C was maintained for the duration of the acclimation and experimental periods by a water chiller. Other water quality parameters, such as pH, nitrate, phosphate,

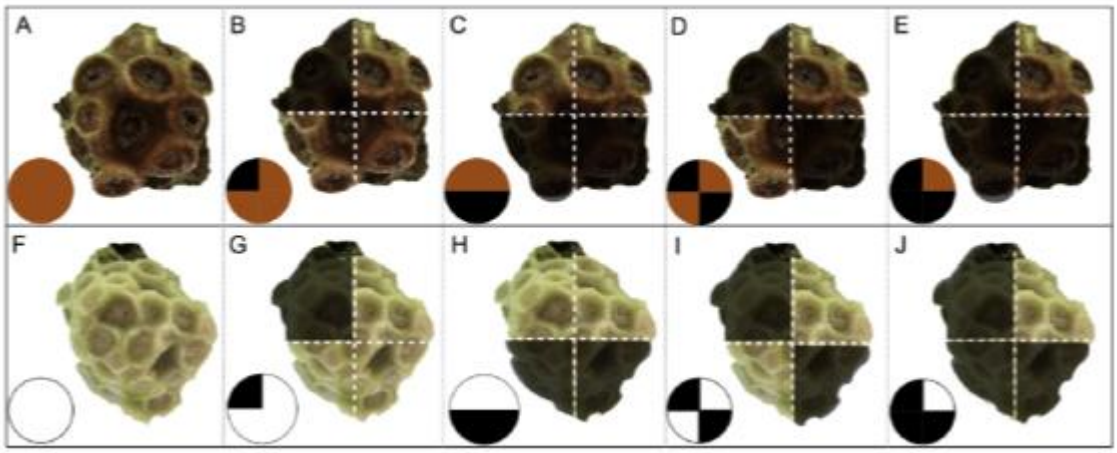

Figure A1. Experimental design for colony wounding. Intact colonies (A,F), 25% (B,G), 50% separate (D,I), and 75% wounded (E, J). Brown and white circles represent wounding schema in symbiotic and aposymbiotic colonies of *A. poculata*, respectively. Shaded areas indicate wounded proportion of the colony. N = 5 colonies for each wound group per symbiotic state.

calcium, and alkalinity were monitored and recorded weekly for the duration of the experiment.

Coral specimens were placed on raised plastic grids, each containing sixteen to eighteen colonies in separate slots to limit inter-colonial antagonism. Each day, *A. poculata* specimens received targeted ad libitum feedings of copepods (JEHMCo., Inc.), and each aquarium was scrubbed and siphoned to remove uneaten food, detritus and algae. Individual colonies were identified with numbered tags that were affixed to the corals' non-living base with cyanoacrylate.

A.3.2 Experimental design

This experiment included eight distinct treatments (four wounding patterns among two symbiotic states) intended to directly model the effects of zooxanthellae symbiosis and lesion P:SA on recovery in *A. poculata* (Fig. 1). Coral specimens (n = 50 colonies, n = 5 of each symbiotic state per wound treatment and control group) were visually categorized as symbiotic or aposymbiotic, and verified as such using a chlorophyll proxy equation generated for *A. poculata* by Dimond and Carrington (2007). Colonies displaying polyps of mixed symbiotic state were not selected for the study, but changes in symbiotic state among individual polyps of aposymbiotic colonies were observed during the acclimation and experimental periods.

For the designation of wounding pattern, the surface of each *A. poculata* colony was measured and considered as four quadrants of equal surface area. In quarter colony (25%) lesions, a single quadrant of the coral was ablated (Fig. 1 B, G). Two quadrants were ablated in the 50% adjacent (Fig. 1 C, H) and 50% separate (Fig. 1 D, I) lesion groups, adjacent to, and opposite of one another respectively to manipulate margin damage while keeping wound area constant. Three contiguous quadrants of the colony were wounded in the 75% lesion group (Fig. 1 E, J). These four wound types were intended to differ relatively predictably in their P:SA, with

the greatest ratio in the 25% and 50% separate groups, followed by the 50% adjacent group, and lowest in the 75% wound group. Total wound perimeter estimates were also measured in ImageJ (NIH) so wound P:SA could be calculated for consideration as a continuous variable. Colony size was evaluated as a continuous variable based on the initial live surface area of each colony. Additionally, 10 colonies were allocated as controls (Fig. 1 A, F) and received no wounding treatment, although the photochemical efficiency of these corals was monitored during the study (Fig. 5 C).

A.3.3 Data collection

Prior to wounding, each *A. poculata* specimen was photographed from the top and all four sides to fully image the entire colony. A two-way ANOVA was used to assess potential biases in colony size (measured as live surface area) between symbiotic states and wound treatment groups. Initial live surface area of colonies was estimated by enveloping their living portions in aluminum foil, trimming it to account for creases and dead areas. The tin foil was then weighed, and a predetermined surface area to weight ratio for the foil was used to calculate the coral's surface area (Marsh, 1970). This method was selected over surface area measurements derived from whole-colony photographs because image analysis can only estimate surface area in two dimensions.

For measuring recovery or mortality, this bias was less of an issue because the three-dimensionality of the colony is less pronounced over the localized spatial scales at which recovery/mortality was observed. However, for estimating an entire colony's size and designating wound area, planar estimates would have grossly underestimated the true surface area of the colony. Aposymbiotic corals exhibited significantly greater live surface area (11.78±5.58 cm^2) compared to symbiotic colonies (8.48±2.54 cm2) ($F(1,44)=7.548$, $p=0.009$). However, this difference is reflective of the size distribution observed at the collection site (DeFilippo, personal observation). Colonies were randomly assigned to wound treatments, and no significant size bias was detected between wound groups ($F(4,44)= 1.508$ $p = 0.216$).

Once total live surface area had been measured, wound area was designated by assigning a percentage of the tin foil's mass corresponding to the coral's wound treatment group (e.g. 25, 50, 75%) for removal. All wound designations were made within ±5% of the target tin foil weight. Wounding consisted of first removing the visible polyp and coenenchyme tissue with a Waterpik©, and then eroding the raised corallite structure until relatively flat with a diamond coated file. No effort was made to destroy the remaining septa once the corallite structure had been leveled, nor to remove any tissue fragments visible in

the lesion after the prescribed treatment. These wounds were not intended to replicate any specific natural lesioning agent, but constitute a generalized surface ablation such as might be incurred from a variety of mechanical stressors including storms and scraping corallivores (Woodley *et al.*, 1981; Bonaldo *et al.*, 2011).

Wounded *A. poculata* specimens were re-photographed within 48– 72 h of wounding, and again at 7, 10, 15, 20, 30 and 60 days after wounding. These time points were selected to yield a fine-scale time series of the early stages of recovery, as well as coarser patterns occurring over longer time periods. Photographs were analyzed in ImageJ (NIH) to measure the surface area of recovered tissue and mortality of live tissue. Total estimates were made by summing planar measurements of these parameters across photographs from the top and all four sides of the coral, excluding redundant area across angles. Photographs for two coral specimens were deemed unreliable due to shifts in coral position across photographs, and were excluded from analysis. When measuring recovery, a distinction was made between tissue regenerating from the perimeter (characteristic of both LR and CI healing) versus the interior (central/PE recovery) of the lesion (Fig. 2).

Maximum quantum yield (F_v/F_m) measures the photosynthetic capacity

of photosystem II (PS II), also known as photosynthetic efficiency. A Walz Junior pulse-amplitude modulated (PAM) fluorescence meter was used to measure the photosynthetic efficiency of each *A. poculata* colony prior to wounding, and again 3, 15, 30, and 60 days after wounding. Readings were taken between 1300 and 1500 h on each day to minimize the effects of diurnal fluctuations (Brown *et al.*, 1999) on the time series data. After 30 min of dark acclimation in a close topped black plastic container, individual colonies were transferred to a glass beaker filled with 2–3 in. of aquarium seawater that was placed within a dark plastic box where PAM readings were taken. A colony's photosynthetic efficiency at each time point was determined as the average maximum quantum yield measured from three haphazardly selected polyps. Briefly, 6 s of far red illumination was given to determine minimal fluorescence in the dark-adapted state (F0), and a saturating pulse (10,000 μmolm−2 s−1) was applied over 0.6 s to determine maximum fluorescence (Fm). Illumination was applied by a light fiber held ~1mm from the oral disk of each polyp at an angle of approximately 45–60°. The change in fluorescence (ΔF) caused by the saturating pulse was divided by maximal fluorescence to yield the maximum quantum yield, F_v/F_m. Polyp color was analyzed from photographs taken before wounding, and 3, 15, 30, and 60 days after wounding. Polyp color values were obtained by quantifying red, green, and

blue (RGB) pixels in 10 randomly selected polyps per colony against a color standard using a custom analysis script written in MATLAB (version R2007b, TheMathWorks, Natick, MA). This method corrects for changes in absolute illumination and any color imparted by ambient light to allow comparison between images. Following the protocol of Dimond and Carrington (2007), RGB values were condensed to a single value using principal component analysis. The resulting principal component (PC) explained an average of 70.6±4.72% of the variation in RGB, and component loadings averaged 88.4 ± 4.04, 93± 3.32, and 66± 18.53 for red, green, and blue respectively across all days measured. Principal component values were multiplied by−1 to induce realistic directionality, and were normalized to zero by adding the absolute value of the lowest transformed measurement to all values. To convert polyp color to approximated chlorophyll density, the adjusted PC values were applied to the equation developed by Dimond and Carrington (2007): $y = 0.044x^2 + 0{:}0335x$, where y= approximated chlorophyll density (μg cm−2) and x= polyp color PC (R2 = 0.89). Although chlorophyll density is not a strict measurement of symbiont density because zooxanthellae pigment concentrations fluctuate (Warner *et al.*, 2002; Cummings, 1983; Fitt *et al.*, 2000), it has been shown to be a reliable symbiosis parameter for distinguishing symbiotic states in *A. poculata* (Dimond and Carrington, 2007).

Additionally, in situ zooxanthellae counts require destructive tissue subsampling, which would inflict a second source of partial mortality to wounded colonies. The use of a symbiosis proxy (approximated chlorophyll density) in *A. poculata* represents an important tool for enabling non-destructive assessments that do not interfere with or confound the recovery potential of colonies.

Additional wounded and control *A. poculata* specimens not associated with the wounding experiment were fixed in formaldehyde, and their skeletons were dissolved in hydrochloric acid for morphological observations of corallite and tissue penetration depth, allowing a more detailed examination via tissue dissection of the wounding treatment's effect on the lesion site.

A.3.4 Statistical Analysis

All statistical analyses were performed using the R software package, version 3.2.0 (R Core Team (2015). All group means are reported as ± standard deviation. Because centrally recovered tissue indicates 'Phoenix effect' (PE) healing, and perimeter recovery is characteristic of both 'colony integration' (CI) and 'localized regeneration' (LR), the amount of central versus perimeter recovery observed was compared with Welch's paired t-test. For perimeter recovery, CI and LR can be further distinguished by a positive relationship between wound P:SA and colony size with recovery, respectively. Thus, wound P:SA, wound treatment, and colony

size, in addition to symbiotic state and residual tissue (tissue visible in the lesion site within 48–72 h after wounding) were evaluated as potential independent variables when modeling recovery. Surface area of recovered tissue was divided by initial wound size and the resulting proportions were fitted to a beta regression model with a logit link function using the 'betareg' package, which accommodates proportional data bounded between 0 and 1 (Ferrari and Cribari-Neto, 2004).

Live tissue mortality was examined for potential associations with continuous independent variables such as colony surface area, but none were detected. Therefore, a factorial approach was used for analysis. A two-way ANOVA was used to compare relative tissue mortality across symbiotic states and wound treatment groups. The mortality data exhibited pronounced heteroscedasticity, which transformations failed to resolve. Since transformations did not correct the violation but altered the ANOVA outcomes, the untransformed results are presented, but should be interpreted cautiously.

To confirm the difference in symbiosis levels that distinguish symbiotic from aposymbiotic *A. poculata* colonies, approximated chlorophyll density was fitted to a restricted maximum likelihood (REML) linear mixed effects (LME) model, with symbiotic state, wound treatment group, and day as potential fixed effects, and coral specimen ID as a random effect. To compare functional

photosynthetic efficiency between symbiotic states and assess possible variation among wound treatment groups, F_v/F_m values were also fitted to an LME model with the same suite of candidate fixed and random effects. While there was no biological basis to expect differences in photosynthetic efficiency or approximated chlorophyll density among wound treatment groups, it was important to assess whether such variation was present and potentially confounding the effects of the wounding treatments themselves on healing or mortality.

Model selection for wound recovery, F_v/F_m, and approximated chlorophyll density was based on Akaike's Information Criterion adjusted for small sample size (AICc), which balances model fit against overparameterization. Models containing every possible combination of candidate independent variables were fitted and ranked according to AICc, using the 'dredge' function of the 'MuMIn' package, and the difference between each model and the best model was calculated according to: Δ_i . $AIC_{c\ i} - AIC_{cmin}$. A Δ_i of 0–2 indicates "substantial" support for model 'i', while 4–7 is "considerably less", and N10 is "essentially none" (Burnham and Anderson, 2002). Simultaneous Tukey pairwise comparisons were performed between levels of factors and interactions when necessary using the 'glht' function of the 'multcomp' package. For all analyses, model assumptions were graphically assessed when necessary using quantile–quantile plots, density

plots, and/or residual by predicted plots. For all response variables except mortality, wound treatment had no observed statistical effect. Therefore, all samples within each symbiotic state were pooled together for analyses, increasing the effective sample size to 20 colonies per symbiotic state.

A.4 RESULTS

To determine the occurrence of central (PE) healing versus perimeter recovery (characteristic of both LR and CI recovery), the surface area of tissue originating within the lesion site from residual tissue fragments was compared to tissue regenerating from the margins of the wound. Perimeter recovery was observed in 15 out of the 38 (39.47%) recovering corals, accounting for only 5.77% of the total surface area of tissue recovered in this study. Among the colonies that did exhibit it, perimeter recovery constituted a relatively small portion of total recovery, averaging only 0.05±0.05 cm^2, or 21.64±21.01% (Fig. 3 D). By contrast, central recovery was observed in 100% of coral specimens examined, contributing an average of 0.35 ± 0.31 cm2 of new tissue per coral, and accounting for 94.23% of total observed recovery (Fig. 3 D). Welch's paired t test confirmed that central recovery was the dominant healing pattern exhibited in this study ($t=6.473, 38.248$, $p > 0.001$) (Fig. 3 D). The infrequency with which perimeter recovery was observed made explanatory statistical analyses intractable, so the final healing model

describes only central (PE) recovery.

Recovery originated primarily from minor tissue remnants visible in the lesion site, which expanded and coalesced to eventually form differentiated structures (e.g. tentacles) and complete functional polyps. In all groups, recovered tissue increased sharply after wounding, stabilizing midway through the experimental period and eventually declining as undifferentiated tissue was overgrown by algae (Figs. 3 A–C, 2 J–N). Out of wound treatment, wound P:SA, colony surface area, symbiotic state, and residual tissue, the most parsimonious beta regression model of recovery included only symbiotic state and residual tissue, with an interaction between the two effects (Table 2.1). The most plausible models that did include initial live surface area, P:SA, or wound treatment lacked substantial support (Table 2). Additionally, each of these models was simply the best model (containing only the interaction between residual tissue and symbiotic state), with either initial live surface area, P:SA, or wound treatment added (Table 2). That these models showed reduced plausibility despite added complexity suggests that these additional parameters were not informative, and that the best model was that which contained only the interaction between residual tissue and symbiotic state. Final recovery was similar among aposymbiotic (20.04 ± 13.47%) and symbiotic corals (21.92 ± 19.46%) (Fig. 3 C). However, the relative amount of

Figure A.2. Time series of wounding and recovery in *A. poculata*. Pre-wounding (A), after 3 days (B), 7 days (D), 10 days (F), 15 days (H), 20 days (J), 30 days (L), and 60 days (N). Insets: close up of single polyp recovery (indicated with a square) post-wounding after 3 days (C), 7 days (E), 10 days (G), 15 days (I), 20 days (K), 30 days (M), and 60 days (O). Newly formed tentacles denoted by "t," areas of algal overgrowth denoted by "a." Circles in the lower right corner represent simplified diagrams of recovery: areas in brown signify live tissue cover while black regions signify removed tissue.

residual tissue remaining in the lesion site was greater among aposymbiotic (9.52 ± 5.33%) compared to symbiotic (7.03 ± 3.99%) colonies. As such, while there was no significant difference in final recovery between symbiotic states, the effect of residual tissue on final recovery was significantly greater in symbiotic corals (Table 2.1).

Mortality of the remaining colony tissue was observed to occur almost exclusively on the coenenchyme rather than the polyps themselves. Mortality was highest early in the experimental period, though early recovery was greater (Figs. 3, 4). A significant interaction between wound treatment and symbiotic state was observed ($F(3, 30) = 3.437$, $p = 0.029$, Table 3), and post hoc Tukey comparisons indicated that the relative mortality of the symbiotic corals in the 50% separate wound group (29.58 ± 26.23%) exceeded that of the symbiotic (5.68±4.22%) and aposymbiotic (3.88±1.57%) corals of the 25% wound group, the symbiotic corals of the 50% adjacent wound group (4.80 ± 0.69%), and the aposymbiotic corals in the 50% separate wound group (7.95 ± 4.94) (Fig. 4 A, B). It should be noted that the large variance in the mortality of symbiotic corals in the 50% separate wound group (Fig. 4 A) was driven by a single individual

exhibiting relatively low mortality.

Maximum quantum yield (F_v/F_m) values were significantly greater among

symbiotic *A. poculata* at every day on which measurements were taken, but temporal trends differed between symbiotic states. Patterns in photosynthetic efficiency were best explained by an interaction effect between symbiotic state and day, with coral specimen as a random effect (Table 4). There was little support ($\Delta AIC_c > 4$) for models containing only main effects of these two parameters or symbiotic state by itself, and essentially no support ($\Delta AIC_c > 10$) for all other candidate models, including those containing wound treatment and all other possible combinations of main and interaction effects (Table 2).

Mean F_v/F_m values across the time series were 0.61 ± 0.06 for wounded symbiotic *A. poculata*, and 0.46 ± 0.09 for wounded aposymbiotic colonies. Wounding had no effect on F_v/F_m, and the values for the control group averaged 0.62 ± 0.07 for symbiotic corals, and 0.45 ± 0.08 for aposymbiotic corals. For symbiotic *A. poculata*, F_v/F_m values on day 3 were significantly greater than those taken prior to wounding, or 30 and 60 days after wounding (Fig. 5 C). Conversely, for aposymbiotic *A. poculata*, F_v/F_m values taken on days 3, 15, 30, and 60 were each significantly greater than those taken prior to wounding, and measurements taken on day 60 were significantly greater than those from days 3, and 30 (Fig. 5 C). Mean baseline polyp color PC values for symbiotic and aposymbiotic *A. poculata* established prior to wounding were 2.84 ± 0.47, and 1.11 ± 0.51 respectively,

Table A.1. Model summary of beta regression for central recovery with logit link function. Pseudo-R^2 = 0.555, Log-likelihood = 39.651, AIC_c = -67.427. Φ (Phi) serves as the precision parameter of the beta density for this model. Aposymbiotic *A. poculata* serve as the reference category for all effects that include symbiotic state.

Parameter	Estimate	Std. error	z	p
Intercept (aposymbiotic)	−2.519	0.324	−7.776	<0.001
Symbiotic	−0.447	0.449	−0.997	0.319
Residual tissue	10.896	2.645	4.119	<0.001
Symbiotic × residual tissue	11.272	4.445	2.536	0.011
ϕ (Phi)	15.550	3.550		

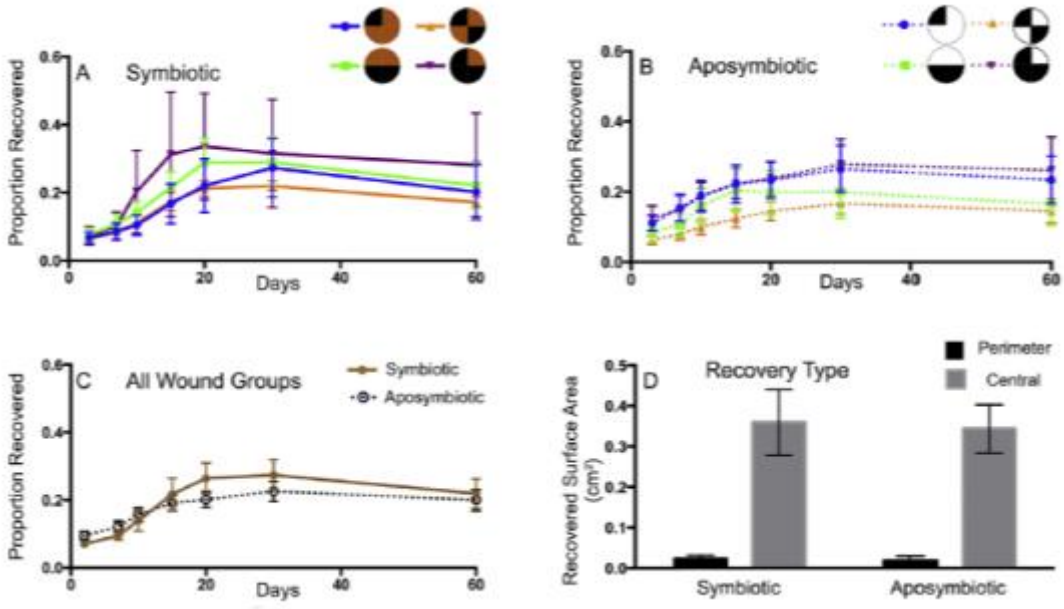

Figure A.3. Healing patterns in *A. poculata*. Mean proportion of the lesion area recovered for each wound group of (A) symbiotic *A. poculata* colonies, (B) aposymbiotic *A. poculata* colonies, and (C) all wound groups of symbiotic and aposymbiotic colonies combines. (D) Mean surface area of new tissue by recovery type (central vs. perimeter). Error bars represent standard error from the mean.

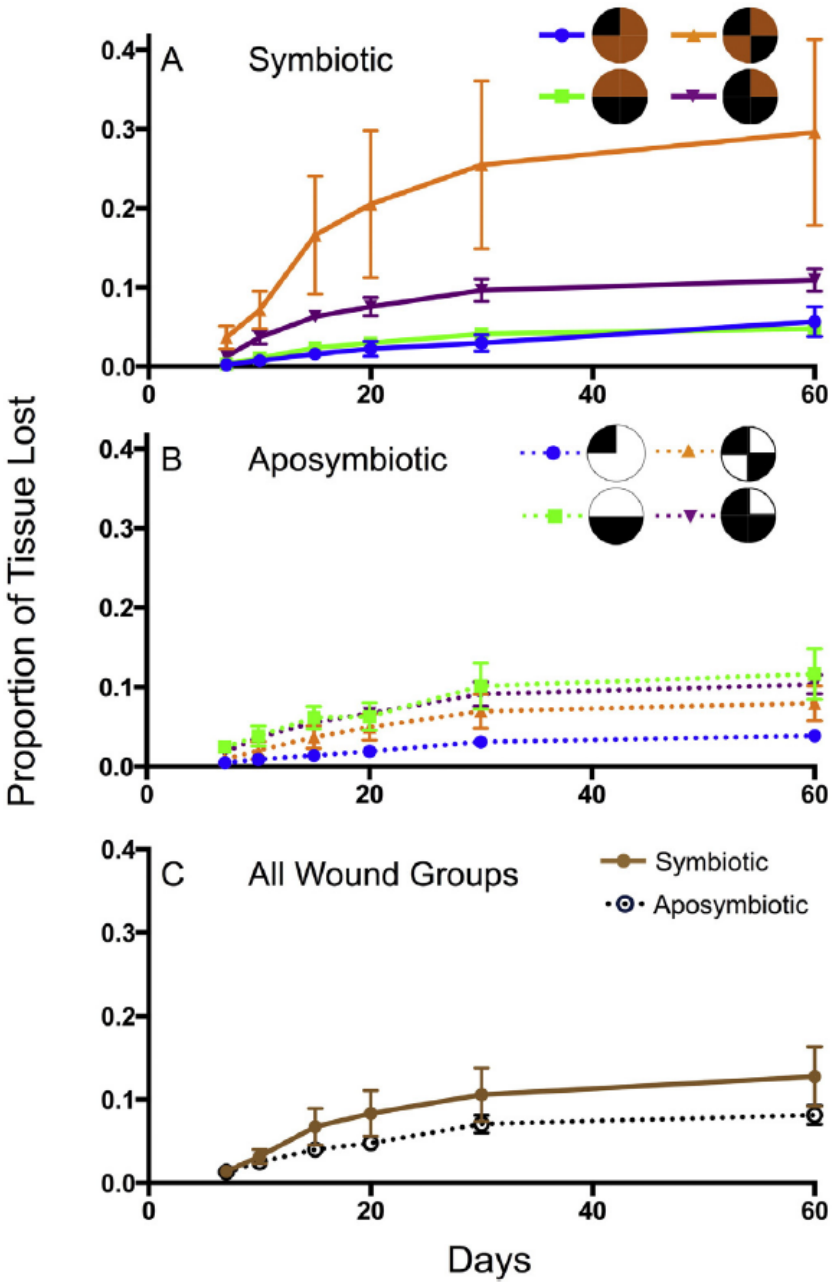

Figure A.4. Tissue mortality patterns in *A. poculata.* Mean proportion of living tissue lost for each wound group of (A) symbiotic *A. poculata* colonies, (B), aposymbiotic *A. poculata* colonies, and (C) all wound groups of symbiotic and aposymbiotic colonies combined. Error bars represent standard error from the mean.

Table A.2. Model selection results for recovery (a), photosynthetic efficiency (b), and approximated chlorophyll density (c). Only candidate models within >10 ΔAIC_c are presented. For each outcome, models are ranked from most plausible to least plausible ($\Delta AIC_c = 0$); df is the degrees of freedom for each model.

Response variable	Model parameters	Log likelihood	df	ΔAIC_c
(a) Recovery	Symbiotic, residual tissue, symbiotic × residual tissue	39.651	5	0.00
	Symbiotic, residual tissue, symbiotic × residual tissue, initial live tissue	39.844	6	2.45
	Symbiotic, residual tissue, symbiotic × residual tissue, P:SA	39.722	6	2.69
	Symbiotic, residual tissue	36.344	4	3.95
	Symbiotic, residual tissue, symbiotic × residual tissue, initial live tissue, P:SA	40.177	7	4.81
	Symbiotic, residual tissue, P:SA	36.743	5	5.82
	Symbiotic, residual tissue, initial live tissue	36.509	5	6.28
	Symbiotic, residual tissue, symbiotic × residual tissue, wound treatment	40.649	8	7.09
	Symbiotic, residual tissue, initial live tissue, P:SA	37.381	6	7.37
	Residual tissue	33.073	3	7.99
	Residual tissue, P:SA	34.070	4	8.50
	Symbiotic, residual tissue, symbiotic × residual tissue, P:SA, wound treatment	41.058	9	9.74
(b) Photosynthetic efficiency	Symbiotic, day, symbiotic × day	287.255	12	0.00
	Symbiotic, day	280.632	8	4.53
	Symbiotic	276.276	4	4.80
(c) Approximated chlorophyll density	Symbiotic	106.446	4	0.00
	Symbiotic, day	105.878	8	9.69

Table A.3. ANOVA summary for adjusted mortality.

Parameter	df	SSE	MSE	F	p
Symbiotic state	1	0.020	0.020	1.920	0.176
Wound treatment	3	0.109	0.036	3.492	0.028
Symbiotic state × wound treatment	3	0.107	0.036	3.437	0.029
Residuals	30	0.311	0.010		

Table A.4. Summary of REML fitted linear mixed effects model for F_v/F_m. For symbiotic state, aposymbiotic corals serve as the reference category, and for the day, the pre-wound measurements serve as the reference category. Log likelihood = 287.255, AIC_c = -549.193. Coral specimen was included in the model as a random effect.

Parameter	Estimate	Std. error	t	p
Intercept (aposymbiotic)	0.389	0.014	28.086	<0.001
Symbiotic	0.187	0.020	9.535	<0.001
Day 3	0.064	0.018	3.477	0.006
Day 15	0.079	0.018	4.326	<0.001
Day 30	0.073	0.018	3.976	0.001
Day 60	0.133	0.018	7.232	<0.001
Symbiotic × day 3	0.026	0.026	0.998	0.320
Symbiotic × day 15	−0.025	0.026	−0.966	0.335
Symbiotic × day 30	−0.051	0.026	−1.972	0.05
Symbiotic × day 60	−0.124	0.026	−4.766	<0.001

Table A.5. Summary of REML fitted linear mixed effects model for chlorophyll density. The reference category for symbiotic state is the aposymbiotic corals. Log likelihood = 106.45, AIC_c = -204.69. Coral specimen was included in the model as a random effect.

Parameter	Estimate	Std. error	t	p
Intercept (aposymbiotic)	0.150	0.028	5.419	<0.001
Symbiotic	0.281	0.039	7.153	<0.001

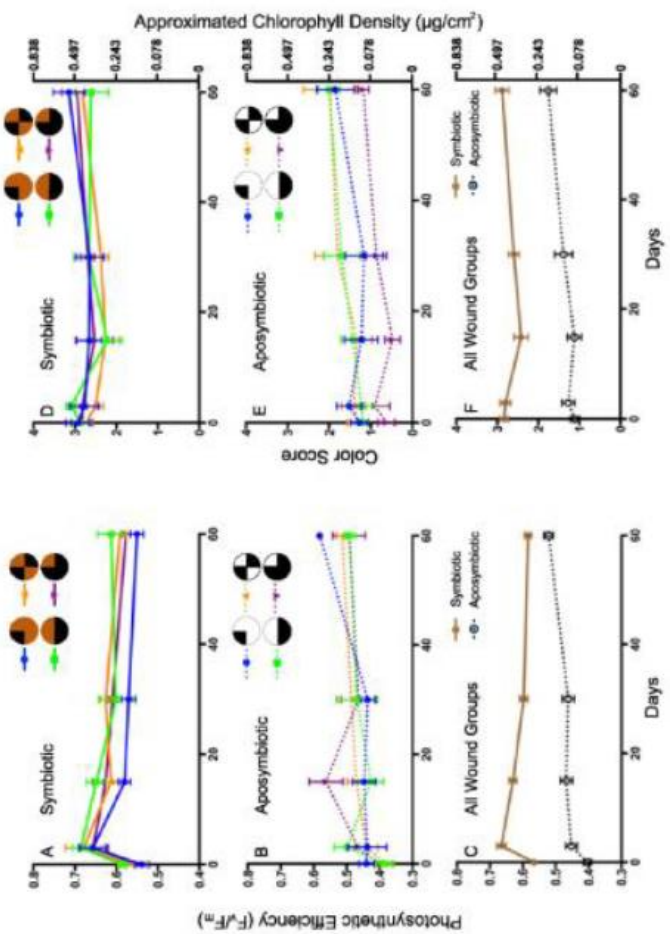

Figure A.5. Photosynthetic efficiency and chlorophyll density in *A. poculata*. Mean photosynthetic efficiency (F_v/F_m) over time for each wound group of (A) symbiotic *A. poculata* colonies, (B) aposymbiotic colonies, and (C) all wound groups combined for symbiotic and aposymbiotic colonies (including unwounded controls). Mean color score and approximated chlorophyll density over time for each wound group of (D) symbiotic *A. poculata* colonies, (E) aposymbiotic *A. poculata* colonies, and (F) all wound groups combined for symbiotic and aposymbiotic colonies. Error bars represent standard error from the mean.

indicating total approximated chlorophyll concentrations of 0.46 ± 0.14 and 0.10 ± 0.06 μg cm−2. 0.06 μg cm−2.

The most parsimonious model for approximated chlorophyll density included only symbiotic state as a fixed effect, with coral specimen as a random effect. Approximated chlorophyll density was significantly greater among symbiotic *A. poculata* for the duration of the experiment (Fig. 5, Table 5) There was very little support ($\Delta AIC_c > 9$) for all other candidate models considered, including those incorporating wound treatment, day, and all possible combinations of interaction and main effects (Table 2).

Dissection of preserved and decalcified *A. poculata* specimens showed unexpectedly deep polyp penetration, extending roughly 4–6 mm into the skeleton. Specimens wounded according to the same protocol as those in this study were similarly dissected, revealing preserved tissue remnants in the lesion site immediately after wounding.

A.5 DISCUSSION

This study makes several new contributions to our understanding of symbiosis in the recovery and maintenance of *A. poculata* coral hosts. First, the physical and temporal patterns of wound recovery in *A. poculata* were examined and no difference between symbiotic states in final recovery was observed,

suggesting that the absence of symbiosis does not preclude timely recovery. However, the effect of residual tissue on final recovery was significantly greater in symbiotic corals, suggesting that photosynthetic capability is advantageous. Most importantly, previously described healing models ('localized regeneration (LR)', 'colony integration (CI)', or 'Phoenix effect (PE)') were evaluated and the dominance of recovery originating from within the lesion site rather than its perimeter suggests that *A. poculata* exhibited primarily PE recovery in this study. This suggests that the mechanism of wound recovery across species should be considered when using healing as a proxy for coral health, since recovery style may influence the rate and likelihood of recovery.

The prevalence of PE recovery in *A. poculata* is likely due to two factors. Firstly, the deep corallite structure provides a refuge for polyp tissue against all but the most invasive lesioning agents. The presence of tissue remnants deep within dissected corallites immediately after wounding strongly suggests that even the most severe natural wounding would not fully extirpate tissue from the lesion site, and that residual polyp tissue would be the main driver of tissue recovery in this species. Corals of the genus *Porites* exhibit deep tissue penetration as well (Davies, 1991), and are also one of the only other coral taxa in which PE healing has been documented (Roff *et al.*, 2014; Jokiel *et al.*, 1993; Meesters *et al.*,

1992), suggesting a morphological basis for this healing mode that may be consistent across taxa. Second, *A. poculata* was observed to have a thin coenenchyme, often partially missing prior to collection or lost to varying extents during the study. This observation may indicate low levels of colony integration (Soong and Lang, 1992), potentially impeding translocation of photosynthate to the wound site from healthy polyps as required for LR and CI healing. Although LR is among the more common mechanisms of healing in corals (Meesters *et al.*, 1994; Bak and Steward-Van Es, 1980; Meesters *et al.*, 1997a; Van Woesik, 1998), in this study there was insubstantial evidence that either wound treatment or wound P:SA influenced recovery. This is consistent with biological expectations, as the LR hypothesis assumes that no tissue remains in the lesion site after wounding (Meesters *et al.*, 1997a) and is predicated on the expectation that recovery originates from the lateral margins of the wound (Meesters *et al.*, 1994; Bak and Steward-Van Es, 1980; Meesters *et al.*, 1997a; Van Woesik, 1998). Our decalcified and dissected colonies indicated tissue remnants in the lesion site, providing further support for a PE-driven recovery mechanism. Moreover, the CI model also assumes that recovery originates from the lesion perimeter, which was seldom observed.

The amount of residual tissue remaining after wounding had a significant

impact on final recovery for multiple possible reasons: (1) given equal rates of recovery, a coral with a greater amount of initial tissue has a 'head start' over other colonies. However, the regression coefficients for residual tissue indicate that its influence is beyond a mere additive contribution (Table 1). (2) If 'Phoenix effect' recovery proceeds only from residual tissue fragments, the number and size of these fragments may constitute a limiting factor in recovery, particularly if they depend on their own photosynthate for expansion. In both LR and CI, the energy for recovery is provided by translocation of photoassimilates from healthy polyps adjacent to, or distant from the lesion site respectively (Taylor, 1977; Gladfelter, 1983; Meesters *et al.*, 1997a, 1994; Oren *et al.*, 2001, 1997). If residual tissue fragments are isolated from the rest of the colony, they may need to provide their own energy for expansion and development of differentiated structures. Residual tissue fragments were never observed bearing feeding tentacles, but they did appear to retain the normal pigmentation of the living colony, suggesting the continued presence of *S. psygmophilum* in symbiotic colonies. If photosynthesis is indeed the primary energy source for recovery, then a greater area of tissue in the wound site would achieve greater net carbon

fixation than a smaller one (Jokiel and Morrissey, 1986), providing more energy for expansion and differentiation. This could also explain why symbiotic *A.*

poculata, with their greater symbiont/chlorophyll densities (Dimond and Carrington, 2007, 2008) and photosynthetic capacity (Jacques *et al.*, 1983), achieved more recovery per unit area of residual tissue, even with daily ad libitum feedings to all colonies.

Previous descriptions of PE recovery have occurred in response to hyposalinity (Krupp *et al.*, 1992; Jokiel *et al.*, 1993) and thermally induced bleaching (Roff *et al.*, 2014). Interestingly, both of these sources of mortality are mediated by contact of the colony surface with the surrounding water, and may not impact deeper portions of the coral. By contrast, more invasive sources of mortality such as excavating sponges (Chaves-Fonnegra and Zea, 2011), and parrotfish (Bonaldo *et al.*, 2011; Rotjan and Lewis, 2005, 2008) severe hurricane damage (Woodley *et al.*, 1981; Bythell *et al.*, 1993), dynamite, and ship groundings (Riegl, 2001) may be less likely to illicit PE healing. Thus, the encouragingly rapid recovery that Roff *et al.* (2014) observed in *Porites* after mass bleaching may not be as likely in response to more invasive wounding agents.

The only significant differences in relative mortality involved the symbiotic corals exposed to the 50% separate wound treatment. The wounding treatment itself likely contributed to the greater mortality of this group by disrupting the living colony's integrity more extensively than the other lesion types (Fig. 1). While

this wounding pattern was designed to maximize the perimeter of living tissue in contact with the wound site to potentially provide greater opportunity for recovery, it also achieved maximal disruption of colony cohesion. Only the symbiotic colonies exposed to this wounding treatment suffered greater mortality, adding to a small but growing body of evidence that algal symbiosis can exert an energetic demand on corals (Sachs and Wilcox, 2006; Burmester and Rotjan, pers. obs.).

As anticipated, photosynthetic efficiency and approximated chlorophyll density were both greater among symbiotic compared to aposymbiotic *A. poculata* on all days measured. Neither parameter differed among wound treatments, suggesting that the greater mortality observed among symbiotic corals of the 50% separate wound group was due to the wounding pattern itself. Moreover, the consistently greater F_v/F_m values of symbiotic *A. poculata* indicate greater photosynthetic capacity of PS II, further suggesting that elevated symbiont densities and photosynthetic yield are responsible for the greater healing capacity observed in these colonies. While chlorophyll density estimated throughpolyp color cannot distinguish between changes in symbiont densities versus changes in the chlorophyll densities of symbionts (Warner *et al.*, 2002; Cummings, 1983; Fitt *et al.*, 2000), it has nonetheless been demonstrated as a viable and non-destructive

tool to estimate symbiosis in *A. poculata* (Dimond and Carrington, 2007). Because direct zooxanthellae counts are destructive, the in situ measurement of symbiont densities would have been a confounding factor, acting as a de facto wound beyond our experimental construct. Interestingly, the approximated chlorophyll densities estimated in this study for both symbiotic states were lower than those described by Dimond and Carrington (2007), possibly reflecting the effects of stress induced by wounding and/or captivity on symbiont/pigment concentrations.

A. 6 CONCLUSIONS

Symbiotic and aposymbiotic varieties of *A. poculata* exist sympatrically, suggesting that both symbiotic states regularly persist in nature. One potential advantage conferred by symbiosis is greater healing capacity with single wounds, regardless of size, most likely attributable to increased photosynthetic yield. However, our results indicate that when multiple large wounds are inflicted, there is little impact on wound size or position on recovery, and corals in both symbiotic and aposymbiotic states were still able to demonstrate recovery.

This study supports a morphological basis for PE recovery in corals, which can be used to predict the occurrence of this healing pattern in response to lesions of varying invasiveness. Considering that PE recovery has been implicated in the

rapid, large scale recovery of corals with deep-bodied polyps, these results will have useful applications towards predicting the ecological consequences of disturbances for reefs, and future studies should consider the role of polyp depth in colony recovery potential. Additionally, our results indicate that different configurations of the same relative lesion size can have markedly different impacts on colony health, informing the use of recovery from artificially inflicted wounds as a proxy for coral status.

A.7 ACKNOWLEDGEMENTS

This research was funded by a grant from the PADI Foundation awarded to EMB, an Undergraduate Research Grant from the Boston University Marine Program awarded to LD, and a grant from the Cell Signaling Technologies Environmental Small Grants Program awarded to RR. Personnel from both Boston University and the New England Aquarium were directly involved in the study design, collection, analysis and interpretation of data, in writing the report, and in the decision to submit the article for publication. However, institutional funding sources were not involved in any of the above. We would like to thank Tasia Blough, Katrina Malakhoff, Aaron Pilnick, Jesse Mathews, Julio Camperio-Ciani, Georgia Luddecke and Nicholas Lawrence for the assistance in data collection and aquarium husbandry. We also thank Jeff Chabot for programming RGB color

analysis in MATLAB, and Thomas Buehrens for the statistical advice.

A.8 PUBLICATION

DeFilippo L, Burmester EM, Kaufman L, Rotjan D (2016) Patterns of surface lesion recovery in the Northern Star Coral, *Astrangia poculata*. J Exp Mar Biol Ecol 481: 15-24.

A.9 AUTHOR CONTRIBUTIONS

LD: Carried out the experiment, analyzed the images, performed the statistical analyses, graphed the data, wrote the manuscript, and contributed funding. EMB: Collected specimens, collaborated in project design and implementation, assisted with figure creation, and manuscript writing, and contributed resources and funding. LK: Contributed useful conversations and input. RR: Conceived and designed the experiment, helped to perform the experiment, assisted with graphics, and manuscript writing and contributed space, other resources, and funding.

BIBLIOGRAPHY

List of Abbreviated Journal Titles

Biol Bull	Biological Bulletin
Biol Rev	Biological Reviews
Bull Mar Sci	Bulletin of Marine Science
Curr Biol	Current Biology
Cons Biol	Conservation Biology
Dis Aquat Org	Disease of Aquatic Organisms
Duke Envtl L & Pol F	Duke Environmental Law & Policy Forum
Ecol Monogr	Ecological Monographs
The FASEB J	The Official Journal of the Federation of Ameriecan Societies for Experimental Biology
Free Radic Biol Med	Free Radical Biology & Medicine
Frontiers Microbiol	Frontiers in Microbiology
Global Change Biol	Global Change Biology
Genome Biol Evol	Genome Biology & Evolution
Internat Rev Hydrobiol	International Review of Hydrobiology
J Appl Stat	Journal of Applied Statistics
J Exp Mar Biol	Journal of Experimental Biology
J Exp Mar Biol Ecol	Journal of Experimental Marine Biology & Ecology
J Invert Pathol	Journal of Invertebrate Pathology
J Invertebr Pathol	Journal of Invertebrate Pathology
J Phycol	Journal of Phycology
J Sea Res	Journal of Sea Research
Limnol Oceanogr	Limnology & Oceanography
Mar Biol	Marine Biology
Mar Biotechnol	Marine Biotechnology
Mar Ecol	Marine Ecology
Mar Ecol Prog Ser	Marine Ecology Progress Series
Mar Genomics	Marine Genomics
Mar Life	Marine Life
Mar Poll Bull	Marine Pollution Bulletin
Marine & Freshwater Res	Marine & Freshwater Research
Microbiol	Microbiology
Nucelic Acid Res	Nucleic Acid Research

Oceanog	Oceanography
PNAS	Proceedings of the National Academy of Sciences of the United States of America
Proc 5th Int Coral Reefs	Proceedings of the Fifth International Coral Reef Congress
Proc Biol Soc Wash	Proceedings of the Biological Society of Washington
Proc Natl Acad Sci	Proceedings of the National Academy of Sciences
Proc R Soc B Biol Sci	Proceedings of the Royal Society of London B: Biological Sciences
R Soc Open Sci	Royal Society Open Science
Rev Trop Biol	Review of Tropical Biology
Sci Reports	Scientific Reports- Nature
Trends Ecol Evol	Trends in Ecology & Evolution

References

Aranda M, Li Y, Liew J, Baumgarten S, Simakov O, Wilson, MC, Piel J, Ashoor H, Bougouffa S, Bajic VB, Ryu T, Ravasi T, Bayer T, Micklem G, Kim H, Bhak J, LaJeunesse TC, Voolstra CR (2016) Genomes of coral dinoflagellate symbionts highlight evolutionary adaptation conducive to a symbiotic lifestyle. Sci Reports 6: 39734

Bailey TL, Williams N, Misleh C, Li WW (2006) MEME: discovering and analyzing DNA and protein sequence motifs. Nucleic Acids Res 34 (suppl 2): W369-W373.

Bak RPM, Steward-Van Es Y (1980) Regeneration of superficial damage in the scleractinian corals *Agaricia agaricites*, *F. purpurea*, and *Porites astreoides*. Bulletin Mar Sci 30(4): 883-887

Bak, RPM (1983) Neoplasia, regeneration and growth in the reef-building coral *Acropora palmata.* Mar Biol 77: 221-227

Baker A, Glynn PW, Riegl B (2008) Climate change and coral reef bleaching: An ecological assessment of long-term impacts, recovery trends and future outlook. Estuarine, Coastal and Shelf Science, 80(4): 435-471

Barshis DJ, Ladner JT, Oliver TA, Seneca FO, Traylor-Knowles NT, Palumbi SR (2012) Genomic basis for coral resilience to climate change. PNAS 110(4): 1387-1392

Bay RA & Palumbi SR (2015) Rapid acclimation ability mediated by transcriptome changes in reef-building coral. Genome Biol Evol 7(6): 1602-1612

Black NA, Voellmy R, Szmant AM (1995) Heat shock protein induction in *Montastrea faveolata* and *Aiptasia pallida* exposed to elevated temperatures. Biol Bull 188(3): 234-240

Bonaldo RM, Krajewski JP, Bellwood DR (2011) Relative impact of parrotfish grazing scars on massive *Porites* corals at Lizard Island, Great Barrier Reef. Mar Ecol Prog Ser 423: 223–233

Burnham KP, Anderson DR. Model selection and multimodel inference: a practical information-theoretic approach (Springer, New York, ed. 2, 2002)

Brainard RE, Weijerman M, Eakin CM, McElhany P, Miller MW, Patterson M, Piniak GA, Dunlap M, Birkeland C (2013) Incorporating climate and ocean change into extinction risk assessments for 82 coral species. Cons Biol 27(6): 1169-78

Brown BE, Ambarsari I, Warner ME, Fitt WK, Dunne RP, Gibb SW, Cummings DG (1999) Diurnal changes in photochemical efficiency and xanthophyll concentrations in shallow water reef corals: evidence for photoinhibition and photoprotection. Coral Reefs 18: 99–105

Bythell JC, Gladfelter EH, Bythell M (1993) Chronic and catastrophic natural mortality of three common Caribbean reef corals. Coral Reefs, 12.3-4: 143-152

Cameron CM, Edmunds PJ (2014) Effects of simulated fish predation on small colonies of massive *Porites* spp. and *Pocillopora meandrina*. Mar Ecol Prog Ser 508, 139–148

Chapman *et al.* (2010) The dynamic genome of *Hydra*. Nature 464: 592-594

Cohen AL & M Holcomb (2009) Why corals care about ocean acidification: Uncovering the mechanism. Oceanog 22(4) Special Issue: On the Future of Ocean Biogeochemisty in a High-CO_2 World: 118-127

Chaves-Fonnegra A, Zea S (2011) Coral colonization by the encrusting excavating Caribbean sponge *Cliona delitrix*. Mar Ecol 32: 162–173

Coyer JA, Ambrose RF, Engle JM, Carroll JC (1993) Interactions between corals and algae on a temperate zone rocky reef: mediation by sea urchins. J Exp Mar Biol Ecol 167: 21-37

Crawley MJ (1983) Herbivory: The Dynamics of Animal–Plant Interactions. Blackwell Scientific Publications, Oxford.

Cummings C (1983) The biology of *Astrangia danae*. PhD Dissertation, University of Rhode Island, Kingston

Cróquer A, Villamizar E, Noriega N (2002) Environmental factors affecting tissue regeneration of the reef-building coral *Montastrea annularis* (Faviidae) at Los Roques National Park, Venezuela. Rev Biol Trop 50: 3-4

Daniels CA, Baumgarten S, Yum LK, Michell CT, Bayer T, Arif C, Roder C, Weil E, Voolstra CR (2015) Metatranscriptome analysis of the reef-building coral *Orbicella faveolata* indicates holobiont response to coral disease. Frontiers Mar Sci. 2:62 doi: 10.3389/fmars.2015.00062

Davies PS (1991) Effect of daylight variations on the energy budgets of shallow-water corals. Mar Biol 108: 137–144.

Davies SW, Marchetti A, Ries JB, Castillo KD (2016) Thermal and pCO_2 stress elicit divergent transcriptomic responses in a resilient coral. Frontiers Mar Sci 3:112 doi: 10.3389/fmars.2016.00112

Descombes P, Wisz MS, Leprieur F, Parravincini V, Heine C, Olsen SM, Swungedouw D, Kulbicki M, Mouillot D, Pellissier L (2015) Forecasted coral reef decline in marine biodiversity hotspots under climate change. Global Climate Change. doi:10.1111/gcb.12868

DeFilippo L, Burmester EM, Kaufman L, Rotjan RD. (2016) Patterns of surface lesion recovery in the Northern Star Coral *Astrangia poculata*. J Exp Mar Biol Ecol 481: 15-24

Denis V, Debreuil J, De Palmas S, Richard J, Guillaume MMM, Bruggemann, JH (2011) Lesion regeneration capacities in populations of the massive coral *Porites lutea* at Réunion Island: Environmental correlates. Mar Ecol Prog Ser 428, 105–117

Denis V, Guillaume MMM, Goutx M, de Palmas S, Debreuil J, Baker A, Boonstra RK, Bruggermann JH (2013) Fast growth may impair regeneration capacity in the branching coral *Acropora muricata*. PLoS ONE 8(8): e72618. doi:10.1371/journal.pone.0072618

DeSalvo MK, Sunagawa S, Voolstra CR, Medina M (2010) Transcriptomic responses to heat stress and bleaching in the elkhorn coral *Acropora palmata*. Mar Ecol Prog Ser 402: 97-113

Diaz-Pulido G, McCook LJ (2002) The fate of bleached corals: patterns and dynamics of algal recruitment. Mar Ecolog Prog Ser, 232: 115-128

Dimond J, Carrington E (2007) Temporal variation in the symbiosis and growth of the temperate scleractinian coral *Astrangia poculata*. Mar Ecol Prog Ser, 348: 161-172

Dimond J, Carrington E (2008) Symbiosis regulation in a facultatively symbiotic temperate coral: zooxanthellae division and expulsion. Coral Reefs, 27: 601-604

Dimond J, Kerwin AH, Rotjan R, Sharp K, Stewart FJ, Thornhill DJ (2012) A simple temperature-based model predicts the upper latitudinal limit of the temperate coral *Astrangia poculata*. Coral Reefs, 32(2): 401-409

Downs CA, Fauth JE, Halas JC, Dustan P, Bemiss J, Woodley CM (2002) Oxidative stress and seasonal coral bleaching. Free Radic Biol Med 33(4):533-543

Downs CA, Woodley CM, Richmond RH, Lanning LL, Owen R (2005) Shifting the paradigm of coral-reef "health" assessment. Mar Poll Bull 51: 486-494

Edmunds PJ, Gates RD (2003) Has coral bleaching delayed our understanding of fundamental aspects of coral–dinoflagellate symbioses? Bioscience 53, 976–980

Dunn SR, Bythel JC, Le Tissier MDA, Burnett WJ, Thomason JC (2002) Programmed cell death and cell necrosis activity during hypothermic stress-induced bleaching of the symbiotic sea anemone *Aiptasia* sp. J Exp Mar Biol Ecol 272(1): 29-53

Edmunds PJ (2005) The effect of sub-lethal increases in temperature on the growth and population trajectories of three scleractinian corals on the southern Barrier Reef. Oecologia. 146(3): 350-364

Edmunds PJ (2009) Effect of acclimatization to low temperature and reduced light on the response of reef corals to elevated temperature. Mar Biol 156, 1797–1808

Edmunds PJ, Lenihan HS (2010) Effect of sub-lethal damage to juvenile colonies of massive *Porites* spp. under contrasting regimes of temperature and water flow. Mar Biol 157, 887–897

Ferrari S, Cribari-Neto F (2004) Beta regression for modelling rates and proportions. J Appl Stat 31: 799–815

Fine M, Zibrowius H, Loya Y (2001) *Oculina patagonica*: a non-lessepsian scleractinian coral invading the Mediterranean Sea. Mar Biol 138(6): 1195-1203

Fine M, Oren U, Loya Y (2002) Bleaching effect on regeneration and resource translocation in the coral *Oculina patagonica*. Mar Ecol Prog Ser 234: 119-125

Fishelson L (1973) Ecological and biological phenomena influencing coral-species composition on the reef tables at Eilat (Gulf of Aqaba, Red Sea). Mar Biol 19: 183-196

Fisher EM, Fauth JE, Hallock PJ, Woodley CM (2007) Lesion regeneration rates in reef-building corals *Montastrea* spp. as indicators of colony condition. Mar Ecol Prog Ser 339: 61-71

Fitt, WK, McFarland FK, Warner ME, Chilcoat GC (2000) Seasonal patterns of

tissue biomass and densities of symbiotic dinoflagellates in reef corals and relation to coral bleaching. Limnol Oceanogr 45: 677–685

Gladfelter EH (1983) Circulation of fluids in the gastrovascular system of the reef coral *Acropora cervicornis*. Biol Bull 165: 619–636

Glynn PW, Peters EC, Muscatine L (1985) Coral tissue microstructure and necrosis: relation to catastrophic coral mortality in Panama. Dis Aquat Org 1: 29–37

Grace S (2004) Ecomorphology of the temperate scleractinian *Astrangia poculata*: Coral-macroalgal interactions in Narragansett Bay. Dissertation: University of Rhode Island

Grajales A & E Rodríguez (2014) Morphological revision of the genus Aiptasia and the family Aiptasiidae (Cnidaria, Actiniaria, Metridioidea). Zootaxa 3826(1): 55-100

Garrett TA, Hwang J, Schmeitzel JL, Schwarz J (2011) Lipidomics of *Aiptasia pallida* and *Symbiodinium*: a model system for investigating the molecular basis of coral symbiosis. The FASEB J 25(1) supplement 938.2

Grottoli, AG, Rodrigues LJ, Palardy JE (2006) Heterotrophic plasticity and resilience in bleached corals. Nature. 440: 1186-1189

Hall, V.R., 2001. The response of Acropora hyacinthus and Montipora tuberculosa to three different types of colony damage: scraping injury, tissue mortality and breakage. J Exp Mar Biol Ecol 264, 209–223.

Harmelin, J.G., Marinopoulos, J., 1994. Population structure and partial mortality of the gorgonian *Paramuricea clavata* (Risso) in the north-western Mediterranean (France, Port-Cros Island). Mar Life 4, 5–13.

Henry L, Hart M (2005) Regeneration from injury and resource allocation in sponges and corals- a review. Internat Rev Hydrobiol 90(2): 125-158

Hill M, Hill A (2012) The magnesium inhibition and arrested phagosome hypotheses: new perspectives on the evolution and ecology of *Symbiodinium* symbioses. Biol Rev 87: 804-821

Hoegh-Guldberg O (1999) Climate change, coral bleaching and the future of the world's coral reefs. Marine & Freshwater Res 50(8): 839-866

Holcomb M, McCorkle D, Cohen AL (2010) Long-term effects of nutrient and CO2 enrichment on the temperate coral *Astrangia poculata*. J Exp Mar Biol Ecol 386: 27-33

Holcomb M, Cohen A, McCorkle D (2012) An investigation of the calcification response of the scleractinian coral *Astrangia poculata* to elevated pCO2 and the effects of nutrients, zooxanthellae and gender. Biogeosciences 9: 29-39

Hughes TP, Jackson JBC (1985) Population dynamics and life histories of foliaceous corals. Ecol Monogr 55: 141-156

Jackson JBC, Winston JE (1981) Modular growth and longevity in bryozoans. In: Larwood GP, Nielson C (Eds.), Recent and Fossil Bryozoa. Olsen & Olsen, Fredensborg, pp. 121–126

Jacques TG, Pilson MEQ (1980) Experimental ecology of the temperate scleractinian coral *Astrangia danae*. I. Partition of respiration, photosynthesis and calcification between host and symbionts. Mar Biol 60: 167–178

Jacques TG, Marshall N, Pilson MEQ (1983) Experimental ecology of the temperate scleractinian *Astrangia danae*: Effect of temperature, light intensity and symbiosis with zooxanthellae on metabolic rate and calcification. Mar Biol 76: 135-148

Jayewardene D (2010) Experimental determination of the cost of lesion healing on *Porites compressa* growth. Coral Reefs 29(1): 131-135

Jayewardene D, Birkeland C (2006) Fish predation on Hawaiian corals. Coral Reefs 25(3): 328-328

Jayewardene D, Donahue MJ, Birkeland C (2009) Effects of frequent fish predation on corals in Hawaii. Coral Reefs 28(2): 499-506

Jokiel PL, Morrissey JI (1986) Influence of size on primary production in the reef

coral *Pocillopora damicornis* and the macroalga *Acanthophora spicifera*. Mar Biol 91: 15-26

Jokiel PL, Hunter CL, Taguchi S, Watarai L (1993) Ecological impact of a fresh-water "reef kill" in Kaneohe Bay, Oahu, Hawaii. Coral Reefs 12: 177–184

Jompa J, McCook LJ (2003) Coral-algal competition: macroalgae with different properties have different effects on corals. Mar Ecolog Prog Ser 258: 87-95

Kaufman L (1981) There was biological disturbance on Pleistocene coral reefs. Paleobiology 7(4): 527-532

Kitahara MV, Cairns SD, Jaroslaw S, Blair D, Miller DJ (2010) A comprehensive phylogenetic analysis of the Scleractinia (Cnidaria, Anthozoa) based on mitochondrial CO1 sequence data. PLOSOne: 5(7): e11490

Knowlton N (2001) The future of coral reefs. PNAS 98 (10): 5419-5425

Kojis BL, Quinn NJ (1985) Puberty in Goniastrea favulus: age or size limited? Proc 5th Int Coral Reefs Congr 4:289-293

Kramarsky-Winter E, Loya Y (1996) Regeneration versus budding in fungiid corals: a trade-off. Mar Ecol Prog Ser 134: 179–185

Kramarsky-Winter E, Loya Y (2000) Tissue regeneration in the coral *Fungia granulose*: The effect of extrinsic and intrinsic factors. Mar Biol 137(5): 867-873

Krupp DA, Jokiel PL, Chartrand TS (1992) Asexual reproduction by the solitary Scleractinian coral *Fungia scutaria* on dead parent coralla in Kaneohe Bay, Oahu, Hawaiian Islands. In: Richmond, B.M. (Ed.), Proceedings of the Seventh International Coral Reef Symposium, Hawaii, pp. 527–534.

LaJeunesse TC, Parkinson JE, Reimer JD (2012) A genetics-based description of *Symbiodinium minutum* SP. NOV. and *S. psygmophilum* SP. NOV. (*Dinophyceae*), two dinoflagellates symbiotic with *Cnidaria*. J Phycol 48: 1380-1391

Lehnert EM, Burriesci MS, Pringle JR (2012) Developing the anemone *Aiptasia* as a tractable model for cnidarian-dinoflagellate symbiosis: the transcriptome of aposymbiotic *A. pallida.* BMC Genomics 13L 271

Lehnert EM, Mouchka ME, Burriesci MS, Gallo ND, Schwarz JA, Pringle J (2014) Extensive Differences in Gene Expression Between Symbiotic and Aposymbiotic Cnidarians. G3: GENES, GENOMES, GENETICS 4(2): 277-295

Lenihan HS, Edmunds PJ (2010) Response of *Pocillopora verrucosa* to corallivory varies with environmental conditions. Mar Ecol Prog Ser 49: 51-63

Lesser MP and Farrell JH (2004) Exposure to solar radiation increases damage to bothhost tissues and algal symbionts of corals during thermal stress. Coral Reefs, 23(3): 367-377

Lin S, Cheng S, Song B, Zhong X, Lin X, Li W, Li L, Zhang Y, Zhang H, Ji Z, Cai M, Zhuang Y, Shi X, Lin L, Wang L, Wang Z, Liu X, Yu S, Zeng P, Hao H, Zou Q, Chen C, Li Y, Wang Y, Xu C, Meng S, Xu X, Wang J, Yang H, Campbell DA, Sturm NR, Dagenais-Bellefeuille S, Morse D (2015) The *Symbiodinium kawagutii* genome illuminates dinoflagellate gene expression and coral symbiosis. Science 350: 691–694

Lin Z, Chen M, Dong X, Zheng X, Huang H, Xu X, Chen J (2017) Transcriptome profiling of *Galazea fascicularis* and its endosymbiont *Symbiodinium* reveals chronic eutrophication tolerance pathways and metabolic mutualism between partners. Sci Reports 7: 42100

Lirman D (2000) Lesion regeneration in the branching coral *Acropora palmata*: effects of colonization, colony size, lesion size, and lesion shape. Mar Ecol Prog Ser 197: 209–215.

Maor-Landaw K, Karako-Lampert S, Ben-Asher HW, Goffredo S, Falini G, Dubinsky Z, Levy O (2014) Gene expression profiles during short-term heat stress in the red sea coral *Stylophora pistillata.* Global Change Biol 20: 3026-3035

Marsh Jr JA (1970) Primary productivity of reef-building calcareous red algae. Ecology 51: 255–263

Marshall AT, Clode P (2004) Calcification rate and the effect of temperature in a zooxanthellate and an azooxanthellate scleractinian reef coral. Coral Reefs. 23: 218-224

Mascarelli PE, Bunkley-Williams L (1999) An experimental field evaluation of healing in damaged, unbleached and artificially bleached star coral, *Montastraea annularis*. Bull Mar Sci 65: 577–586

Mayfield AB, Wang YB, Chen CS, Lin CY, Chen SH (2014) Compartment-specific transcriptomics in a reef-building coral exposed to elevated temperatures. Mol Ecol 23: 5816-5830

Meesters EH, Bak RPM (1993) Effect of coral bleaching on tissue regeneration potential and colony survival. Mar Ecol Prog Ser 96, 189–198

Meesters EH, Bos A, Gast GJ (1992) Effects of sedimentation and lesion position on coral tissue regeneration. Proc 7th International Coral Reef Symposium 2: 681-688

Meesters EH, Noordeloos M, Bak RPM (1994) Damage and regeneration: links to growth in the reef-building coral Montastrea annularis. Mar Ecol Prog Ser 112: 119-128

Meesters EH, Wesseling I, Bak RPM (1996) Partial mortality in three species of reef-building corals (*Scleractinia*) and the relation with colony morphology. Bull Mar Sci 58: 838-852

Meesters EH, Pauchli W, Bak RPM (1997) Predicting regeneration of physical damage on a reef-building coral by regeneration capacity and lesion shape. Mar Ecol Prog Ser 146: 91-99

Meesters EH, Wesseling I, Bak RPM (1997b) Coral colony tissue damage in six species of reef-building corals: partial mortality in relation with depth and surface area. J Sea Res 37: 131–144

Meszaros, A, Bigger C (1999) Qualitative and quantitative study of wound healing processes in the coelenterate, *Plexaurella fusifera*: spatial, temporal, and

environmental (light attenuation) influences. J Invertebr Pathol 73: 321–331

Miller MW (1995) Growth of a temperate coral: effects of temperature, light, depth, and heterotrophy. Mar Ecol Prog Ser 122: 217-225

Mistri M, Ceccherelli VU (1995) Damage and partial mortality in the gorgonian *Paramuricea clavata* in the Strait of Messina (Tyrrhenian Sea). Mar Life Vol 5: 43–49 Marseille

Mitchelmore CL, Ringwood AH, Weis VM (2003) Differential accumulation of cadmium and changes in glutathione levels as a function of symbiotic state in the sea anemone *Anthopleura elegantissima*. J Exp Mar Biol Ecol 284: 71–85

Moya A, Huisman L, Ball EE, Hayward DC, Grasso LC, Chua CM, Woo HN, Gattuso JP, Forêt S, Miller DJ (2012) Whole transcriptome analysis of the coral *Acropora millepora* reveals complex responses to CO_2-driven acidification during the initiation of calcification. Mol Ecol 21(1): 2440-2454

Muscatine L. The role of symbiotic algae in carbon and energy flux in reef corals. In *Coral Reefs: Ecosystems of the World* vol. 25 1990 pp. 75–87. Eds. New York, NY:Elsiever

Nagelkerken I, & Bak RPM (1998) Differential regeneration of artificial lesions among sympatric morphs of the Caribbean corals *Porites astreoides* and *Stephanocoenia michelinii*. Mar Ecol Prog Ser 171, 279–283

Nagelkerken I, Meesters EH, Bak RPM (1999) Depth-related variation in regeneration of artificial lesions in the Caribbean corals *Porites astreoides* and *Stephanocoenia michelinii*. J Exp Mar Biol Ecol 234: 29–39

Nugues MM, Roberts CM (2003a) Partial mortality in massive reef corals as an indicator of sediment stress on coral reefs. Mar Poll Bull 46(3): 314-323

Nugues MM, Roberts CM (2003b) Coral mortality and interaction with algae in relation to sedimentation. Coral Reefs 22(4): 507-516

Oakley CA, Ameismeier MF, Peng L, Weis VM, Grossman AR, Davy SK (2016) Symbiosis induces widespread changes in the proteome of the model cnidarian *Aiptasia*. Cell Microbiol doi: 10.1111/cmi.12564

Oldach MJ, Workentine M, Matz MV, Fan TY, Vize PD (2017) Transcriptome dynamics over a lunar month in a broadcast spawning acroporid coral. Mol Ecol 26: 2514-2526

Oren U, Benayahu Y.,Loya Y (1997) The effect of lesion size and shape on regeneration of the Red-Sea coral *Favia favus*. Mar Ecol Prog Ser 146: 101-107

Oren U, Benayahu Y, Lubinevsky H, Loya Y (2001) Colony integration during regeneration in the stony coral *Favia favus*. Ecology 82(3): 802-813

Ortiz-González IC, Rivera-Vicéns RE, Schizas NV (2017) *De novo* transcriptome assembly of the hydrocoral *Millepora alcicornis* (branching fire coral) from the Caribbean. Mar Genomics 32: 27-30

Palardy JE, Rodrigues LJ, Grottoli AG (2008) The importance of zooplankton to the daily metabolic carbon requirements of healthy and bleached corals at two depths. J Exp Mar Biol Ecol 367(2): 180-188

Palumbi SR, Barshis DJ, Traylor-Knowles N, Bay RA (2014) Mechanisms of reef coral resistance to future climate change. Science 344:6186 895-897

Perez SF, Cook CB, Brooks WR (2001) The role of symbiotic dinoflagellates in the temperature-induced bleaching response of the subtropical sea anemone *Aiptasia pallida*. J Exp Mar Biol Ecol 256(1): 1-14

Peters EC, Cairns SD, Pilson MEQ, Wells JW, Jaap WC, Lang JC, Vasleski CJ, St. Pierre Gallohan L (1988) Nomenclature and biology of *Astrangia poculata* (=*A. danae*, = *A. astreiformis*) (*Cnidaria*: *Anthozoa*). Proc Biol Soc Wash 101: 234-250

Peters EC, Pilson MEQ (1985) A comparative study of the effects of sedimentation on symbiotic and asymbiotic colonies of the coral *Astrangia danae* Milne Edwards and Haime 1849. J Exp Mar Biol Ecol 92: 215–230

Pinheiro J, Bates D, DebRoy S, Sarkar D and R Core Team (2017). *nlme: Linear and Nonlinear Mixed Effects Models*. R package version 3.1-130, https://CRAN.R-project.org/package=nlme.

Pinzón JH, Kamel B, Burge CA, Harvell CD, Medina M, Weil E, Mydlarz LD (2015) Whole transcriptome analysis reveals changes in expression of immune-relates genes during and after bleaching in a reef-building coral. R Soc Open Sci 2: 140214

Poole AZ, Kitchen SA, Weis VM (2016) The role of complement in cnidarian-dinoflagellate symbiosis and immune challenge in the sea anemone *Aiptasia pallida*. Frontiers Microbiol 7:519

R Core Team (2013). R: A language and environment for statistical computing. R Foundation for Statistical Computing, Vienna, Austria. URL http://www.R-project.org/.

Riegl B (2001) Degradation of reef structure, coral and fish communities in the Red Sea by ship groundings and dynamite fisheries. Bull Mar Sci 69: 595–611

Mansour TA, Rosenthal JJC, Brown CT, Roberson LM (2016) Transcriptome of the Caribbean stony coral *Porites astreoides* from three developmental stages. GigaScience 5:33 doi: 10.1186/s13742-016-0138-1

Maor-Landaw K, Ben-Ascher HW, Karako-Lamper S, Salmon-Divon M, Prada F, Caroselli E, Goffredo S, Falini G, Dubinsky Z, Levy O (2017) Mediterranean versus Red Sea corals facing climate change, a transcriptome analysis. Sci Reports 7: 42405

Mass T, Putnam HM, Drake JL, Zelzion E, Gates RD, Bhattacharya D, Falkowski PG (2017) Temporal and spatial expression patterns of biomineralization proteins during early development in the stony coral *Pocillopora damicornis*. Proc R Soc B 283: 20163022

Mulhall M (2008) Saving the Rainforest of the Sea: An Analysis of International Efforts to Conserve Coral Reefs. Duke Envtl L & Pol F 19:321

Muscatine L and Hand C (1958) Direct evidence for the transfer of materials from symbiotic algae to the tissues of a coelenterate. Proc Natl Acad Sci USA 44(12): 1259-1263

Riegl B, Velimerov B (1991) How many damaged corals in the Red Sea reef systems? A quantitative survey. Hydribiologia 216/217 (1): 249-256

Rinkevich B (1996) Do reproduction and regeneration in damaged corals compete for energy allocation? Mar Ecol Prog Ser 143, 297–302

Rinkevich B, Loya Y (1989) Reproduction in regenerating colonies of the coral *Stylophora pistillata*. In: Spanier E, Steinberger Y, Luria M (eds) Environmental quality and ecosystem stability. Hebrew University, Jerusalem, pp 257–265

River GF, Edmunds PJ (2001) Mechanisms of interaction between macroalgae and scleractinians on a coral reef in Jamaica. J Exp Mar Biol Ecol 261(2): 159-172

Rodolfo-Metalpa R, Peirano A, Houlbrèque F, Abbate M, Ferrier-Pagès M (2008) Effects of temperature, light and heterotrophy on the growth rate and budding of the temperate coral *Cladocora caespitosa*. Coral Reefs 27: 17-25

Roff G, Bejarano S, Bozec YM, Nugues M, Steneck RS, Mumby PJ (2014) *Porites* and the Phoenix effect: unprecedented recovery after a mass coral bleaching event at Rangiroa Atoll, French Polynesia. Mar Biol 161: 1385–1393

Roth KE, Jeon K, Stacey G (1988) Homology in endosymbiotic systems: the term "Symbiosome". Molecular Genetics of Plant-Microbe Interactions, pages 220-225

Roth MS (2014) The engine of the reef: photobiology of the coral-algal symbiosis. Front Microbiol 5:422

Rosic N, Kaniewska P, Chan CKK, Ling EYS, Edwards D, Dove S, Hoegh-Guldber O (2014) Early transcriptional changes in the reef-building coral *Acropora aspera* in response to thermal and nutrient stress. BMC Genomics 15:1052

Rotjan RD, Dimond JL (2010) Discriminating causes from consequences of persistent parrotfish corallivory. J Exp Mar Biol Ecol 390(2): 188-195

Rotjan RD, Dimond JL, Thornhill D, Leichter J, Helmuth B, Kemp D, Lewis SM (2006) Chronic parrotfish grazing impedes coral recovery after bleaching. Coral Reefs 25: 361-368

Rotjan RD, Lewis SM (2005) Selective predation by parrotfishes on the reef coral *Porites* astreoides. Mar Ecol Prog Ser 305: 193-201

Rotjan RD, Lewis SM (2006) Parrotfish abundance and selective corallivory on a Belizean coral reef. J Exp Mar Biol Ecol 335: 292-301

Rotjan RD, Lewis SM (2009) Predators selectively graze reproductive structures in a clonal marine organism. Mar Biol 156(4): 569-577

Rotjan RD, Lewis SM (2008) The impact of coral predators on tropical reefs. Mar Ecol Prog Ser 367: 73-91

Rowan R (2004) Coral bleaching: Thermal adaptation in reef coral symbionts. Nature 430: 742

Ruiz-Jones LJ & Palumbi SR (2015) Transcriptome-wide changes in coral gene expression at noon and midnight under field conditions. Biol Bull 228: 227-242

Sachs JL, Wilcox TP (2006) A shift to parasitism in the jellyfish symbiont *Symbiodinium microadriaticum*. Proc R Soc Lond B Biol Sci 273: 425–429

Shinzato C, Shoguchi E, Kawashima T, Hamada M, Hisata K, Tanaka M, Fujie M, Fujiwara M, Koyanagi R, Ikuta T, Fujiyama A, Miller DJ, Satoh N (2011) Using the *Acropora digitifera* genome to understand coral responses to environmental change. Nature. 476: 320-323

Shinzato C, Inoue M, Kusakabe M (2014) A snapshot of a coral "holobiont": A transcriptome assembly of the scleractinian coral, *Porites*, captures a wide variety of genes from both the host and symbiotic zooxanthellae. PLOSOne 9(1): e85182

Shoguchi E, Shinzato C, Kawashima T, Gyoja F, Mungpakdee S, Koyanagi R, Takeuchi T, Hisata K, Tanaka M, Fujiwara M, Hamada M, Seidi A, Fujie M,

Usami T, Goto H, Yamasaki S, Arakaki N, Suzuki Y, Sugano S, Toyoda A, Kuroki Y, Fujiyama A, Medina M, Coffroth MA, Bhattacharya D, Satoh N (2013) Draft assembly of the *Symbiodinium minutum* nuclear genome reveals dinoflagellate gene structure. Curr Biol 23: 1399–1408

Soong K, Lang JC (1992) Reproductive integration in reef corals. Biol Bull 183: 418–431

Steen RG (1986) Evidence for heterotrophy by zooxanthellae in symbiosis with *Aiptasia pulchella*. Bioll Bull 170: 267-278

Suggett DJ, Borowitzka MA, Prášil O (Eds.) Chlorophyll a Fluorescence in Aquatic Sciences: Methods and Applications, Developments in Applied Phycology 4, Springer Science+Business Media B.V. 2010

Sullivan JC, Ryan JF, Watson JA, Webb J, Mullikin JC, Rokhsar D, Finnerty JR (2006) *StellaBase*: The *Nematostella vectensis* Genomics Database. Nucleic Acids Res 34(Database issue): D495-D499

Sun J, Chen Q, Lun JCY, Xu J, Qiu JW (2013) PcarnBase: Development of a Transcriptomic Database for the Brain Coral *Platygyra carnosus*. Mar Biotechnol 15(2): 244-251

Sunagawa S, Wilson EC, Thaler M, Smith ML, Caruso C, Pringle JR, Weis VM, Medina M, Schwarz JA (2009) Generation and analysis of transcriptomic resources for a model system on the rise: the sea anemone *Aiptasia pallida* and its dinoflagellate endosymbiont. BMC Genomics 10:258

Szmant-Froelich A, Pilson MEQ (1980) The effects of feeding frequency and symbiosis with zooxanthellae on the biochemical composition of *Astrangia danae* Milne Edwards and Haime, 1849. J Exp Mar Biol Ecol 48: 85-97

Szmant-Froelich A, Pilson MEQ (1984) Effects of feeding frequency and symbiosis with zooxanthellae on nitrogen metabolism and respiration of the coral *Astrangia poculata*. Mar Biol 81: 153-162

Taylor, D.L., 1977. Intra-colonial transport of organic compounds and calcium in some Atlantic reef corals. International Proceedings of the 3rd International Coral Reef Symposium. Vol. 1, pp. 431–436.

Thornhill DJ, Kemp DW, Bruns BU, Fitt WK, Schmidt GW (2008) Correspondence between cold tolerance and temperate biogeography in a western Atlantic *Symbiodinium* (*Dinophyta*) lineage. J Phycol 44:1126-1135

Titlyanov EA, Titlyanova TV, Chapman D (2008) Recovery dynamics of mechanically damaged scleractinian corals of the genus *Porites* under different light intensities. Galaxea, J Coral Reef Stud 10: 69–76

The UniProt Consortium (2017) UniProt: the universal protein knowledgebase. Nucleic Acids Res 45: D158-D169

Van Veghel MLJ, Bak RPM (1994) Reproductive characteristics of the polymorphic Caribbean reef building coral *Montastraea annularis*. III. Reproduction in damaged and regenerating colonies. Mar Ecol Prog Ser 109: 229-233

Van Woesik R (1998) Lesion healing on massive *Porites* spp. corals. Mar Ecol Prog Ser 164: 213-220

Warner M, Chilcoat G, McFarland F, Fitt W (2002) Seasonal fluctuations in the photosynthetic capacity of photosystem II in symbiotic dinoflagellates in the Caribbean reef-building coral *Montastraea*. Mar Biol 141: 31–38

Weis VM, Davy SK, Hoegh-Guldberg O, Rodriguez-Lanetty M, Pringle JR: Cell biology in model systems as the key to understanding corals. Trends Ecol Evol. 2008, 23: 369-376. 10.1016/j.tree.2008.03.004.

Woodley JD, Chornesky EA, Clifford PA, Jackson JBC, Kaufman LS, Knowlton N, Lang JC, Pearson MP, Porter JW, Rooney MC, Rylaarsdam KW, Tunnicliffe VJ, Wahle CM, Wulff JL, Curtis ASG, Dallmeyer MD, Jupp BP, Koehl MAR, Neigel J, Sides EM (1981) Hurricane Allen's impact on a Jamaican coral reef. Science 214: 749–754

Wolfowicz I, Baumgarten S, Voss PA, Hambleton EA, Voolstra CR, Hatta M, Guse A (2016) *Aiptasia* sp. larvae as a model to reveal mechanisms of symbiont selection in cnidarians. Sci Reports doi: 10.038/srep323666

Work TM, Aeby GS (2010) Wound repair in *Montipora capitata*. J Invert Pathol 105: 116-119

Wright RM, Aglyamova GV, Meyer E, Matz MV (2015) Gene expression associated with white syndromes in a reef building coral, *Acropora hyacinthus*. BMC Genomics 16:371 doi: 10.1186/s12864-015-1540-2

Yuan C, Zhou Z, Zhang Y, Chen G, Xiaopeng Y, Ni X, Tang J, Huang B (2017) Effects of elevated ammonium on the transcriptome of the stony coral *Pocillopora damicornis*. Mar Poll Bull 114(1): 46-52

CURRICULUM VITAE